SYNTHESIS AND CHARACTERISATION OF TOUGH AND PERMEABLE MACROPOROUS POLYMERS

Ranting Wu

A dissertation submitted to Imperial College London

in fulfilment of the requirements for the degree of

Doctor of Philosophy

and the Diploma of Membership of Imperial College London

Department of Chemical Engineering

Imperial College London

July 2011

Abstract

Emulsion templating using high internal phase emulsions is an effective route to prepare low density, high porosity macroporous polymers known as polyHIPEs (poly(high internal phase emulsion)). Conventional polyHIPEs, synthesised from surfactant stabilised w/o (water-in-oil) emulsions, have low permeabilities and poor mechanical properties. This thesis describes an investigation into developing and characterising one type of tough and permeable macroporous polymers via emulsion templating. Increasing the continuous phase volume from HIPEs (high internal phase emulsion) to MIPEs (medium internal phase emulsion) is an effective way to improve the mechanical properties of resulting macroporous polymers. The influence on morphology and physical properties of the resulting macroporous polymers caused by the usage of different initiators and surfactants in MIPEs was initially discussed to optimise the formulation of MIPEs based on styrene and divinylbenzene (DVB). The MIPEs based on styrene and DVB used azobis(isobutyronitrile) (AIBN) as initiator produced macroporous polymers possessing desired open porous interconnected pore structure no matter which surfactant (surfactant mixture) was used while potassium persulfate (KPS) and redox initiator system cannot produce open porous macroporous polymers from MIPEs consisting of styrene and DVB. Then tough and permeable low density polymers were developed, produced by polymerising the continuous phase of emulsion templates, which contained styrene, polyethyleneglycoldimethacrylate (PEGDMA) and silylated silica particles. PEGDMA and the silylated silica particles acted as crosslinker. The functionalised silica particles were incorporated into the polymer, which resulted in a significant improvement of the mechanical properties of the polyHIPEs without

affecting the interconnected and permeable pore structures. The physical and mechanical properties of the tough and permeable macroporous polymers were characterised. Especially the mechanical properties, including shear properties and fracture toughness (mode II) were investigated using the Arcan fixture. Both the shear properties and fracture toughness (mode II) increased significantly with increasing the organic phase volume in emulsion templates and the further improvements can be obtained by the incorporation of silica filler in the emulsion templates. Finally, approaches to directly synthesise hydrophilic macroporous polymers based on styrene and DVB were presented since most of macroporous polymers produced from HIPEs are hydrophobic and need modification after polymerisation to improve the surface wettability. The incorporation of silylated silica particles in the emulsion templates improved the wettability of the resulting macroporous polymer but not the water uptake. The water uptake of macroporous polymers can be increased by the introduction of methacrylic acid (MA) and dimethylaminoethyl methacrylate (DMAEMA) into the aqueous phase of emulsion templates as additional monomers in order to synthesise hydrophilic polymer/polymer macroporous composites.

Declaration

I hereby certify that the work presented in this thesis is the result of my own Investigation carried out at Imperial College London during the period from January 2007 to June 2010, except where otherwise stated.

Ranting Wu

July 2011

Contents

List of Figures

List of Tables

List of Scheme

Acknowledgements

First of all I want to express my profound gratitude to my supervisor Prof. Alexander Bismarck. Without his inspirational ideas and thoughtful guidance I would not have been here to finish my PhD research. His financial support has made my daily life easier throughout my study.

I also want to specially thank Dr. Angelika Menner who has guided me through the whole research. She is my first and most important teacher in emulsion templating technique. In addition she has offered intensive help in the characterisation of my specimens.

I also want to thank my colleagues and friends in the PaCE group at Imperial College, for their help and support during my stay in UK. Their kindness and humour has left me with wonderful memories.

Finally, I want to show my deepest gratitude to my parents, to whom this thesis is dedicated. Without their unselfish love and whole-hearted support I would never have achieved anything.

List of Abbreviations

AETMS	2-(acryloxyethoxy) trimethylsilane
AIBN	2,2'-azobis(isobutyronitrile)
AM	acrylamide
APS	ammonium persulfate
C/W	CO_2-in-water
CNT	carbon nanotubes
CTAB	cetyltrimethylammonium bromide
DDBSS	dodecylbenzenesulfonic acid sodium salt
DMAEMA	dimethylaminoethyl methacrylate
DMTA	dynamic mechanical thermal analysis
DVB	divinylbenzene
DVS	dynamic vapour sorption
EHA	2-ethylhexyl acrylate
EHMA	2-ethylhexyl methacrylate
HDAM	1,6-hexanediol acrylate methacrylate
HDDA	6-hexanediol diacrylate
HIPE	high internal phase emulsion
HLB	hydrophilic-lipophilic balance
I-HIPE	inverse (reverse) high internal phase emulsion
KPS	potassium persulfate
LIPE	low internal phase emulsion
MA	methacrylic acid

MBA	N,N′-methylene bisacrylamide
MIPE	medium internal phase emulsion
MPS	methoxysilyl propylmethacrylate
o/w	oil-in-water
o/w/o	oil-in-water-in-oil
PEG	poly(ethylene glycol)
PEGDMA	poly(ethylene glycol) dimethacrylate
PolyHIPE	poly(high internal phase emulsion)
PolyMIPE	poly(medium internal phase emulsion)
PPF	poly(propylene fumarate)
PS	poly(styrene)
PVA	poly(vinyl alcohol)
PVC	poly(vinylchloride)
SCF	supercritical fluid
SDS	sodium dodecyl sulfate
SEM	scanning electron microscopy
THF	tetrahydrofuran
TKMES	tetrakis(methacryloxyethoxy) silane
w/o	water-in-oil
w/o/w	water-in-oil-in-water

Nomenclature

Symbol	Parameter	Units
a	Crack or notch length	mm
A	Cross sectional area of sample	m^2
c	Specimen length	mm
D	Displacement	mm
E	Tensile modulus,	Pa
f	Fraction	-
G	Shear modulus	Pa
G_{IIC}	Mode II critical strain energy release rate	J/m^2
K	Permeability coefficient	$m^2\ s^{-1}$
k	Viscous permeability	m^2
K_0	Knudsen permeability coefficient	m^2
K_{IC}	Critical mode I stress intensity factor	$MPa*m^{1/2}$
K_{II}	Stress intensity factor	$MPa*m^{1/2}$
K_{IIC}	Mode II critical stress intensity factor	$MPa*m^{1/2}$
L	Sample length	m
M	Molecular weight of gas	$g\ mol^{-1}$
P	Applied load	N
P	Porosity	%
p_0	Pressure at which Q is measured	Pa
p_1	Upstream pressure	Pa
p_2	Downstream pressure	Pa

p_m	Mean pressure	Pa
Q_2	Volumetric flow rate downstream of sample	$m^3 s^{-1}$
R	Gas constant	$J K^{-1} mol^{-1}$
T	Temperature	K
V	Volume	m^3
$Y_I(a/c)$	Mode I finite correction factor	-
$Y_{II}(a/c)$	Mode II finite correction factor	-
ρ_e	Foam density	gcm^{-3}
ρ_m	Skeleton density	gcm^{-3}
θ	Loading angle in Arcan jig	°
θ_c	Effective contact angle	°
σ	Stress	Nm^{-2}
τ	Shear stress	Nm^{-2}
μ	Fluid viscosity	Pa.s
ε	Strain	%

1 Introduction

1.1 Background

Highly porous polymers are attractive materials in a diverse range of applications, from structural materials to energy technologies. Although there are many different types of porous polymer foams, they are usually prepared by the gas blowing technique [1] and tend to possess irregular morphologies and closed cell structure. In recent years, a type of macroporous polymer, produced from high internal phase emulsions (HIPEs), so-called polyHIPEs, with open and well defined pore structures has gained increasing interest. PolyHIPEs are obtained by polymerising the continuous phase of these emulsion templates containing monomers, crosslinker and surfactant, followed by the removal of the dispersed or templating phase [2-4]. HIPEs are defined as emulsions whose internal phase occupies at least 74 % of the total volume of the emulsions which corresponds to the maximum packing fraction for identical spheres [5] and it was long suspected to be a key requirement to produce open porous polymers. However, recent research revealed that even the polymerisation of less concentrated emulsions produced macroporous polymers with an interconnected microstructure and low density, which means the definition of the HIPEs ratios, may be extended [6-9]. PolyHIPEs are famous for their unique permeable structure which contains both pore and pore throats. Pores are large cavities of micrometre dimensions and they are interconnected by a series of smaller pores referred to as pore throats (Figure 1-1). The pore throats form at the contact points of neighbouring droplets in the emulsion template and allow neighbouring

pores to communicate with each other. Therefore, they result in the permeability of polyHIPEs. It has been proven that polyHIPEs duplicate the structure of the HIPEs at the gel point of the polymerisation [10]. As a consequence of this characteristic, well defined polymer foams (polyHIPEs) can be obtained by tailoring the composition of HIPEs; such tailor-made polyHIPEs have the potential to be adopted for a large variety of applications varying from filter membranes [11], ion exchange resins [12] even to the scaffolds used in tissue engineering [13-15]. However, numerous potential applications of polyHIPEs could not be realized in industry because of the poor mechanical performance.

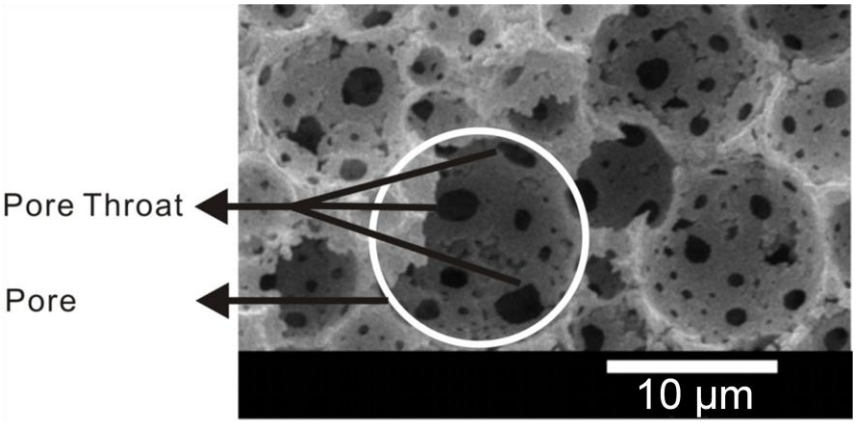

Figure 1-1 Definition of pore and pore throats of polyHIPEs

1.2 Motivation for the research

In order to explore the potential applications of polyHIPEs, many researchers [8, 9] aimed to improve the mechanical performance of conventional polyHIPEs without affecting the highly porous interconnected and permeable structure of the macroporous polymers. There are two different approaches reported in the literature. One is optimising the formulation of emulsion templates, such as changing monomers or introducing a reinforcement and the other is to polymerise less

concentrated emulsions resulting in macroporous polymers with increased foam density.

Furthermore, the full characterisation encompasses the determination of physical and mechanical properties of the polymerised macroporous polymers. However, there seems to be no reliable approach to investigate the mechanical performance, especially the shear properties and fracture toughness, of these macroporous polymers. In fact, the shear properties of these macroporous polymers is the key parameter determining many applications, i.e if they are to be used as core materials in sandwich composites or filter media, which have to resist flow through them. Fracture toughness is an indication of the amount of stress required to propagate a preexisting flaw and it is another most important parameter of any material.

In summary, the motivation of this project is to develop and fully evaluate open porous, permeable, interconnected macroporous polymers via emulsion templating technology.

1.3 Research objectives

The main objective in the work described in this thesis is to develop and characterise open porous polymer foams with improved mechanical properties via emulsion templating. Furthermore, the impact of the addition of fillers on the wetting properties of the macroporous polymers is to be explored. The overall research objectives are as follows:

1 Investigate the relationship between the components of emulsion templates and the morphological and physical properties of the resulting macroporous polymers

in order to optimise the formulation of emulsion templates without affecting the desired interconnected pore structure.

2 Synthesise low density, high porosity and permeable macroporous nanocomposites with significantly improved mechanical properties comparing to "standard" polyHIPEs via emulsion templating.

3 Explore a new approach to evaluate the tensile and shear properties of macroporous polymers and determine various mechanical parameters including tensile modulus, tensile strength, shear modulus, shear strength and fracture toughness of these macroporous polymers.

4 To investigate the effect of the emulsion formulation on the wetting behaviour of macroporous polymers.

1.4 Structure of the thesis

This thesis presents work on the development and characterisation of interconnected and tough macroporous polymer foams via emulsion templating. The whole thesis is divided in to eight chapters. Chapter 2 comprehensively reviews the relevant background literature based on the formulation and the influence factors in emulsion templates. The applications of macroporous polymers via emulsion templating and the approaches to tailor the mechanical properties of these macroporous polymers are discussed. In Chapter 3, the materials used and experimental processes, including sample preparation and characterisation procedures are presented. Chapter 4 presents the influence of using different surfactants for stabilisation of emulsion templates as well as different initiation methods, on the morphological and physical properties of resulting macroporous polymers. Chapter 5 describes a new type of tough, interconnected and low density open porous polymers developed via emulsion

templating and in Chapter 6 describes the adaptation of the Arcan test to determine the shear and tensile properties and fracture toughness of macroporous polymers. Chapter 7 discusses the impact of changing the emulsion formulation on the surface of macroporous polymers. Finally, Chapter 8 draws overall conclusions from the study and makes suggestions for future work.

2 Background and literature review of the emulsion templating technique

2.1 Fundamentals of high internal phase emulsions

Porous polymers can be used in extensive applications in daily life. In recent years, macroporous polymer produced from high internal phase emulsions (HIPEs) so-called polyHIPEs, with an organic continuous phase consisting of monomers, crosslinker and surfactant gained increasing interest due to their unique interconnected pore structure [16]. The following reviews some fundamentals of the emulsion templating technique.

2.1.1 Definition of high internal phase emulsions

Lissant [5] was the first to class HIPEs as emulsions containing an internal phase volume of 70 vol % or greater. Nowadays, HIPEs are generally defined as emulsions with internal phase occupying at least 74 % of the total volume of the emulsions [16, 17]. The ratio is the maximum packing fraction of uniform and undeformed droplets [17]. When the internal phase volume exceeds 74% of emulsions, the droplets have to be nonuniform in size or deformed to polyhedra [18]. Lissant stated the dispersed phase droplets should assume a rhomboidal dodecahedral (RDH) packing between 74% to 94% of internal phase volume while the packing changes to tetrakaidecahedral (TKDH) mode when the dispersed droplets volume exceeds 94%. (Figure 2-1). According to the definition of HIPEs, after polymerisation of the continuous phase of a HIPE and removal of the internal phase, the resulting

polyHIPEs exhibit an interconnected pore structure, low foam densities and very high porosities up to 95% [7].

Although the definition of HIPEs has existed for many years, the definition may extend to a wider range depending on recent research. Manley et al. reported that even the polymerised products of less concentrated low [6] or medium [7-9] internal phase emulsions (LIPEs or MIPEs), which have by definition internal phase volumes of less than 30 vol.% and between 30 vol.% and 70 vol.%, respectively [18], exhibit low densities and interconnected permeable structures, which are considered to be the most important characteristics of polyHIPEs.

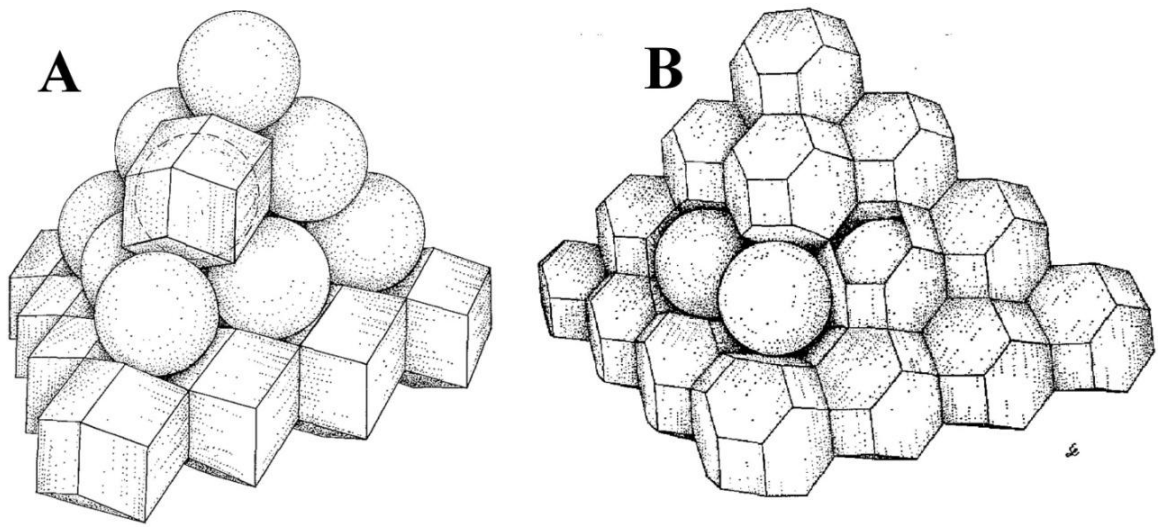

Figure 2-1 Droplet packing and ordering systems in HIPEs: A: Rhomboidal dodecahedral packing B: Tetrakaidecahedral packing [18]

As discussed before, the most unique feature of polyHIPEs is the interconnected microstructure which contains both pore and pore throats. It has been proven that polyHIPEs duplicate the structure of the HIPEs at the gel point of the polymerisation [13, 19]. As a consequence of this characteristic, the pore diameter of polyHIPEs can be tailored by adjusting the composition of HIPEs. Generally speaking, increasing emulsion stability accompanied by a lower interfacial tension, leads to smaller

droplets in emulsion templates [16, 20]. In other words, the polyHIPEs with large pore size can be obtained by lowering the emulsion stability, such as changing the concentration or type of surfactant [10], or adding specific solvents into the emulsion templates to promote Ostwald ripening, which describes the phenomenon that many small crystals form in a system slowly disappear to grow larger ones, which at the expense of the small crystals [20]. Therefore, the average pore diameter of polyHIPEs can vary from around 1 μm to more than 100 μm [16].

Pore throats appear at the contact points of neighbouring pores and make the whole polyHIPEs interconnected and permeable. The mechanism of pore throats formation is complex and conflicting views are expressed. Cameron et al. [21] suggested that pore throats are formed during the polymerisation process at the gel point of the polymerisation because of an internal shrinkage of the polymer matrix during conversion of monomers to polymer. However, more recent evidence suggests that the pore throats may initially be covered by thin polymer films [22]. It was hypothesised that the surfactant, which is insoluble in the aqueous internal phase, becomes increasingly insoluble in the growing polymer during the polymerisation of the continuous phase of the emulsion template. This leads to the formation of a surfactant rich third phase located in areas of close contact between neighbouring droplets. This surfactant rich-monomer poor phase forms a thin film, which ruptures during post-polymerisation purification or drying process.

2.1.2 Water-in-oil and oil-in-water emulsion template

Generally, high internal phase emulsions consist of an organic phase (oil phase) and another aqueous phase (water phase). Both the organic phase as well as aqueous phase can act as dispersed phases of emulsion templates. Usually, w/o (water phase

is dispersed in oil continuous phase) emulsions are defined as HIPEs whereas o/w (oil phase is dispersed in water continuous phase) emulsions are called inverse (or reverse) - HIPEs (I-HIPEs).

The first and most studied emulsion templates are those using styrene as monomer and divinylbenzene (DVB) as crosslinker [21, 23-28]. The HIPEs are commonly stabilised by surfactants with low hydrophilic-lipophilic balance (HLB value) between 2 and 6 [29], such as sorbitan monooleate (Span 80) [13, 21, 29-30]. However, most macroporous polymers form HIPEs which are hydrophobic and are impeded in some applications, such as tissue engineering since the hydrophobic polyHIPEs are considered not to be a very suitable environment for cell growth without surface modification.

In order to solve the problem, I-HIPEs are prepared to produce hydrophilic macroporous polymers directly. I-HIPEs consist of an aqueous continuous phase containing a hydrophilic monomer and a hydrophilic crosslinker, and an organic dispersed phase, such as toluene [32] or cyclohexane [33]. Comparing to HIPEs, the I-HIPEs are usually stabilised by surfactants with higher HLB value between 8.5 and 16.5, such as polyethylene glycol tert-octylphenyl ether (Triton X405) [33-38]. After polymerisation and complete removal of the dispersed phase, hydrophilic macroporous polymers are obtained. However, compared to conventional HIPEs, I-HIPEs are more difficult to stabilise [39] and furthermore, it is hard to remove and to dispose of the internal organic phase completely as well.

2.1.3 An example of manufacture process of polyHIPEs

There are two steps in the conventional batch processing of fabricating polyHIPEs. The first step is the formation of a stable HIPE template. The components of the continuous phase, which include monomer(s), crosslinker and surfactant(s), are mixed in a reaction vessel (Figure 2-2). The initiator, which is the trigger for the polymerisation, is dissolved in either the continuous organic phase or the aqueous phase depending on its solubility. After obtaining a homogeneous continuous organic phase, the aqueous phase, often containing salt(s), is gradually added to the reaction vessel. During the entire addition process, shear agitation is provided by the stirrer to increase homogeneity of emulsion templates. The final emulsion shows high viscosity and homogeneity.

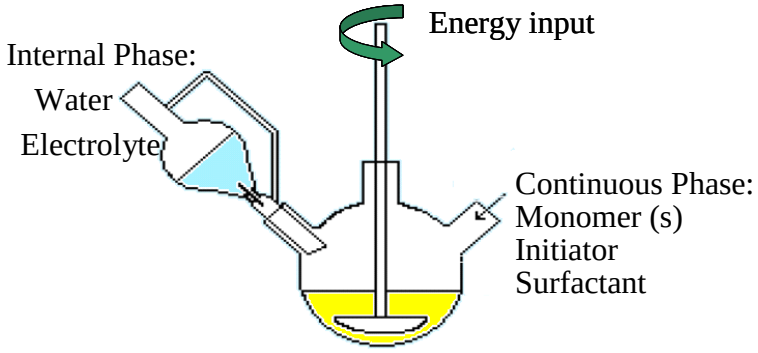

Figure 2-2 Schematic diagram for the preparation of emulsion templates

Afterwards, the viscous emulsion is transferred from the reaction vessel into a mould and polymerised at a specific temperature according to the initiator system used. After polymerisation, the polymer is removed from moulds and purified to remove residual surfactants or unreacted monomers. Finally, the purified polymer is dried to a constant weight.

2.2 Components of emulsion templates

Although several types of emulsions, including w/o emulsions, o/w emulsions and Pickering emulsions are used as templates for the production of macroporous polymers, the components of all emulsions are similar. In HIPEs systems, the continuous phase normally consists of monomers, which are polymerised to form the final macroporous polymers and emulsifiers, either surfactant(s) or particles, which are required to stabilise the emulsions. The discontinuous phase needs to be removed after the polymerisation. The polymerisation of monomers can be triggered by addition of initiators. Initiators can be dissolved in either the organic phase such as α,α'-azoisobutyronitrile (AIBN) [6-9,26] or the aqueous phase such as potassium persulfate (KPS) [40-43] depending on their solubility. The following sections list details and the influence factors of each component.

2.2.1 Monomers

The first and most studied emulsion templates used styrene and divinylbenzene (DVB) as co-monomers [23-28]. However, the resulting macroporous polymers are very brittle. In order to decrease the brittleness, various combinations of monomers such as 2-ethylhexyl acrylate (EHA) or 2-ethylhexyl methacrylate (EHMA) [40, 44-47] were used to synthesise polyHIPEs. However, the compression modulus and glass transition temperatures decreased with increasing EHA content in emulsion templates [45].

Changing the monomer in emulsion templates not only changes the mechanical performance but also modifies the surface characteristics, hydrophilic monomers such as acrylamide (AM) and N,N′-methylene bisacrylamide (MBA) [48, 49] and 2-

hydroxyethyl methacrylate [33] are introduced into the aqueous continuous phase and hydrophilic foams are manufactured by polymerising these I-HIPEs. Furthermore, even hydrophilic/hydrophobic superabsorbent polymer/polymer composite [50-55] can be developed. The continuous organic phase normally contains hydrophobic monomers, such as styrene and DVB, while the dispersed aqueous phase consists of hydrophilic monomers, such as MBA and AM. The emulsions are stabilised by an appropriate surfactant, such as Span 80 [51], sodium dodecylsulfate (SDS) [52]. Oil-soluble initiator, such as benzoyl peroxide [51] or AIBN [53-55] and water-soluble initiator, such as potassium persulfate (KPS) [53-55] can be used to initiate the polymerisation in the continuous phase and dispersed phase, respectively. Hydrophobic and hydrophilic monomers are simultaneously polymerised within the continuous phase and dispersed phase and a polymer/polymer composite is subsequently produced.

Various functional monomers are introduced to emulsion templates as components as well. The flame resistance of final macroporous polymers can be improved by the addition of chloroprene, dichloroprene, pentabromophenyl acrylate and 4-chlorostyrene into the organic continuous phase to copolymerise with styrene and DVB [56]. Biodegradable and/or compostable macroporous polymers are obtained by polymerising emulsion templates containing 2,3-dimethyl-1,3-butadiene and or isoprene as monomers and ethylene glycol dimethacrylate, trimethylolpropane dimethacrylate, 1,6-hexanediol diacrylate, 1,4-butanediol dimethacrylate, 2-butene-1,4-dioldimethacrylate or diethylene glycol dimethacrylate as crosslinkers in the organic continuous phase [57].

The polymerisation time of polyHIPEs can be reduced by using specific monomers. The use of a combination of especially reactive monomers such as 2-ethylhexyl acrylate (EHA), 6-hexanediol diacrylate (HDDA), 1,6-hexanediol acrylate methacrylate (HDAM) and 2-ethylhexylmethacrylate (EHMA) instead of conventional styrene and DVB reduces the polymerisation time and so less than 5 min are needed at polymersation temperatures [58].

All polymer foams produced from HIPEs discussed above are crosslinked. Uncrosslinked polyHIPEs can also be polymerised from HIPEs containing isobornyl acrylate and 2-ethylhexyl acrylate or only containing stearyl acrylate [59].

2.2.2 Emulsifiers

An emulsion is a mixture of two immiscible liquids. One liquid, the dispersed phase, is dispersed in the other, the continuous phase, in the form of droplets. The two immiscible phases of the emulsion templates can be stabilised either by surfactants or particles. There are three types of surfactants, non-ionic, anionic and cationic surfactants and the non-ionic surfactants are the most widely used surfactants. HIPEs are commonly stabilised by surfactants with low hydrophilic-lipophilic balance (HLB) value between 2 and 6 [29], whereas I-HIPEs are normally stabilised by surfactants with higher HLB value between 8.5 and 16.5, respectively [60, 61].

The most commonly used non-ionic surfactant to stabilise HIPEs is sorbitan monooleate (Span 80) with a HLB value of 4.3 [13, 16, 21, 43, 51, 62]. Similar to Span 80, some other sorbitan ester surfactants, such as sorbitan monolaureate (Span 20) [63, 64], sorbitan monopalmitate (Span 40) [65] and sorbitan trioleate (Span 85) [30, 66] have been used to stabilise HIPEs as well. However, Span 80 is not a good

candidate to stabilise less concentrated emulsions, such as MIPEs. In order to stabilise low or medium internal phase emulsions (LIPEs or MIPEs), which have by definition internal phase volumes of less than 30 vol.% and between 30 vol.% and 70 vol.%, respectively [18], Hypermer 2296 [6, 67-69] containing ethoxylated ester with a HLB value of 4.9 and Hypermer B246sf [6, 70] consisting of hydrophobic polyhydroxy fatty acid and hydrophilic polyethylene glycol blocks with a HLB value of 6.0 were used to stabilise such emulsion templates in the PaCE research group.

Besides the non-ionic surfactant discussed above, various other non-ionic surfactants were adopted to stabilise HIPEs, such as Hypermer 1070 [71, 72], polyoxyethylene sorbitan monooleate (Tween 80) [13, 16]. Furthermore, non-ionic surfactants were used to stabilise I-HIPEs as well, such as polyethylene glycol tert-octylphenyl ether (Triton X405) [33-38] and polyethylene glycol dodecyl ether (Brij 35) [73].

Though non-ionic surfactants are the most widely used surfactants, anionic and cationic surfactants have also been found to be useful to stabilise both HIPEs and I-HIPEs. The anionic surfactants, such as bis-tridecyl sulphosuccinic acid [64], sodium dodecyl sulphate [74] were used to stablise HIPEs while sodiumdodecyl sulphate [37] was adopted in I-HIPEs as a surfactant. The cationic surfactants, cetyltrimethylammonium bromide (CTAB) [75], distearyl dimethyl ammonium chloride and dioleyl dimethyl ammonium chloride [64] were also used to stabilise HIPEs.

The usage of a mixture of nonionic, anionic and cationic surfactants: sorbitan monolaureate (Span20), dodecylbenzenesulfonic acid sodium salt (DDBSS) and cetyltrimethylammonium bromide (CTAB) was also described in a previous patent

to stabilise HIPEs [76]. This mixture of surfactants is claimed to stabilise emulsions more effectively than Span 80 alone [76, 77].

The concentration of the surfactant in the continuous phase is important for the formation of stable HIPEs and the subsequent formation of open porous polyHIPEs. Williams et al. [10, 78] described the relationship between the morphology of macroporous polymers using styrene/DVB as monomers and the concentration of surfactant Span 80. HIPEs stabilised by 3-5% surfactant yield upon polymerization closed-cell macroporous polymers. However, small pore throats begin to develop as the surfactant level exceeds 7%. Subsequently, the pore throat sizes continue to increase with increasing surfactant concentration. However, if the surfactant concentration in the emulsion templates is larger than 80%, the resulting macroporous polymers are fragile; they easily disintegrate into a powder. Therefore, the optimal levels of surfactant in emulsion templates are between 20 wt.% and 50 wt.%.

Besides surfactant, colloidal particles, such as inorganic oxide particles [79-82] carbon nanotubes (CNT) [83, 84], microgel particles [85, 86] or bacterial celluloses [87] have also been used to stabilise HIPEs instead of surfactants and these emulsions are referred to as Pickering emulsions. Pickering emulsions are extremely stable due to the irreversible adsorption of particles at the interface between the continuous and dispersed phases which acts as a barrier to avoid droplets coalescence [88].

The wettability of particles is a key factor in the stabilisation mechanism. More hydrophobic particles preferentially stabilise HIPEs while more hydrophilic particles preferentially stabilise I-HIPEs. From previous research, several hydrophobic

particles, such as titania nanoparticles [79], surface modified silica particles [80], bacterial celluloses [87] have been reported to stabilise HIPEs while hydrophilic silica particles [82] and poly(N-isopropylamide)-co-(methacrylic acid) microgel particles [85] have been proved to effectively stabilise I-HIPEs.

Compared to conventional surfactants, using particles to stabilise emulsion templates has a number of advantages. Firstly, the required amount of particles to stabilise an emulsion is much smaller than that of surfactants, at least 5% [10, 78] of surfactant relative to the continuous phase is needed to stabilise HIPEs effectively while even 1 wt. % [79, 80, 89] of particles with respect to monomers can stabilise HIPEs or even MIPEs due to the extremely high capability to stabilise emulsions [90, 91]. Furthermore, the macroporous polymers produced from particle-stabilised HIPEs may lead to other benefits; for example, the pore walls of the final materials will be packed with a layer of particles which may contain functional groups and lead to a variety of further applications [84, 92]. For example, using titania nanoparticles (TNPs) to stabilise Pickering emulsion templates also introduce other benefits to the resulting nanocomposite foams including [93-96], for example, catalytic activity, UV-absorption or enhanced surface roughness which may lead to a variety of applications in the future.

2.2.3 Initiators

The polymerisation of monomers is triggered by initiators. There are three types of initiators including thermal initiators, redox initiators and photoinitiators. In addition, each type of initiator can be divided into water-soluble and oil soluble initiators depending on their solubility but most redox initiators are water-soluable.

Thermal initiators generally form free radicals by application of heat. The most commonly used water-soluble initiator in HIPEs is KPS [40-43]. Other water-soluble initiators used to initiate the polymerisation in emulsion templates include ammonium persulfate [97] and sodium persulphate [64]. The most commonly used oil-soluble initiator is AIBN [6-9, 26, 67, 68, 70, 80, 83]. Other oil soluble initiators used in emulsion templates are benzoyl peroxide, di-2-ethyl-hexyl-peroxydicarbonate [64], 1,1'-azobis(cyclohexanecarbonitrile) [98], lauroyl peroxide [99], 2,2'-azobis(2-methylbutyronitrile), 4,4'-azobis(4-cyanopentanoic acid) and 2,2'-azobis(N,N'-dimethyleneisobutyramidine) [59]. These initiators can only be used at elevated temperature to produce sufficient radical concentrations. For example, AIBN and KPS can usually be used in a temperature range between 50 ℃ and 100 ℃.

In order to initiate the polymerisation of monomers in emulsion templates at ambient temperatures, redox initiators can be adopted. Redox initiators usually consist of a pair: an oxidising agent and a reducing agent. Many redox initiator combinations are water-soluble. One typical example of redox initiator system used in emulsion templates is L-ascorbic acid and ferrous sulfate heptahydrate (reducing agent) and hydrogen peroxide (oxidising agent) [100,101]. Other redox initiator combinations used in emulsion templates include sodium hydrogen sulfite (reducing agent) and potassium persulfate (oxidising agent), sodium hydrogen sulfite (reducing agent) and sodium persulfate (oxidising agent) [100].

Photoinitiators rapidly and efficiently respond to light sources, such as UV light, and produce radicals or other species initiating the polymerisation. Normally, photoinitiators are oil soluble. Typical examples of photoinitiators used in emulsion templates include α-,α-dimethoxy-α-hydroxy acetophenone (DAROCUR 1173),

benzyl dimethyl ketal (IRGACURE 651), bis(2,4,6-trimethylbenzoyl)-phenylphosphineoxide (IRGACURE 819) [40,59] and benzil dimethyl ketal (ESACURE KB-1) [99].

The usage of an oil soluble initiator together with a water soluble initiator usually decreases the polymerisation time [102]. The oil soluble initiator t-butylperoxy-2-ethylhexanoate (Perbutyl 0) was used in combination with the water soluble KPS to trigger the polymerisation of HIPEs containing EHA and DVB and the polymerisation time of the emulsion can be reduced to less than 10 min.

2.2.4 Additives to the aqueous phase of emulsion templates

Salts are usually added into the aqueous phase of HIPEs as an additive in order to suppress Ostwald ripening by preventing monomers to dissolve in aqueous phase or vice versa. Generally, a water-soluble salt of alkali metals and alkaline earth metals such as calcium chloride, potassium sulphate, potassium chloride and magnesium sulphate are used as electrolytes in the aqueous phase of HIPEs [103, 104]. The addition of electrolytes enhances the stability of emulsions since the droplet size of emulsions was decreased and the resistance to droplets coalescence is increased [103].

The presence in the aqueous phase of small quantities of organic additives such as tetrahydrofuran (THF) and poly(ethylene glycol) (PEG) have been found to increase the average pore and pore throat diameters of macroporous polymers obtained. It is suggested that these additives enhance Ostwald ripening and decrease the emulsion stability [105].

2.3 Processing of producing macroporous polymers from emulsion templates

In addition to laboratory polyHIPEs batch production methods, there are several new processing protocols used to produce macroporous polymers from emulsion templates. The following describes the details.

2.3.1 Continuous process of synthesising polyHIPEs

Compared to laboratory batch process, the continuous polymerisation of HIPEs allows obtaining products in a relatively short time period and improves the economics by increasing production rate.

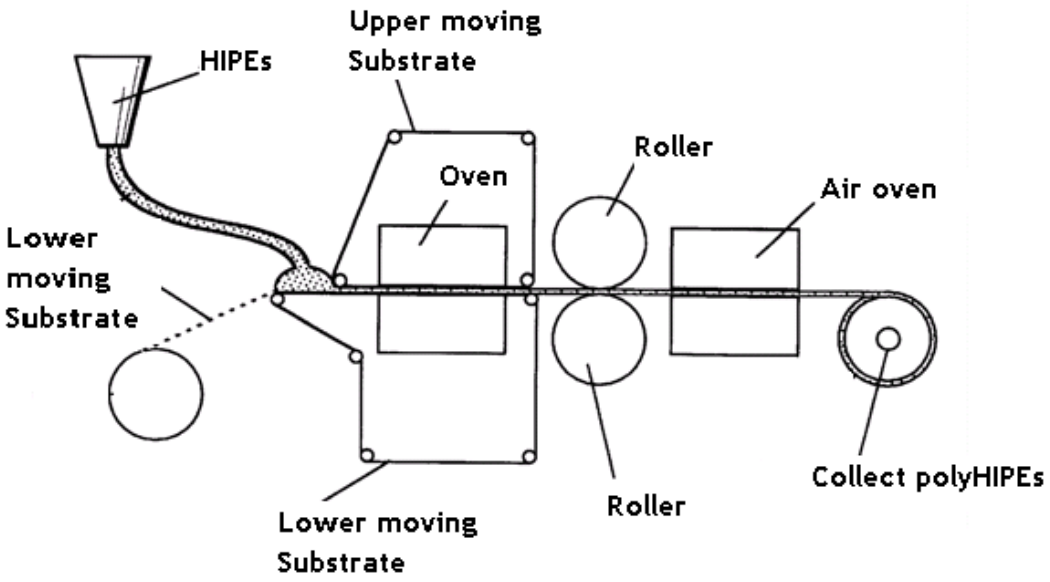

Figure 2-3 Schematic description of continuous processing of synthesising polyHIPEs [106]

Mork et al. [106] reported that polyHIPEs can be produced continuously by firstly mixing the continuous phase and internal phase in one vessel and forming a HIPE. The emulsion template is transferred by a delivery tube onto a lower moving support

substrate and then running the support through a heating zone for a time sufficient to polymerise at least 75% of the monomers in the HIPEs. Then, the polymerised macroporous foam is first passed through an aqueous and methanol bath to remove the remaining monomers and surfactants and then passed through an air oven to remove internal phase. The polyHIPEs were collected afterwards. Optionally, the polymerised macroporous foams can be squeezed to press out the internal water by passing through rollers. Furthermore, an upper moving substrate can be positioned at a fixed distance to produce macroporous polymer foams with desired a thickness (Figure 2-3).

2.3.2 Process of emulsion-templated microbeads

In order to use polyHIPEs in chromatography packings, polyHIPEs materials need to be reduced to particulate form by grinding. However, grinding results in particles with very irregular shape/sizes and causes wastage of original materials. Emulsion-templated macroporous polymers in the form of monodisperse beads were invented to circumvent this problem.

Emulsion-templated microbeads can be produced by sedimentation polymerisation, which was proposed by Ruckenstein et al. [107, 108]. In this process, individual HIPE droplets are partially polymerised during sedimentation through an immiscible sedimentation medium. Usually, w/o/w (water-in-oil-in-water) emulsions are used. This process includes two steps; the first step is combining an oil continuous phase, which consists of water-insoluble monomers, such as styrene and DVB, and surfactant, such as Span 80, with an aqueous internal phase to form a HIPE and then adding the HIPE template into another aqueous suspension medium to form a HIPE-in-water suspension system. The oil phase contained an oil-soluble initiator, such as

AIBN and both the aqueous internal phase and aqueous suspension medium included a water-soluble initiator, such as KPS. Once a stable suspension of HIPE microdroplets formed, the polymerisation was initiated by increasing the temperature of the aqueous suspension medium. In order to increase the sedimentation time, shear agitation was provided during the addition of the HIPEs into the aqueous suspension medium and during the entire polymerisation process. A further increase of sedimentation time was achieved by adding a gelling agent, such as acacia gum into the aqueous suspension medium [109]. The microbeads were left in the aqueous suspension medium at 60 ℃ overnight and purified with water and acetone to remove residual components.

Recently, oil-in-water-in-oil (o/w/o) emulsion based microbeads were developed by Zhang et. al [110]. Firstly, an oil-in-water I-HIPE was formed by slowly adding cyclohexane to an aqueous solution of monomers while stirring. Acrylamide (AM) and N,N′-methylenebisacrylamide (MBA) were chosen as monomers because of their rapid polymerisation ability under sedimentation polymerisation conditions [107, 108]. Water-soluble ammonium persulfate (APS) was used as the initiator and sodium dodecyl sulfate, (SDS) plus poly(vinyl alcohol) (PVA) were used as surfactant to form a stable I-HIPE. Then, the I-HIPE was injected into a glass column containing a heated mineral oil sedimentation medium. The droplets sank slowly through the sedimentation medium and were collected at the bottom of the glass column. After sedimentation, the beads were left in the heated sedimentation column for an additional 3 h to complete the polymerisation. Finally, the beads were purified with hexane and acetone.

2.3.3 Supercritical fluid treated I-HIPEs

I-HIPEs as templates to synthesise macroporous polymers are uneconomic since the procedure is extremely solvent intensive. Usually, large amounts of oil or organic solvent are required for the internal phase (>75 vol.%), which brings about the disadvantage of high levels of organic waste. Furthermore, the solvent used as the internal phase may be very difficult to remove completely. A possible solution to this problem is templating supercritical CO_2-in-water (C/W) emulsions [49,111-113]. The general procedure for C/W emulsions templating is shown in Figure 2-4. CO_2 with the pressure = 100-300 bar is introduced into emulsion templates to replace a part or the entire internal organic phase to form $scCO_2$–in-water emulsions. The aqueous phase contained AM and MBA as monomers and perfluoropolyether (PFPE) ammonium carboxylate with low molecular weight (Mw = 567 g /mol) was used as surfactant [111, 113]. The C/W emulsion templates were polymerised at 60 ℃, 250–290 bar, 12 h [113]. After polymerisation, the removal of carbon dioxide is easy since carbon dioxide reverts to the gaseous state upon depressurisation.

Compared to conventional organic solvent used as the internal phase in I-HIPEs, supercritical carbon dioxide ($scCO_2$) is a sustainable solvent because it is nontoxic, non-flammable and naturally abundant [114-116]. However, the supercritical fluid (SCF) technique involves either a foaming mechanism, gelation of the SCF medium or a combination of both. Therefore, only limited macroporous polymers can be accessed via this route since many materials cannot be foamed or derived from CO_2-soluble precursors [111]

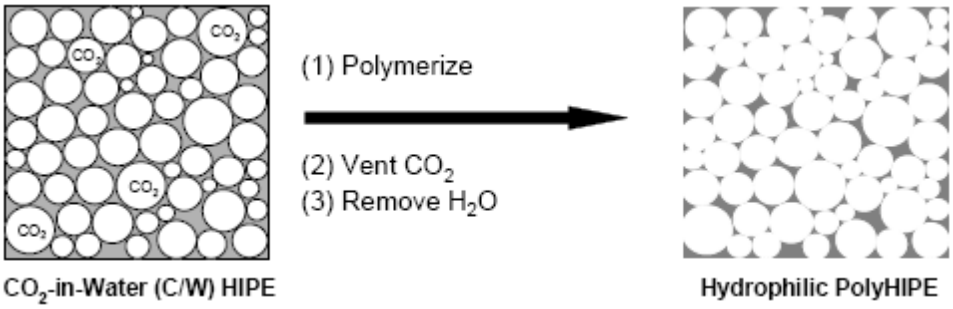

Figure 2-4 Preparation of a macroporous polymer via supercritical emulsion templating. External phase is an aqueous solution containing monomers, internal phase is $scCO_2$ [111]

2.4 Applications of macroporous polymers made from emulsion templates

Because of their unique interconnected pore structure, emulsion templated macroporous polymers have been explored for several applications including filter membranes [11], ion exchange resins [12], ultraporous polymer supports for organic synsthesis [117], chromatographic supports [118] and even scaffolds for tissue engineering [13-15]. Besides monolithic polyHIPEs, other forms of macroporous polymers made from emulsion templates such as microbeads and films have been explored. However, there are no real industrial applications of polyHIPEs due to their poor mechanical properties. The following summarises the applications of emulsion templated macroporous polymers.

2.4.1 Applications of polyHIPEs

a) As separation media

PolyHIPEs have the potential to be used as filter materials because of their unique interconnected pore structure. The open porous structure allows fluids to pass

through while particles, which are larger than the pore throats, are trapped. Therefore, polyHIPEs can be adopted as ion-exchange media for the separation of biological materials and the removal of salts, metals or acids from aqueous solutions.

Compared to conventional separation membranes, the size and number of pores and pore throats of resulting polyHIPEs can be refined by optimising the formulation of the emulsion template and the manufacturing procedure. In addition, if the porous polymer contains a polyelectrolyte [119], the polyelectrolyte acts as a diffusion barrier to control the speed at which charged species are transported through the porous foams to an underlying adsorbent material because of charge interactions, hydrophobic interactions and steric hindrance.

b) As absorbent materials

Macroporous polymer foams produced from emulsion templates, especially hydrophilic/hydrophilic porous foams [50] are a type of superabsorbent material. Since the organic continuous phase contains water-insoluble monomers and the aqueous internal phase includes water-soluble monomers, the resulting macroporous polymer showed a capability to acquire and distribute rapidly both aqueous and organic fluids. Therefore, it can be used as a superabsorbent material for fluid acquisition/distribution applications. For example, these polymer foams can be employed as environmental waste oil sorbents; absorbent cores of disposable nappies and many other applications. Furthermore, the type of absorbent materials shows both relatively high capillary absorption pressures and capacity-per-weight properties, which allow them to acquire fluid with or without the aid of gravity. As a consequence, this type of absorbent material is particularly useful as the upper component in a “multi-layer" absorbent system.

c) As scaffold in tissue engineering

PolyHIPEs is a potential candidate for tissue engineering scaffolds due to their high porosity. The high porosity and interconnected pore structure of these macroporous polymers allow reactants and metabolic waste to pass in and out and a higher through-put rate can be achieved comparing to conventional scaffolds [120]. Furthermore, polyHIPEs are considered as scaffold materials for growth of multiple cells [98]. They can provide multi zones where selected cell types are confined to the specific regions of the polyHIPE while other cell types grow throughout the other regions. Depending on various types of cells to be grown, the pore diameter has to be adjusted over a wide range from 0.5 to 100 μm.

PolyHIPE scaffolds based polystyrene (PS) [121], poly(propylene fumarate) (PPF) [15] and polyurethane [122] have been studied as scaffolds for tissue engineering. However, these polymers are hydrophobic, which are considered not to be a very suitable environment for cell growth. With the aim to improve the biocompatibility of these macroporous polymers, I-HIPEs were prepared. Barbetta et al. [32, 123, 124] have extended the application of inverse polyHIPEs as scaffolds in tissue engineering by using derivatised polysaccharide and gelatine as the polymer.

2.4.2 Applications of emulsion-templated microbeads

Compared to conventional polyHIPEs monolith, emulsion-templated microbead is a better candidate in a variety of chromatographic techniques due to its spherical particulate forms [109, 110]. The emulsion-templated microbeads can be used as a substrate in ion-exchange chromatography. They can be employed as either cation-

exchange resin or anion-exchange resin by providing acidic groups or basic groups on the microbeads surface, respectively.

Emulsion-templated microbeads have the potential to be adopted in cell culturing [109]. The microbeads protect the cell from external disturbance and can be used in conventional bioreactors. Furthermore, the w/o/w emulsion-templated microbeads can be modified by sulphonation to increase the hydrophility of the microbeads and the cell attachment to the polymers is improved.

2.5 Approaches to improve and determine the mechanical properties of macroporous polymers

2.5.1 Approaches to improve the mechanical properties of macroporous polymers

Most conventional polyHIPEs are produced from emulsion templates using styrene and DVB as co-monomers and the resulting macroporous polymers are very brittle and chalky. In order to improve the mechanical performance of the resulting macroporous polymers, various combinations of monomers such as 2-ethylhexyl acrylate (EHA) or 2-ethylhexyl methacrylate [40,44] or monomers based on silicon [125], such as tetrakis(methacryloxyethoxy) silane (TKMES) or 2-(acryloxyethoxy) trimethylsilane (AETMS) have been used to synthesise polyHIPEs. The chalkiness and brittleness of polyHIPEs based on styrene and DVB can be reduced by using 2-ethylhexyl acrylate (EHA) as a co-monomer in the emulsion templates, however the glass transition temperature decreases with increasing EHA content in the continuous phase [40, 44-47]. Alternative routes such as the step-growth reaction of

diisocyanate with poly(ε-caprolactone) have also been explored [122]. Such polyHIPEs have however Young's modului well below 10 MPa [46, 122].

Silane coupling agents have been used for several decades to improve the adhesion between polymer matrices and reinforcing glass fibres [126]. The interfacial shear strengths of resulting glass/resin composites were improved [13, 127]. For optimum composite performance 0.1 to 0.25% of a silane coupling agent is deposited onto glass fibres [128]. Polysiloxanes have attracted attention because of their outstanding heat and fire resistance but their brittleness has prevented any utilisation of their potential [129]. Tai et al. [130] successfully synthesised polyHIPEs which combined an inorganic polysiloxane network with an organic polystyrene network to improve both mechanical properties at elevated temperatures and the thermal stability of the macroporous polymers [129]. The organic-inorganic hybrid macroporous polymers were prepared by copolymerising methoxysilyl propylmethacrylate (MPS) radically with styrene and DVB. In order to enhance the mechanical performance at room temperature, Menner et al. [8, 9] successfully developed low density but tough macroporous polymers via emulsion templating. Poly(ethylene glycol) dimethacrylate (PEGDMA) was used as a crosslinker [8] to reduce brittleness instead of DVB and copolymerised with MPS and styrene. A further improvement of the mechanical performance was obtained by the incorporation of silica particles into the polymer network [8, 9]. However, the produced macroporous polymers did not possess an open porous network structure. Furthermore, approximately 20 μm thick walls with a porous microstructure surrounded the pores (Figure 2-5). The formation of methanol during the polycondensation of MPS and the reaction with the surface of silica particles caused the emulsion template to destabilise rapidly (Scheme 2-1).

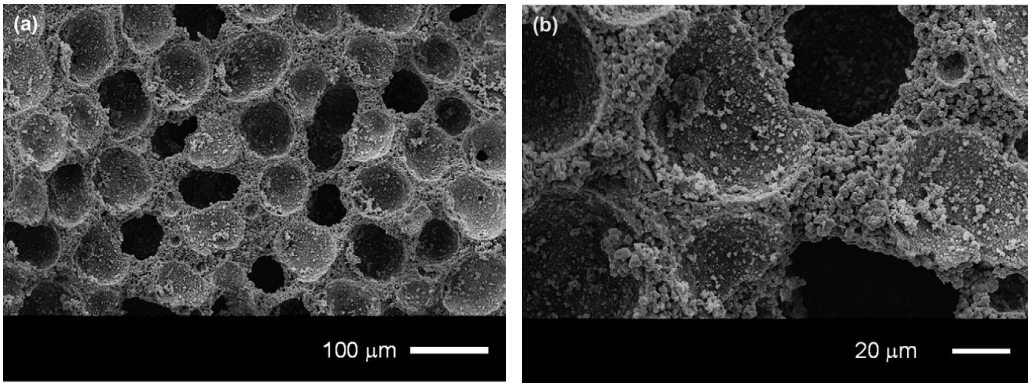

Figure 2-5 SEM images of the macroporous polymer containing 30 wt.-% of silica particles in emulsion template [70]

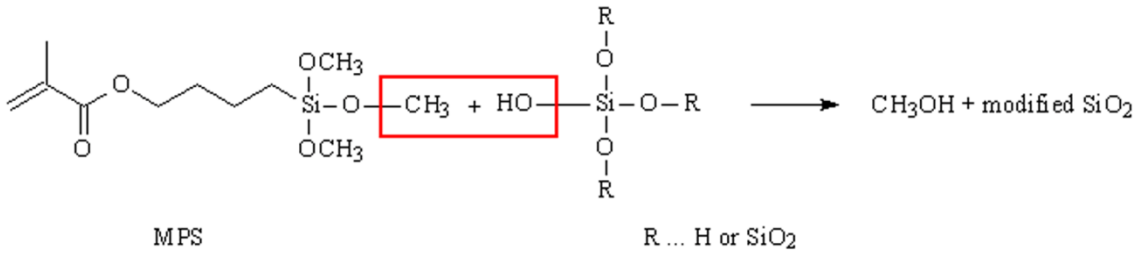

Scheme 2-1 Schematic illustration of the reaction involved in grafting particles

Subsequently, various open celled and tough macroporous polymer nanocomposites have been produced using carbon nanotubes, titania nanorods [68] and clay [131] as reinforcement for the pore walls. Recently, functionalised silica particles [70] were incorporated into the polymer, which resulted in a significant improvement in the mechanical properties of polyHIPEs without affecting the interconnected and permeable pore structures.

A further increase in the mechanical properties of macroporous polymer nanocomposites can be achieved by increasing the continuous phase volume of the emulsion templates to 75 vol.% in order to increase the foam density [6-8, 70, 132]. The polymerised products of less concentrated medium internal phase emulsions (MIPE, 60 vol.% of internal phase) was proven to exhibit low densities and highly interconnected structures, which are considered to be the most important characteristics of polyHIPEs but have much improved mechanical properties.

2.5.2 Approaches to determine the mechanical performance of macroporous polymers

There are two methods to determine the mechanical properties of polyHIPEs reported in the literature. The first is using dynamic mechanical thermal analysis (DMTA) to investigate the dynamic mechanical properties of polyHIPEs as a function of temperature [133-136]. The second is determining the elastic moduli of macroporous polymers under compressive force at ambient temperatures [7, 8, 70, 137] according to British Standard BS ISO 844 [138]. The specimen should be either of square or circular shape and loaded between compression plates until the test specimen thickness is reduced to at least 85 % of the original thickness. The elastic modulus obtained is termed compression modulus, which is defined as the initial linear slope of the stress–strain plot in the compression test.

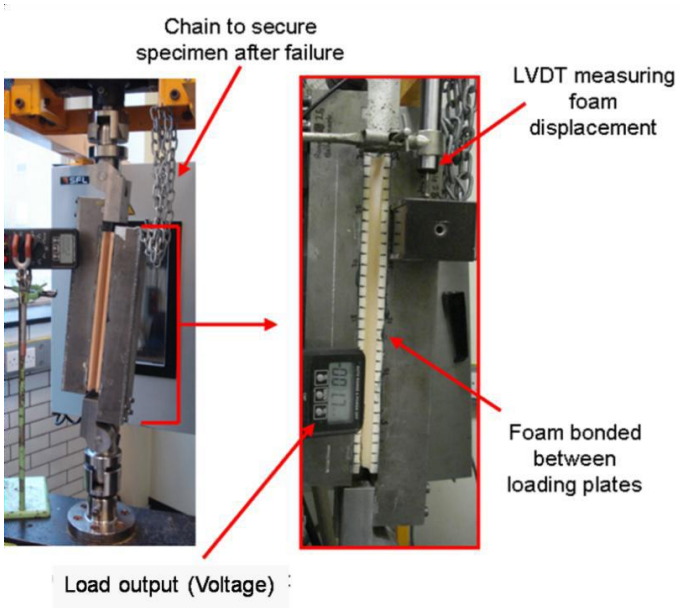

Figure 2-6 Specimen bonded between two steel plates and loaded in the test fixture [141]

The brittleness and chalkiness of conventional polyHIPEs is an expression of the poor shear properties of these macroporous polymers. However, there is no reliable

method to investigate the shear properties of these open porous polymers until now. Rogers et.al. [139-141] investigated the shear behaviour of polyvinylchloride (PVC) foam (Divinycell® H200) following the ASTM standard C-273 [142]. The specimen was firstly bonded between the loading plates. Then, the loading plates and bonded specimen were attached to the test machine fixtures via a simple tongue and groove joint, and secured (Figure 2-6). During testing a linear variable displacement transducer (LVDT) was used to measure the vertical specimen deflection, by measuring the difference in displacement along the length of the loading plates. Shear modulus and fracture toughness can be calculated afterwards. However, PVC foams are very rigid closed cell compared to polyHIPEs. Therefore, the method cannot be used to investigate the shear properties of polyHIPEs since the polyHIPEs crushed during the procedures of bonding the specimen to the steel loading plates or attaching the bonded specimen and loading plates to the test machine.

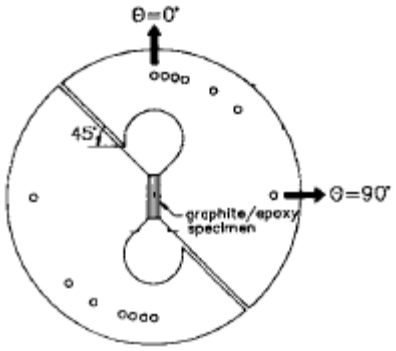

Figure 2-7 Arcan test jig and specimen geometry [145]

Another approach to investigate the fracture mechanics of graphite/epoxy composites [143-146] is using a test jig developed by Arcan et.al. [147] with the objective of producing a uniform biaxial stress condition in the test area (Figure 2-7). Pure shear is produced in the test region when the jig is loaded in the direction $\theta = 0°$ while the specimen is loaded in tension when load is applied in the direction of $\theta =$

90 °. The specimen was bonded to the fixture and secured in place by screws to separate Arcan plates which were connected to the test instrument. The load angle was selected by fastening the two adjacent holes in each Arcan plate to the test machine. Besides the shear and tensile moduli (strength), the fracture toughness can be evaluated experimentally by the introduction of a suitably shaped specimen containing a crack or notch. The fracture toughness can be calculated from shear and tensile properties obtained from the tests as follows [145]:

$$K_{IC} = \sigma \sin\theta \sqrt{\pi a}\, Y_I\,(a/c)$$

$$K_{IIC} = \tau \cos\theta \sqrt{\pi a}\, Y_{II}\,(a/c)$$

where K_{IC} is fracture toughness under tensile mode, K_{IIC} fracture toughness under shear mode, σ tensile stress at fracture, θ loading angle, a crack or notch length, c specimen length, $Y_I\,(a/c)$ a finite correction factor under tensile mode, τ the shear stress at fracture, $Y_{II}\,(a/c)$ a finite correction factor under shear mode

The Arcan test provides the potential to measure the mechanical properties of polyHIPEs since the very heavy steel loading plates are not needed during the specimen preparation process and both the shear and tensile properties of polyHIPEs can be evaluated using the method.

2.6 Summary

In recent years, macroporous polymers, so-called polyHIPEs, produced from high internal phase emulsions (HIPEs) with an organic continuous phase consisting of monomers, cross-linker and surfactant have gained increasing interest. The most attractive feature of polyHIPEs is their interconnected pore structure containing both

pore and pore throats. Furthermore, the pore structure of final macroporous polymer foams can be tailored by modifying the emulsion template formulation. Even microbeads plus polymer composites can be synthesised via emulsion templating. Although polyHIPEs show potential in various applications, real industrial applications are limited because most of conventional polyHIPEs are very brittle and chalky, which is an expression of the poor shear properties of these macroporous polymers. Unfortunately, there has been no literature discussed the investigation of the shear properties of these macroporous polymers until now.

The current research is aimed at solving the problem. The formula of emulsion templates will be optimised and reinforcements will be introduced into the organic phase of the emulsion templates. In addition, a new approach for the mechanical characterisation of resulting macroporous polymers will be explored.

3 Experimental and Instrumentation

3.1 Materials

Styrene, divinylbenzene (DVB), α,α'-azoisobutyronitrile (AIBN), potassium persulfate (KPS), iron (II) sulfate heptahydrate, L-ascorbic acid, hydrogen peroxide (27.5 % w/w solution in water), Sorbitan monooleate (Span80), dimethylaminoethyl methacrylate (DMAEMA), methacrylic acid (MA) and calcium chloride dehydrate ($CaCl_2 \cdot 2H_2O$) were purchased from Sigma-Aldrich (Gillingham, UK). Trimethoxysilyl propylmethacrylate (MPS) was purchased from Acros (Geel, Belgium) and poly(ethylene glycol) dimethacrylate (PEGDMA) with a molecular weight of 330 g/mol was kindly supplied by Cognis (Southampton, UK). The silica particles (200 nm average diameter) were kindly provided by Ortwin Rave Produkte and Dienstleistungen (Koblenz, Germany) and the surfactants Hypermer 2296 and Hypermer B246sf by Croda (East Yorkshire, UK). Oxygen free nitrogen was purchased from BOC Edwards Ltd. (Guildford, UK). Araldite® Precision Adhesive and epoxy adhesive Araldite® 2020, Araldite® 420A/B were purchased from RS components Ltd. (Corby, UK). Styrene and DVB were purified by passing them through a Buchner funnel containing layered basic and neutral aluminium oxide (Sigma-Aldrich, Gillingham, UK) while all other chemicals were used as received.

3.2 Modification and characterisation of silica particles

3.2.1 Silylation of SiO_2 particles

1 g "as received" silica particles were suspended in 5 ml MPS and 5 ml distilled water and stirred for 12 h. The silylated silica particles were isolated by centrifugation and decantation of excess MPS and water. Afterwards, the silylated silica particles were re-dispersed in methanol using an ultrasonic nozzle followed by centrifugation and decantation to remove any remaining unreacted MPS. The purification step was repeated at least three times in order to remove all unreacted MPS. Afterwards, the silylated particles were dried under vacuum at 70 ℃ for 24h.

3.2.2 Characterisation of the silylated particles

Thermo Gravimetric Analysis (TGA): The MPS loading of the surface of the silica particles was determined by TGA (TA Q500, TA Instrument, New Castle, Delaware, USA) in air. The weight loss of approx. 10 mg of silylated silica particles was recorded over a temperature range from 40 ℃ to 600 ℃ at a heating rate of 10 ℃/min.

3.3 Preparation of emulsion templates

3.3.1 Preparation of emulsions in the investigation of effect of emulsion formulation on the pore structure of polyMIPEs

All emulsion templates contained 44 vol.% of the continuous phase, which consisted of 85 vol.% monomers and 15 vol.% surfactant. The aqueous phase of all emulsion templates contained 0.035 mol/L $CaCl_2 \cdot 2H_2O$. When Hypermer B246sf was used to stabilise the emulsion, the surfactant was dissolved in styrene using a magnetic stirrer before adding DVB and surfactant mixture into the reaction vessel.

Both AIBN and KPS, which need to be operated higher than 50 ℃, were used as initiator and the concentration of these two types of initiators was 1 mol % with respect to the monomers. The initiator KPS was added into the aqueous phase and dissolved with $CaCl_2 \cdot 2H_2O$ while AIBN was added to the organic phase. All components of the organic phase were transferred to reaction vessel and stirred with an anchor stirrer, which was connected to an overhead stirrer (IKA RW20 DIGITAL, Fisher Scientific, Leicestershire, UK). After 5 min of stirring, the aqueous phase was added dropwise into the reaction vessel using a dripping funnel. During the entire addition phase of organic phase, the stirring speed of was kept constant at 400 rpm. After complete addition of the aqueous phase, the stirring speed was increased to 2000 rpm for another 5 min to obtain homogeneous emulsions.

In order to trigger the polymerisation of emulsion templates at ambient temperatures, a redox initiator system which consisted of ascorbic acid (0.33 g, 1.87 mmol) and iron (II) sulfate heptahydrate (0.065 g, 0.23 mmol) was used. The initiator system was dissolved in the aqueous phase together with $CaCl_2 \cdot 2H_2O$. The organic phase components were transferred to the reaction vessel and stirred using an anchor stirrer. After 5 min of stirring, the aqueous phase was dropwise added into the reaction vessel using a dripping funnel. During the entire addition phase, the stirring speed was kept constant at 400 rpm. After complete addition of the aqueous phase, the stirring was continued for 5 min to obtain homogeneous emulsions. Afterwards, hydrogen peroxide (1.64g, 13.28mmol) was added to these emulsion templates. Then, the stirring speed was increased to 1000 rpm for a further 5 min to guarantee a homogeneous distribution of the hydrogen peroxide within the emulsions. The formulation of all emulsion templates will be summarised in Chapter 4.

3.3.2 Preparation of emulsions used for the preparation of tough interconnected macroporous polymers

The continuous phase of all emulsion templates consisted of styrene (40 vol.%) and PEGDMA (40 vol.%) as monomers, 20 vol.% surfactant Hypermer B246sf and 1 mol% initiator AIBN with respect to the monomers. Both the HIPEs containing 80 vol.% of internal phase and MIPEs consisting of 60 vol.% of internal phase were prepared. Furthermore, various amount of silylated silica particles ranging from 0 to 60 wt.% silylated with respect to the monomers were added to the continuous phase of these emulsions. The aqueous phase of all emulsion templates contained 0.56 mol/L $CaCl_2 \cdot 2H_2O$.

Since Hypermer B246sf can only be dissolved in styrene, the surfactant, styrene and the initiator were first mixed until all components were dissolved using a magnetic stirrer. PEGDMA and MPS silylated silica particles were mixed separately using a high speed homogenizer (Polytron PT 1600E, Kinematica Inc., Lucerne, Switzerland) operating at 15000 rpm for 15 min to obtain a homogeneous suspension of the filler. Then, these homogeneous mixtures were transferred to the reaction vessel and stirred using an anchor stirrer, which was connected to an overhead stirrer. After 5 min of stirring, the aqueous phase was added dropwise to the reaction vessel using a dripping funnel. During the entire addition phase, the stirring speed was kept constant at 400 rpm. After complete addition of the aqueous phase, the stirring speed was increased to 1000 rpm for 30 s to obtain homogeneous but very viscous emulsions. The composition of all emulsions will be summarised in Chapter 5.

3.3.3 Preparation of emulsions used to prepare tough interconnected macroporous polymers to study their shear and tensile properties

Both the MIPEs containing 60 vol.% internal phase and HIPEs containing of 80 vol.% internal phase were prepared for the investigation of the shear and tensile properties of tough interconnected macroporous polymers. The preparation of emulsion templates was identical to 3.3.2. However, only up to 20 wt.% silylated silica particles with respect to the monomers were introduced into the continuous phase of these emulsions and these emulsion templates were transferred to specially made polytetrafluoroethylene (PTFE) mould. The composition of all emulsion templates will be summarised in Chapter 6.

3.3.4 Preparation of emulsions used to prepare macroporous polymers to investigate their wetting properties

Both MIPEs containing 60 vol.% of internal phase and HIPEs containing 80 vol.% of internal phase were prepared. They were all mixed in a glass reaction vessel using an anchor stirring rod, which was connected to an overhead stirrer, at 400 rpm. The continuous phase of all emulsions consisted of 80 vol.% of monomers (styrene and DVB), 20 vol.% of the surfactant Hypermer 2296 and 2 mol% of the initiator AIBN with respect to monomers. Furthermore, one MIPE contained 40 wt.% silylated silica particles with respect to the monomers while the other MIPE did not contain any silylated silica particles. The aqueous phase of all emulsion templates which contained 0.035 mol / L $CaCl_2 \cdot 2H_2O$ was gradually added to the organic phase using a dripping funnel. Besides the electrolyte, 6 vol.% of DMAEMA or 6 vol. % of MA were added to the aqueous phase of HIPEs as additional monomers. In order to avoid portioning of these monomers from the aqueous phase to the organic phase, a

suitable pH value of the aqueous phase was chosen to form the corresponding monomer salts either pH 1 or pH 11 respectively. The aqueous phase was added dropwise into the reaction vessel using a dripping funnel after mixing the organic phase. The stirring speed was kept constant at 400 rpm. Once all components were added, the stirring speed was increased to 2000 rpm for 10 min to obtain homogeneous but very viscous emulsions. The composition of all emulsion templates will be summarised in Chapter 7.

3.4 Preparation of macroporous polymers

3.4.1 Preparation of macroporous polymers using AIBN and KPS as initiator

The ready-made emulsion templates were transferred into free standing polypropylene (PP) centrifuge Falcon® tubes and sealed. The filled Falcon® tubes were placed in an oven and polymerised at 70 ℃ for 24 h. The polymerised samples were removed from the tubes and purified with distilled water for 24 h, followed by methanol for 24 h using a Soxhlet apparatus. These purified macroporous polymer monoliths were dried to constant weight under vacuum at 70 ℃.

3.4.2 Preparation of macroporous polymers using redox initiator

The ready-made emulsion templates were transferred into free standing centrifuge Falcon® tubes and sealed. The filled Falcon® tubes were polymerised at room temperature for one week. The polymerised samples were removed from the tubes and purified with distilled water for 24 h, followed by methanol for 24 h using a Soxhlet apparatus. These purified macroporous polymer monoliths were dried to constant weight under vacuum at 70 ℃.

3.4.3 Preparation of macroporous polymers used for the characterisation of shear and tensile properties

The ready-made emulsion templates were transferred into a PTFE rectangular mould with the following dimensions: length, 300 mm; width, 75 mm; thickness, 25 mm. The filled PTFE mould was sealed securely with screws and placed into an oven and polymerised at 70 ℃ for 24h. The polymerised samples were removed from the PTFE mould and purified with distilled water for 24 h, followed by methanol for 24 h. These purified macroporous polymer monoliths were dried to constant weight under vacuum at 70 ℃.

3.5 Characterisation of physical properties of macroporous polymers

3.5.1 Morphology

Scanning electron microscopy (SEM): To investigate the internal structure of the macroporous polymers images of hand-fractured surfaces of each macroporous polymer were taken using a scanning electron microscope (Jeol JSM 5610 LV, Jeol Ltd., Welwyn Garden City, UK). Prior to the observation, approximately 1 cm^3 of each macroporous polymer was placed on a sample holder using a carbon sticker and sputtered with gold for 2 min in an argon atmosphere using a Scan coat six (Edwards Ltd., Crawley, UK) to guarantee sufficient electrical conductivity.

3.5.2 Determination of the density and porosity

The matrix or skeleton density ρ_m of the resulting macroporous polymers was determined using Helium Pycnometry (Accupyc 1330, Micrometrics Ltd, Dunstable,

UK). The foam or envelope density ρ_e as well as the porosity of the macroporous polymers were obtained using an envelope density analyzer (Geopyc 1360, Micrometrics Ltd, Dunstable, UK). The porosity *P* was calculated using the following equation:

$$P = (1 - \frac{\rho_e}{\rho_m}) \bullet 100\%$$

3.5.3 Surface area measurement

The surface area of polyHIPEs and polyMIPEs was determined using a Surface Area and Porosity Analyzer (Tristar, Micrometrics Ltd, Dunstable, UK) applying the Brunauer-Emmet-Teller (BET) model [68]. The polymer foams were subjected to a "degassing" step prior to the measurement. Small cubic samples of about 1 cm^3 in volume were placed inside a glass cell and heated under vacuum at 100 ℃ overnight. Afterwards, the nitrogen adsorption isotherms were measured at -196.15 ℃.

3.5.4 Thermal properties measurement

Differential scanning calorimetry (DSC): The glass transition temperature (T_g) was investigated using DSC (DSC Q2000, TA Instrument, New Castle, Delaware, USA). Approximately 5 mg of each macroporous polymer was investigated in a temperature range from 25 to 250 ℃ at a rate of 10 ℃/min. The heat flow was measured and two heating and cooling curves were recorded.

3.5.5 Determination of permeability

A homebuilt pressure rise apparatus (Figure 3-1) designed by Manley et.al. [6, 132] was used to measure the gas permeability of the macroporous polymers. Briefly, the gas flow through porous media can be described as follows:

$$K = \frac{Q_2 p_2 L}{\Delta p A} = \frac{V\left(dp_2/dt\right)L}{p_1 A} = \frac{k}{\mu} p_m + \frac{4}{3} K_0 \sqrt{\frac{8RT}{\pi M}}$$

where K is the permeability coefficient, Q_2 the volumetric flowrate at the outlet, p_2 the pressure on the outlet side of the sample, L the sample length, A the cross-sectional sample area and Δp the pressure difference across the sample. V is the known volume of the vessel used to collect the gas that permeats through the sample $\frac{dp_2}{dt}$ the rate of pressure-rise, p_1 the pressure on the inlet high pressure side of the sample, k the viscous permeability, μ the gas viscosity and p_m the mean pressure, being defined as the average of the pressure on the inlet high pressure side of the sample p_1 and the pressure on the outlet low pressure side of the sample p_2. Since the pressure on the outlet side of the sample was kept low using a vacuum pump, the mean pressure is $p_m = p_1 /2$. K_0 is the Knudsen permeability coefficient, R the gas constant, T the temperature, M the molar mass of gas. The rate of pressure-rise $\frac{dp_2}{dt}$ is measured experimentally at set p_1, so the viscous permeability k can be determined from the gradient of a linear plot of K as a function of p_m.

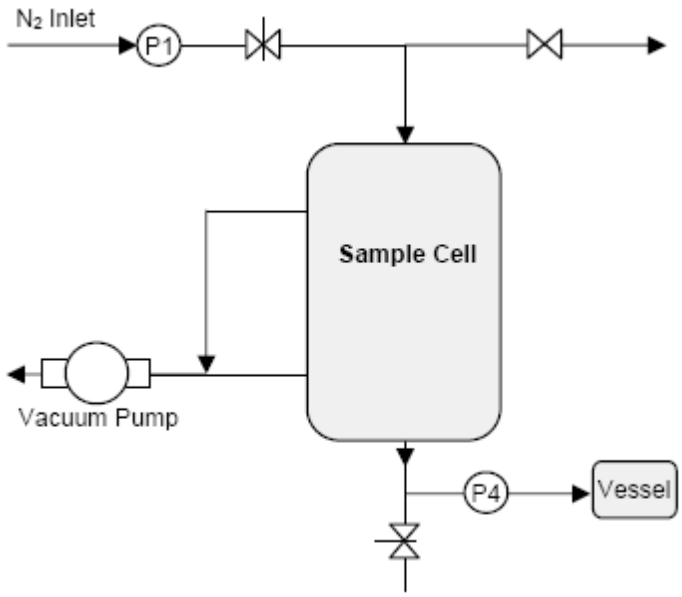

Figure 3-1 Schematic of the gas pressure rise apparatus [132]

Oxygen free nitrogen was used for this measurement. The gas pressure at one side of the macroporous polymer was maintained at a constant higher pressure while the other side of the sample was kept at a low pressure using a vacuum pump. Gas permeated from the high pressure to the low pressure side and was then collected in a vessel with known volume. The rate of pressure rise at the low pressure side was recorded to determine the viscous permeability of the samples. In order to avoid any cross flow around the sample, samples were set into an epoxy resin prior to being placed into the sample cell. The porous cores were initially coated with non-permeable Araldite® Precision Adhesive and left to cure at room temperature. The coated cores were then inserted into the mould cylinder and the two–component epoxy adhesive Araldite® 2020 was poured into the mould cylinder around the coated cores and left at room temperature for 24 h to cure. Afterwards, two samples, which were 25 mm in height and 31 mm in diameter, were cut from the same coated macroporous polymer monolith (Figure 3-2). Two pieces of each sample were measured from both directions. The samples were rotated and re-measured;

therefore, four independent measurements were obtained for each sample at each inlet pressure. Five different inlet pressures were chosen for each sample.

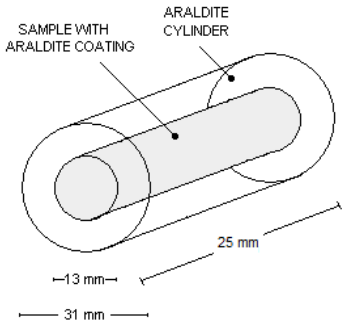

Figure 3-2 Dimensions of coated sample used in gas permeability test [132]

3.6 Characterisation of the mechanical performance of macroporous polymers

3.6.1. Determination of the compression modulus of macroporous polymers

Compression tests were performed according to British Standard BS ISO 844:2001 using a universal Lloyds machine (Lloyds EZ50, Lloyds Instruments Ltd, Fareham, UK) equipped with a 50 kN load cell to investigate the mechanical properties of macroporous polymers. Before testing any macroporous polymers, compliance, which means the two loading plates compress each other without sample, was performed. At least five samples, which were 10 mm in height and 26 mm in diameter, were cut from the same macroporous polymer monolith using a band saw (Titan SF8R, Screwfix, Somerset, UK) and polished using sand paper in order to ensure the top and bottom surfaces flat and parallel. The height of samples at three different points was measured by digital calliper. The difference in height of the

sample was less than 0.3mm and the average value of height was used to calculate the strain of the sample. Samples were loaded between compression plates at a speed of 1 mm/min until a displacement of half the original sample height was reached and the load vs displacement was recorded. The compression modulus is defined as the initial linear slope of the stress–strain plot and the crush strength is the maximum value of the stress–strain curve at the end of the initial linear region (Figure 3-3).

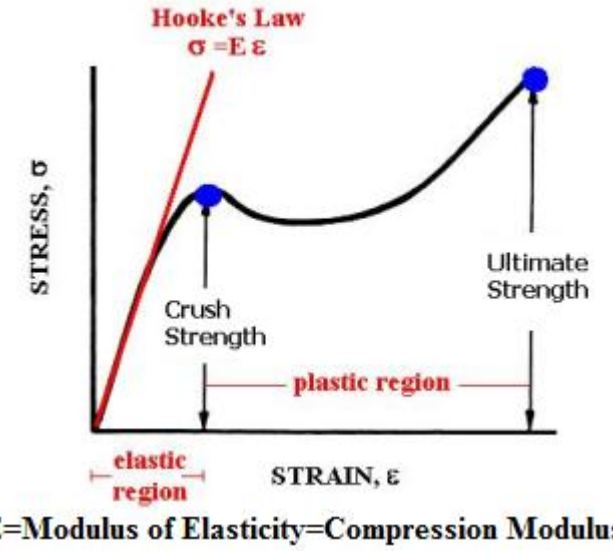

Figure 3-3 Illustration of compression modulus and crush strength [148]

3.6.2 Determination of shear and tensile properties of macroporous polymers using the Arcan test

3.6.2.1 Compliance of the displacement of specimens

During the test of the shear and tensile properties of macroporous polymers, the displacement the machine detected is the sum of both specimen displacement and test instrument displacement. In order to measure the true displacement of specimen, the compliance of the test system had to be determined before the shear and tensile tests of the actual specimens. An aluminium block which was manufactured using

same material as Arcan jig was treated as specimen to calculate the displacement caused by the test instrument (Figure 3-4 (a)). The whole block was secured into the Arcan jig and tested following the same procedure as actual tests.

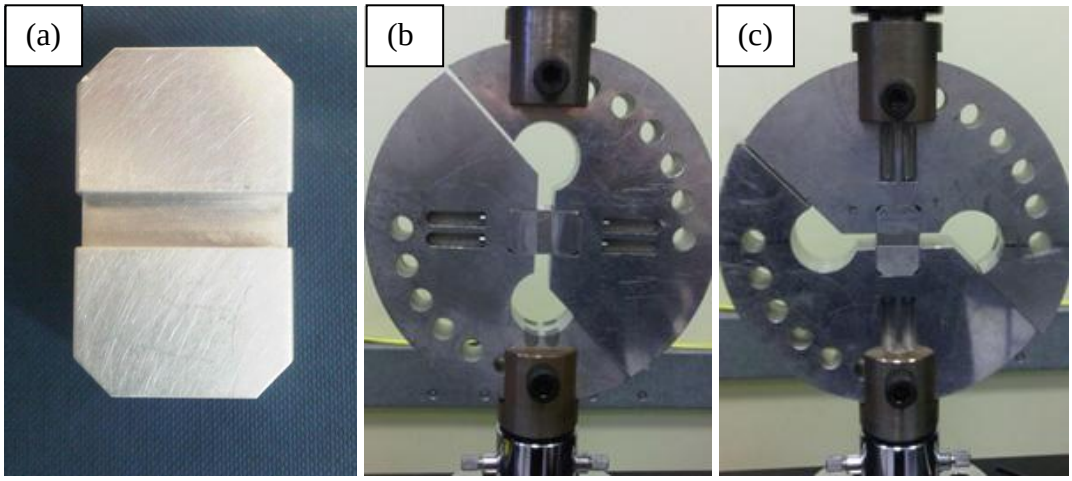

Figure 3-4 Aluminium specimen and setup of the Arcan jig for the Compliance test
(a) Aluminium specimen
(b) Arcan jig setup with compliance specimen under shear mode testing
(c) Arcan jig setup with compliance specimen under tensile mode testing

The load angle was selected by fastening the two holes in the test fixture, which correspond to the desired load angle, to the test machine. Both shear (Figure 3-4 (b)) and tensile (Figure 3-4 (c)) modes were selected. The compliance measurement was performed using a universal Instron machine (Instron 4502, Instron Instruments Ltd, Bucks, UK) equipped with a 1 kN load cell and loaded at a crosshead speed of 0.1 mm/min until the load achieved 900N. When a successful test was completed, the test machine returned to its initial position and the compliance specimen was released. The test procedure was repeated at least five times. The load and displacement were recorded. Shear (tensile) modulus is defined as the initial linear slope of the stress–strain plot.

$$G\ (E) = \frac{\sigma}{\varepsilon} = \frac{P}{A} \times \frac{L}{D}$$

where G is shear modulus, E tensile modulus, σ stress, ε strain, P the applied load, A the cross-sectional area of the specimen, L the length of sample, D the displacement.

The shear modulus of aluminium is 26 GPa and the tensile modulus of aluminium is 72 GPa. The load is recorded and the cross-sectional area and length of specimen are known. Therefore, the displacement of aluminium specimen can be calculated. The total displacement which was recorded by the machine minus the displacement caused by aluminium specimen is the displacement caused by Arcan jig.

3.6.2.2. Determination of shear and tensile properties of macroporous polymers

The shear and tensile properties of macroporous polymers were determined using the Arcan test jig. The fixture was connected to a universal Instron machine (Instron 4502, Instron Instruments Ltd, Bucks, UK) equipped with a 1 kN load cell. A minimum of five specimens with the following dimensions: length = 25mm; width = 8mm; thickness =12mm were cut from the same macroporous polymer monolith using a band saw (Titan SF8R, Screwfix, Somerset, UK). The specimens were polished using sand paper and checked by digital calliper in order to ensure the top and bottom surfaces flat and parallel. Once the specimens were manufactured, they were bonded to the insert aluminium fixtures using Araldite® 420A/B and cured at room temperature for at least 24 hours (Figure 3-5 (a)). To obtain an adequate bond between the foam and the insert aluminium fixtures, it was essential to increase the surface roughness of the insert aluminium fixtures by sand blasting the surface of each fixture with 150 grit (Fox 50 Blasting Machine, Vixen surface treatment Ltd., Stockton on Tees, UK). Afterwards, a thin layer of viscous adhesive was applied to

the specimen and the insert aluminium fixtures. The specimen was sandwiched between the insert aluminium fixtures and aligned to ensure the specimen was fully contacted with aluminium fixtures, then a 2 kg weight steel plate was placed on top to apply an even pressure along the bonding faces.

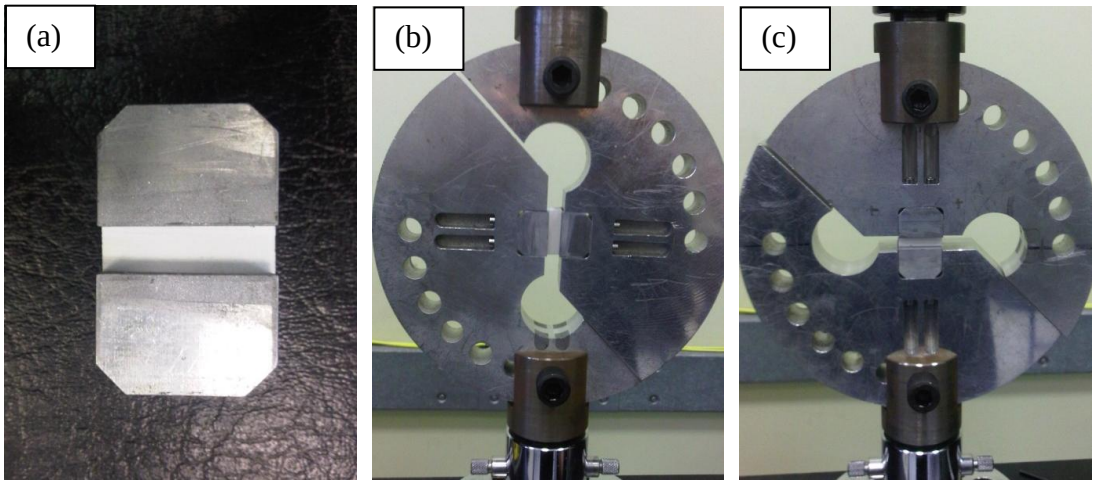

Figure 3-5 Actual specimen and setup of the Arcan jig for shear and tensile properties measurements of poly(M)HIPEs
(a) Actual specimen bonded to insert aluminium fixtures (b) Arcan jig system setup with actual specimen under shear mode testing (c) Arcan jig system setup with actual specimen under tensile mode testing

Afterwards the two insert aluminium fixtures holding the macroporous polymer specimen were secured to the Arcan jig by attaching them with alignment screws, which were connected to the Instron machine (Figure 3-5 (b) and (c)). Specimens were loaded at a crosshead speed of 0.1 mm/min until complete failure. When a successful test was completed, the fractured specimen was removed together with the insert aluminium fixtures and the lower frame of the test machine returned to its initial position. The insert aluminium fixtures were refinished and reused after removal of the fractured macroporous polymer.

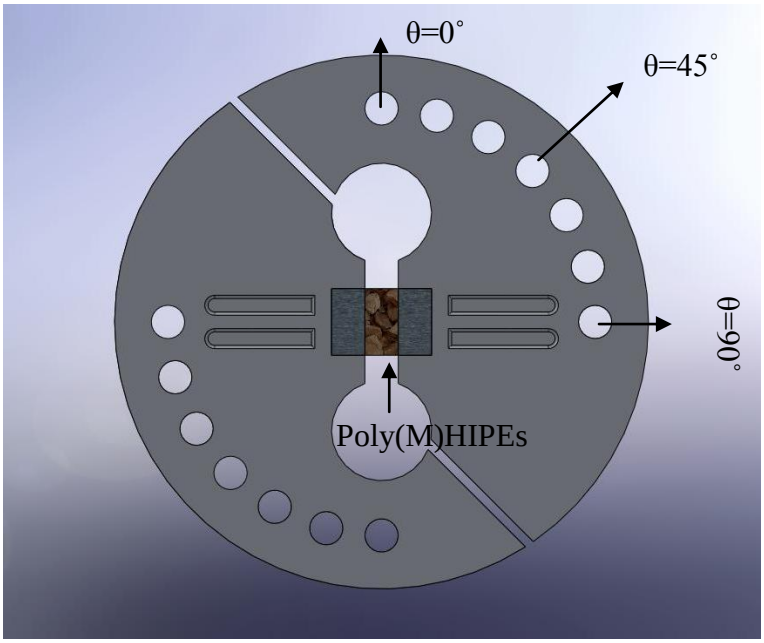

Figure 3-6 Arcan test fixture and specimen geometry

As seen in Figure 3-6, pure shear is produced in the test region when load is applied in the direction $\theta = 0°$, which was already proven by photoelastic methods for isotropic materials [143, 147]. Similarly, the specimen is loaded in equal tension when load in the direction of $\theta = 90°$. Arcan et. al. [147] showed that if the stresses acting on a specimen are uniform, then the tensile and shear stresses are:

$$\sigma = \frac{P}{A} \sin\theta \qquad (1)$$

$$\tau = \frac{P}{A} \cos\theta \qquad (2)$$

where P is the applied load, θ the loading angle and A the cross-sectional area of specimen

The shear (tensile) modulus is defined as the initial linear slope of the stress–strain plot and the shear (tensile) strength is the maximum value of the stress–strain curve at the end of the initial linear region. The real displacement of polyM(H)IPEs specimen which used to calculate strain was corrected by using the total

displacement which was recorded by the machine minus the displacement caused by the Arcan jig.

3.6.2.3. Determination of fracture toughness of macroporous polymers

Furthermore, the Arcan test method was further adapted to the study of interlaminar fracture behaviour of composite materials [143, 144, 146, 149]. The fracture toughness is characterised by stress-intensity factors or the energy release rates at fracture of the specimen [146]. The fracture toughness measurements of macroporous polymers in this project were performed using the Arcan test using a universal Instron machine (Instron 4502, Instron Instruments Ltd, Bucks, UK) equipped with a 1 kN load cell.

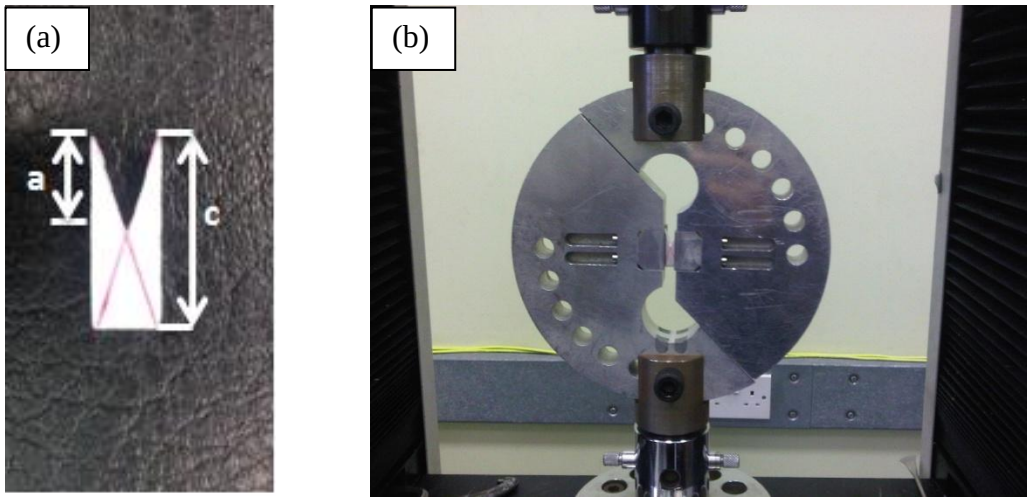

Figure 3-7 Specimen and setup of the Arcan jig for fracture toughness measurement of poly(M)HIPEs
(a) Specimen (b) Arcan jig setup for shear mode fracture toughness testing

The specimens used in the determination of fracture toughness of macroporous were cut from the same macroporous polymer monolith using a band saw with the same dimension as the specimens used in the study of shear and tensile properties of these macroporous polymers. To evaluate the fracture toughness of materials experimentally, cracks or notches are normally introduced into the specimen

[143,146, 150, 151]. Therefore, a V-notch (Figure 3-7 (a)) with the notch length of half specimen length (a/c = 0.5) was cut using a Continuous Loop Diamond Wire Saw (Murg 394, Well Diamond Wire Saws Incorporated, Norcross GA, USA). The tip of V-notch was the crosspoint of two diagonals and is the centre of specimen. A minimum of five specimens were needed. Once the test specimens were manufactured, they were bonded to insert aluminium fixtures using Araldite 420A/B. After the adhesive was cured, the insert aluminium fixtures were secured to Arcan fixtures by screws (Figure 3-7 (b)). Specimens were loaded at a crosshead speed of 0.1 mm/min until complete failure. The experimental procedure was same as shear and tensile properties measurements.

A parameter called the stress-intensity factor (K) is used to determine the fracture toughness of most materials and a Roman numeral subscript indicates the mode of fracture. The fracture toughness in this project was assessed by determining the stress intensity factor (K_{II}) at fracture under shear mode. The critical mode II stress intensity factor (K_{IIC}), which is defined as K_{II} at fracture under 0 ° loading angle using Arcan jig, can be expressed as [143, 145, 146, 152,153]:

$$K_{IIC} = \tau \cos\theta \sqrt{\pi a}\, Y_{II}\,(a/c)$$

where τ is the shear stress at fracture, θ loading angle. $Y_{II}\,(a/c)$ a finite correction factor under shear mode, c specimen length, a V-notch length

The finite correction factor (Y_{II}) is calculated as follows [146]:

$$Y_{II}\,(a/c) = -0.81550 + 12.39517(a/c) - 32.82199\,(a/c)^2 + 39.26487(a/c)^3 - 16.24160\,(a/c)^4$$

This equation can be used for fracture specimens with a crack (notch) length $0.3 \leq a/c \leq 0.7$ and the a / c ratio is 0.5 in this case.

3.7 Investigation of wetting behaviour of macroporous polymers

3.7.1. Contact angle

The water contact angle of macroporous polymer was measured using the Krüss DSA 10 Mk2 Drop Shape Analysis System (Krüss Optronic, Hamburg, Germany) using the sessile drop method. Water drops (about 2 mm diameter) were placed onto the surface of each specimen at room temperature. The static contact angle was measured, 10 s after placing the water droplet onto the surface. The average angle values were determined from five measurements taken at the middle of samples of macroporous polymers.

3.7.2. Dynamic vapour sorption (DVS)

The water vapour uptake was measured using a Dynamic Vapour Sorption apparatus (DVS Advantage, Surface Measurement Systems Ltd., London, UK). The apparatus consists of a microbalance housed inside a temperature-controlled cabinet. DVS provides extremely accurate gravimetric data in conjunction with a control of relative humidity (RH). All experiments were performed at 25 ℃. Approximately, 40 mg of vacuum oven dried macroporous polymer was weighed onto the flat sample pan. Each sample was firstly conditioned at 0% RH using dry nitrogen for 60 min until dried completely. Then, dry nitrogen was bubbled through water to give 95% RH for 24h. The weight of macroporous polymers was recorded as function of time.

4 Investigation of the effect of the emulsion formulation on the pore structure of polyMIPEs based on styrene and DVB

4.1 Introduction

The first and most studied emulsion templates contain styrene and divinylbenzene (DVB) as co-monomers [23-28]. HIPEs are commonly stabilised by non-ionic surfactants with low hydrophilic-lipophilic balance (HLB value) between 2 and 6 [29], such as Span 80 [13, 16, 21, 43, 51, 62], Hypermer B246sf [6, 70] and Hypermer 2296 [6, 67-69]. The concentration of the surfactant in the continuous phase is important for the formation of stable HIPEs and the subsequent formation of open porous polyHIPEs [22]. Williams et al. [10, 78] described the relationship between the morphology of macroporous polymers using styrene/DVB as monomers and the surfactant Span 80 concentration. HIPEs stabilised by 3-5% surfactant yield upon polymerisation closed-cell macroporous polymers. However, small pore throats begin to develop as the surfactant level exceeds 7%. Subsequently, the pore throat sizes continue to increase with increasing surfactant concentration. However, if the surfactant concentration in the emulsion templates is larger than 80%, the resulting macroporous polymers are fragile; they easily disintegrate into a powder. Therefore, the optimal levels of surfactant in emulsion templates are between 20 wt.% and 50 wt.%. The polymerisation of monomers is triggered by initiators. Initiators can be dissolved in either the organic continuous phase or the aqueous internal phase

depending on their solubility. The most commonly used initiators include the oil-soluble initiator α,α'-azoisobutyronitrile (AIBN) [6-9, 26, 67, 68, 70, 80, 83] and the water-soluble initiator potassium persulfate (KPS) [40-43]. However, these initiators are usually employed in a specific temperature range, in which the decomposition rate is high and, therefore, the half-life time is short enough to produce a sufficient amount of radicals. The initiator decomposition rate increases with increasing temperature; e.g. AIBN has a half-life time of 92 h at 50 ℃, 23 h at 60 ℃ and 6 h at 70 ℃ while KPS has a half-life time of 202 h at 50 ℃, 60 h at 60 ℃ and 8 h at 70 ℃ [154]. Therefore, AIBN and KPS are usually used higher than 50 ℃. However, redox initiator systems such as iron (II) sulfate heptahydrate, L-ascorbic acid (reducing agent) and hydrogen peroxide (oxidising agent) can be adopted even at ambient temperature [100,101]. In order to enhance the stability of the emulsions by suppressing Ostwald ripening, electrolytes, such as $CaCl_2$, are added to aqueous phase of HIPEs [16, 17].

HIPEs are generally defined as emulsions whose internal phases occupy at least 74 % of the total volume of the emulsion [29] and the monolithic polymers, which are the result of the polymerisation of the continuous phase, are called polyHIPEs. However, even the polymerised products of less concentrated low [6] or medium [7, 8, 70] internal phase emulsions (LIPEs or MIPEs) also exhibit a low density and interconnected permeable structures, which are considered as the most important characteristics of polyHIPEs from recent research. LIPEs or MIPEs have by definition internal phase volumes of less than 30 vol.% and between 30 vol.% and 70 vol.%, respectively [18]. PolyHIPEs possess many unique properties such as a low density and interconnected pore structure. Pores are large cavities of micrometre dimensions produced by the removal of the water template, which are interconnected

by a series of small interconnects called pore throats. Pore throats are formed in the areas of contact points between neighbouring droplets in the emulsion template and allow neighbouring pores to communicate with each other [21, 22]. Due to the attractive interconnected microstructure, polyHIPEs have the potential to be adopted in variety of applications. However, real industrial applications are limited due to poor mechanical properties of polyHIPEs.

In the present research, MIPEs rather than HIPEs were used in order to increase the organic phase volume of the emulsion templates and subsequently to raise the foam density (reduce the porosity) of the resulting polymer, which lead to improved mechanical performance. The influence caused by surfactant and initiator in the emulsion templates on the morphological and physical properties of resulting macroporous polymers were investigated.

4.2 Summary of sample formulations

Three types of initiators and various surfactants and surfactant mixtures were adopted in emulsion templates. After polymerisation of these emulsions, the macroporous polymers **1**-**12** were produced. The sample preparation procedure was presented in Chapter 3.3 and 3.4. The compositions of all emulsion templates are summarised in Table 4-1.

Table 4-1 Composition of the emulsion templates

Sample ID	Organic phase volume [a]	Organic phase composition Styrene/DVB /Surf. (vol.%) [b]	Surfactant	Surfactant Amount (vol.%) [c]	Initiator	Initiator Amount (g / mmol)
1	44	76 / 9 /15	Hypermer 2296	15	AIBN	0.20 / 1.22
2	44	76 / 9 /15	Span 80	15	AIBN	0.20 / 1.22
3	44	76 / 9 /15	Hypermer 2296	7.5	AIBN	0.20 / 1.22
			Span 80	7.5		
4	44	76 / 9 /15	Hypermer 2296	7.5	AIBN	0.20 / 1.22
			Hypermer B246sf	7.5		
5	44	76 / 9 /15	Hypermer 2296	15	Potassium persulfate	0.33 / 1.22
6	44	76 / 9 /15	Span 80	15	Potassium persulfate	0.33 / 1.22
7	44	76 / 9 /15	Hypermer 2296	7.5	Potassium persulfate	0.33 / 1.22
			Span 80	7.5		
8	44	76 / 9 /15	Hypermer 2296	7.5	Potassium persulfate	0.33 / 1.22
			Hypermer B246sf	7.5		
9	44	76 / 9 /15	Hypermer 2296	15	Ascorbic acid	0.33 / 1.87
					Iron (II) sulfate	0.065 / 0.23
					Hydrogen peroxide	1.64 / 13.28
10	44	76 / 9 /15	Span 80	15	Ascorbic acid	0.33 / 1.87
					Iron (II) sulfate	0.065 / 0.23
					Hydrogen peroxide	1.64 / 13.28
11	44	76 / 9 /15	Hypermer 2296	7.5	Ascorbic acid	0.33 / 1.87
			Span 80	7.5	Iron (II) sulfate	0.065 / 0.23
					Hydrogen peroxide	1.64 / 13.28
12	44	76 / 9 /15	Hypermer 2296	7.5	Ascorbic acid	0.33 / 1.87
			Hypermer B246sf	7.5	Iron (II) sulfate	0.065 / 0.23
					Hydrogen peroxide	1.64 / 13.28

[a] Volume of the organic phase relative to the total volume of the emulsion

[b] Content of styrene, DVB and surfactant relative to the organic phase volume

[c] Content of various surfactants relative to the organic phase volume

4.3 Results and Discussion

As discussed above, the various potential applications of polyHIPEs are limited due to their poor mechanical performance. The continuous phase volume of the emulsion templates was increased by using MIPEs instead of HIPEs in order to produce macroporous polymers with a high foam density which results in improved mechanical properties of the resulting monoliths [70]. All emulsion templates had 44 vol.% of continuous phase, which contained styrene as monomer, DVB as crosslinker and a surfactant. 20 wt.% of surfactant relative to the continuous phase was employed to produce highly interconnected macroporous polymers.

The samples were divided into three groups based on different initiators used in the emulsion templates. Firstly, the oil soluble initiator AIBN was chosen since it is commonly used in the PaCE research group [6-9, 26, 67, 68, 70, 80, 83]. Secondly, the water soluble initiator KPS was used since it the preferred initiator of other researchers to produce polyHIPEs [40-43]. However, these two initiators can only decay at elevated temperatures to produce a sufficient radical concentration. In order to initiate the polymerisation at ambient temperatures (e.g. 20 ℃), a redox initiator system consisting of iron (II) sulfate heptahydrate, L-ascorbic acid and hydrogen peroxide was added into the aqueous emulsion phase to initiate the polymerisation [100,101, 155].

In addition, four types of surfactants including individual surfactant and surfactant mixtures were introduced in the three groups of emulsion templates. The first candidate was the non-ionic, polymeric surfactant Hypermer 2296 with a hydrophilic-lipophilic balance (HLB value) of 4.9. Hypermer 2296 is an ethoxylated

ester and is used in oilfield applications and by other industries. Moreover, it is commonly used to stabilise HIPEs and MIPEs in the PaCE research group [6, 67-69]. Another noticeable surfactant which is widely used by many other researchers to stabilise HIPEs is a non-ionic, surfactant sorbitan monooleate (Span 80) with a HLB value of 4.3 [13, 16, 21, 43, 51, 62]. Due to the outstanding performance in the stabilisation of low concentrated emulsions (LIPEs or MIPEs) [6, 70], Hypermer B246sf was also considered. Hypermer B246sf is a polymeric, non-ionic surfactant consisting of hydrophobic polyhydroxy fatty acid and hydrophilic polyethylene glycol blocks with a HLB value of 6.0. However, since the resulting macroporous polymers are predominately closed cell if solely Hypermer B246sf is used to stabilise the emulsion template it is advisable to use it in a surfactant mixture [6]. Therefore, a mixture of Hypermer 2296 and Hypermer B246sf was employed to stabilise emulsion templates. The two widely used surfactants Hypermer 2296 and Span 80 were mixed to form a mixture to stabilise emulsions as well. Table 4-1 summarises the composition of the MIPEs and Table 4-2 lists the properties of all resulting polyMIPEs.

The absence of a glass transition in the temperature range of 25-250 ℃ may be due to the high degree of crosslinking of the final macroporous polymers. For MIPEs **1-4** AIBN was used as initiator. Therefore, the emulsions were polymerised at 70 ℃. Various surfactants were used to stabilise the emulsion templates. MIPE **1** and MIPE **2** were solely stabilised by Hypermer 2296 and Span 80, respectively. MIPEs **3** and **4** were stabilised by a 1:1 mixture of Hypermer 2296 and Span 80 and Hypermer 2296 and Hypermer B246sf, respectively (Table 1). After polymerisation, polyMIPEs **1-4** were white and non-chalky porous materials. The SEM images of polyMIPEs **1-4** revealed that they all possessed a homogeneous and open porous

interconnected pore structure, which is similar to the microstructure of typical polyHIPEs (Figure 4-1). The average values of pore and pore throat sizes were analysed by UTHSCSA Image tool software and at least 50 pores (pore throats) were measured and the data are summarised in Table 4-2. The pore diameter of polyMIPE **1** ranged from approximately 3 μm to 5 μm and the pores were interconnected via pore throats of 0.8 μm in diameter. The average pore diameter of polyMIPEs **1**-**4** slightly decreased from 3.5 μm (polyMIPE **1**) to 2.8 μm (polyMIPE **4**) due to the usage of different surfactant (surfactant mixtures) while the pore throat sizes of polyMIPEs **2**-**4** remained similar. The slight reduction of the pore size indicates that the droplet size in emulsion templates decreased, which depends on the surfactants used to stabilise the emulsion since the pore structure of polyMIPEs is the replica of the emulsion structure at the gel point of the polymerisation [13, 19]. The smallest pore diameters of polyMIPE **4** were resulted from the surfactant Hypermer B246sf; it improves the emulsion stability the most with the same emulsification process as other surfactants, which is evidenced by the smaller average droplet diameters and, therefore, the smallest average pore size [16, 20].

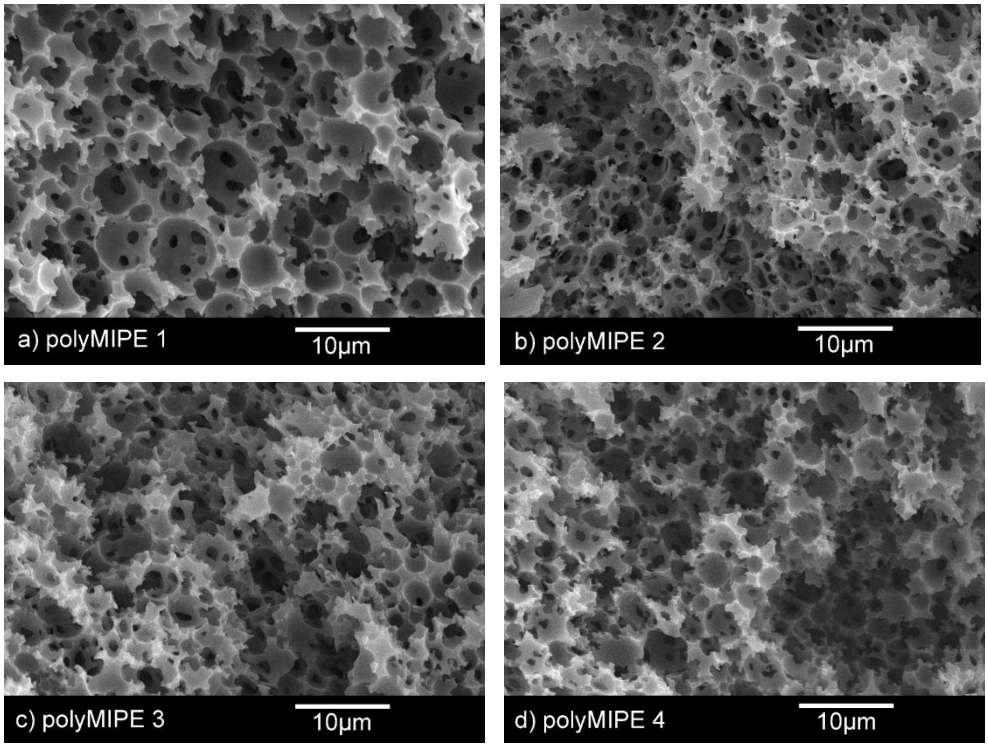

Figure 4-1 SEM images of polyMIPEs 1-4 resulting from the emulsion templates containing AIBN as initiator

As expected, the skeleton density of the synthesised macroporous polymers remained constant at about 1.067 g/cm^3 since the skeleton density is the density of final polymer and, therefore, only depends on the composition of the organic phase. Furthermore, the foam density and porosity of all polyMIPEs **1-4** were similar since all emulsion templates contained the same amount of internal phase volume. The foam density and porosity remained constant at approximately 0.360 g/cm^3 and about 67 %, respectively (Table 4-2). The porosity of polyMIPEs **1-4** is at 67% slightly larger than the internal phase volume of emulsion templates (56%). This is caused by the removal of non-converted monomers and surfactant. All polyMIPEs **1-4** had a surface area of about 2 m²/g. This is in the range expected for emulsion templated macroporous polymers [17, 20].

AIBN seems to be a good initiator for the polymerisation of MIPEs consisting of styrene and DVB to produce macroporous polymers possessing desired the open

porous interconnected microstructure no matter which surfactant (surfactant mixture) was used.

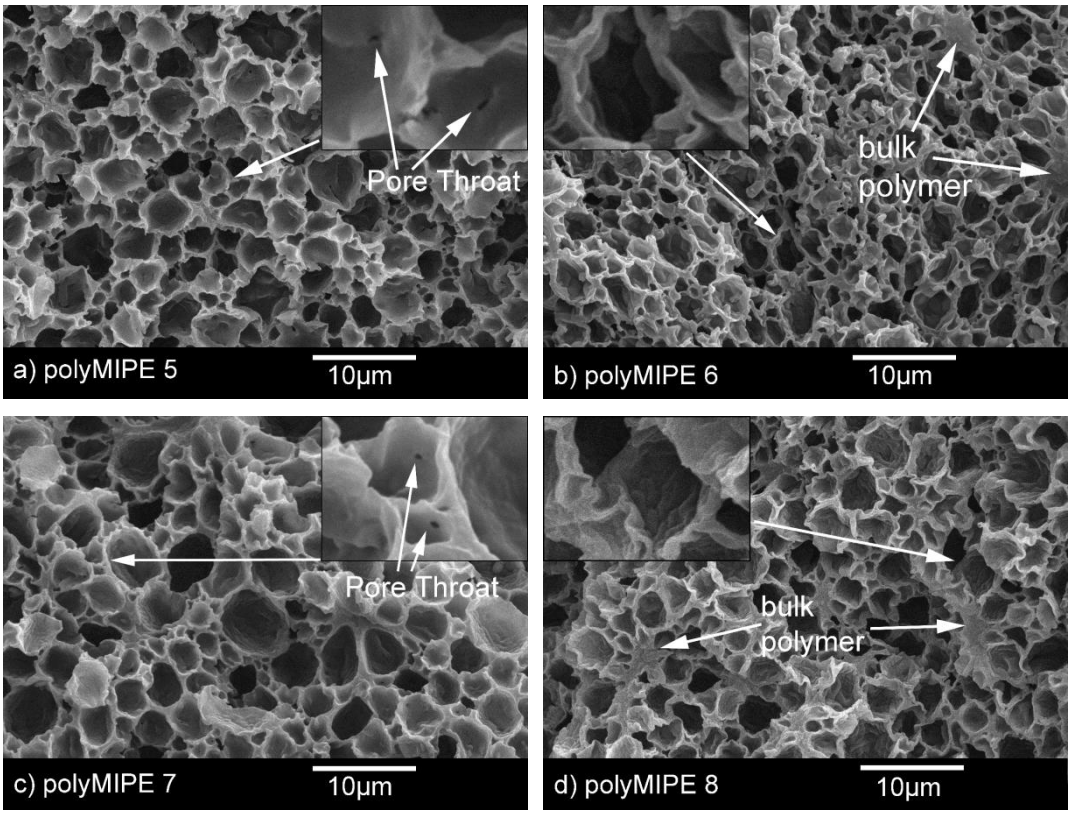

Figure 4-2 SEM images of polyMIPEs 5-8 resulting from the emulsion templates containing KPS as initiator

Similar to MIPEs **1-4**, four types of surfactants were used to stabilise MIPEs **5-8** and the recipes are listed in Table 4-1. However, for the initiation of the polymerisation at 70 ℃ of MIPEs **5-8**, the water soluble initiator KPS was used instead of the oil soluble initiator AIBN. After polymerisation, all resulting macroporous polymers were white, non-chalky materials. PolyMIPEs **5-8** possess similar pore sizes ranging from 1.8 μm to 2.5 μm. However, the resulting polyMIPEs **5-8** did not possess the desired interconnected pore structure; no pore throats can be found in SEM images of polyMIPEs **6** and **8** while very few pore throats can be seen in some of pores of polyMIPEs **5** and **7** about 0.17 μm in diameter (see high resolution sections in Figure 4-2). Furthermore, all polyMIPEs **5-8** possess thick pore walls and some areas

consisting solely of bulk polymer. The bulk polymer regions are more pronounced in polyMIPEs **6** and **8**. In addition, the polyMIPEs **6** and **8** shrunk by approximately 20% during drying. Therefore, the pores were deformed especially the pores close to a bulk polymer area. As the formulations of MIPEs **1-4** are identical to the formulation of MIPEs **5-8** apart from the initiator, the significant change in microstructure of polyMIPEs **5-8** was most likely caused by the changed locus of the initiation of the polymerisation of the continuous phase of MIPEs **5-8**. KPS is a water-soluble initiator; the initiator decay leads to the formation of radicals in the aqueous phase rather than the continuous monomer phase as in case of AIBN. Therefore, the polymerisation occurred first at the oil-water interface. It is worth noting that KPS is commonly used by other researchers to polymerise HIPEs, which results in highly interconnected macroporous polymers. Although they employ similar molar concentrations with respect to monomers as this case, they initiate the polymerisation at lower temperatures [20, 27, 156, 157]; commonly between 55 ℃ [27] and 60 ℃ [20, 153, 154]. However, the polymerisation was initiated at 70 ℃ in the project in order to compare KPS and AIBN under same experiment conditions, which means the initiator decay rate is higher, the half-life time significantly shorter and, therefore, the overall radical concentration in the aqueous phase is much higher in comparison to the radical concentration achieved under the above mentioned experiment conditions. This high radical concentration might lead to the fast formation of a solid closed cell skin (shell) surrounding the water droplets, which suppressed the formation of pore throats.

Table 4-2 Physical properties of macroporous polymer foams

Sample ID	Skeleton density (g/cm^3)	Foam density (g/cm^3)	Porosity (%)	Surface area (m^2/g)	Pore size (μm)	Pore throat size (μm)
1	1.070±0.001	0.347±0.044	68±2	1.99±0.01	3.5±1.3	0.8±0.3
2	1.073±0.003	0.360±0.036	67±2	1.86±0.01	3.2±0.9	0.8±0.3
3	1.070±0.001	0.373±0.028	66±2	1.99±0.01	3.1±0.9	0.8±0.3
4	1.055±0.001	0.359±0.022	66±2	2.45±0.01	2.8±1.0	0.7±0.2
5	1.035±0.003	0.367±0.007	63±2	-	2.2±1.0	0.17±0.09
6	1.030±0.002	0.556±0.091	46±4	-	1.8±0.8	-
7	1.047±0.003	0.383±0.017	64±2	-	2.5±1.2	0.17±0.04
8	1.040±0.003	0.608±0.013	43±2	-	1.9±1.0	-
9	1.102±0.004	0.396±0.029	64±2	0.20±0.02	3.1±1.9	0.6±0.3
10	1.101±0.005	0.402±0.055	64±2	2.23±0.01	3.0±1.2	0.6±0.3
11	1.091±0.005	0.352±0.029	68±2	2.00±0.01	2.8±1.2	0.6±0.3
12	1.094±0.005	0.390±0.016	65±1	0.39±0.03	2.9±1.7	0.4±0.2

Theoretically, the skeleton density of polyMIPEs **1**-**8** should be identical because the skeleton density or bulk density of the polymer only depends on the monomer ratio of the organic phase in emulsion templates assuming all surfactant and the entire internal phase are removed during purification and drying. Therefore, polyMIPEs **5**-**8** exhibited at 1.038 g/cm^3 silimar skeleton densities as polyMIPEs **1**-**4**. It is

suspected that polyMIPEs **5** and **7** are sufficiently interconnected to allow the removal of the surfactant and un-reacted monomers during purification. Therefore, the samples did not shrink during drying. As a consequence, the foam densities and porosities of polyMIPEs **5** and **7** are approximately 0.375 g/cm^3 and 64%, respectively, similar to that of polyMIPEs **1-4**. However, polyMIPEs **6** and **8** had a significantly higher foam density (0.582 g/cm^3) and lower porosity (45%) in comparison to the previously discussed samples due to the volume shrinkage during drying. The shrinkage was most likely caused by the residual surfactant which could not be removed during purification due to the completely closed cell structure of polyMIPEs **6** and **8**. In this case, the residual surfactant acted as plastizer during drying at temperatures between 70 ℃ and 120 ℃.

These results show that although the polymerisation of the continuous phase can be successfully initiated by radicals originating in the aqueous phase, under the above discussed conditions only almost closed cell polyMIPEs can be manufactured. Although pore throats can be found in the polyMIPEs **5** and **7**, the number is very limited and the sizes are quite tiny. This is most likely caused by the high radical concentration due to the high decay rate of KPS at 70 ℃. Therefore, it was decided to employ redox initiator systems since they can both reduce the initiation temperature and initiator decay rate.

The redox initiator system consisted of iron (II) sulfate heptahydrate, $_L$-ascorbic acid (reducing agent) and hydrogen peroxide (oxidising agent) can initiate the polymerisation in HIPEs [155] and is a component of the aqueous phase of MIPEs **9-12** here. The continuous phase of MIPEs **9-12** is identical to the continuous phase of

MIPEs **1**-**4** and **5**-**8**, respectively; the compositions are summarised in Table 4-1. The polymerisation of MIPEs **9**-**12** produced white, non-chalky porous polymers.

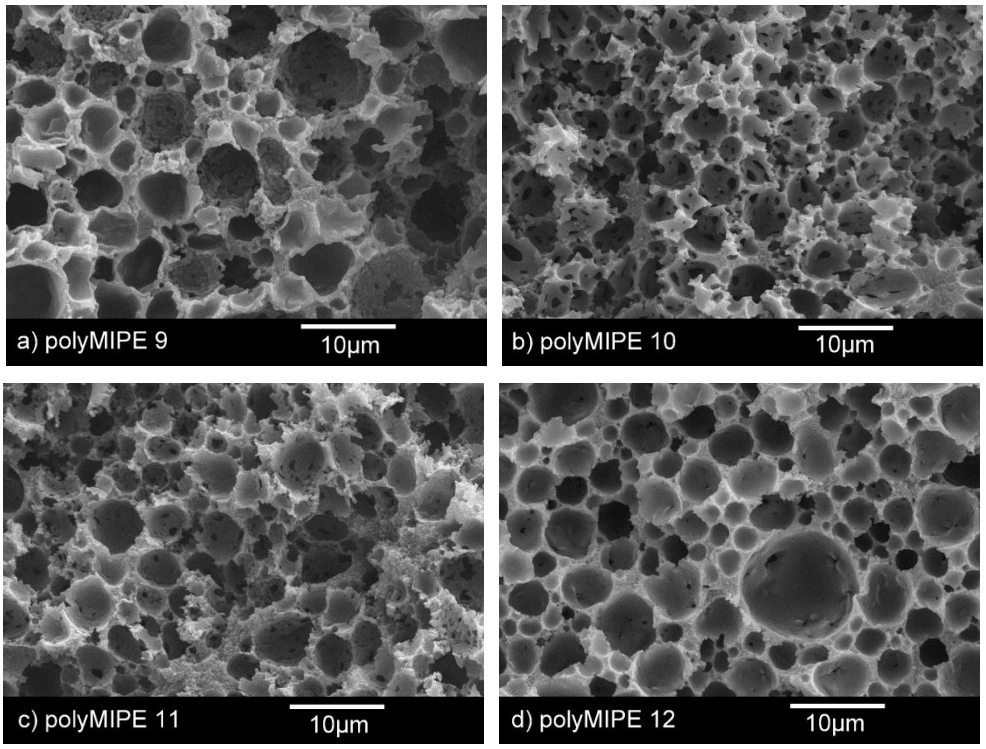

Figure 4-3 SEM images of polyMIPEs 9-12 resulting from the emulsion templates containing redox initiator system

PolyMIPEs **9**-**12** exhibited interconnected pore structures although the degree of interconnectivity, which means the degree of pore throats coverage in terms of pore throats number and size per pore, of polyMIPEs **9** and **12** is considerably lower than that of polyMIPEs **10** and **11** (Figure 4-3). Comparing polyMIPEs **9**-**12** to polyMIPEs **1**-**4,** the sample with same surfactant showed significantly smaller degree of interconnectivity. Although it is easily to find pore throats in the SEM image of polyMIPE **10** and **11**, thick walls, which affect the degree of interconnectivity, can be found as well. Furthermore, they all possess similarly thick pore walls as polyMIPEs **5**-**8**. This indicates that similarly to the polymerisation of MIPEs **5**-**8**, a skin was formed at the oil-water interface during the polymerisation as the initiator

radicals originated in the aqueous phase. However, in order to completely polymerise MIPEs **9**-**12** the polymerisation time had to be increased from 24h (MIPEs **1**-**8**), which is more than twice longer than the half life time of the initiators, to one week (MIPEs **9**-**12**). It took, therefore, longer to reach the gel point of the polymerisation, which indicates that the skin formed at the oil-water interface remained soft for a relatively long period of time. This promoted the phase separation of the continuous phase into a surfactant rich and polymer rich phase and subsequently the formation of pore throats [28]. Solely based on the degree of interconnectivity of the resulting polyMIPEs, it appears that Span80 is the most suited surfactant to stabilise a MIPE containing the used redox initiator system. However, based on pore structure of the resulting polyMIPEs, it seems Hypermer B246sf is the best surfactant to stabilise MIPEs containing the used redox initiator system.

The skeleton density of the synthesised macroporous polyMIPEs **9**-**12** remained constant at about 1.097 g/cm^3, which is similar to that of polyMIPEs **1**-**4**. The foam density and porosity remained at about 0.385 g/cm^3 and about 65 % (Table 4-2). The surface areas of polyMIPEs **10** and **11** are at approximately 2 m²/g similar to the values found for polyMIPEs **1**-**4**. However, the surface area of polyMIPE **9** and **12** was much lower than that of polyMIPEs **10** and **11** due to the low degree of interconnectivity.

4.4 Summary

Numerous potential applications of conventional polyHIPEs are impeded because of their poor mechanical properties such as brittleness and chalkiness. Increasing the

organic phase volume of the emulsion templates from HIPEs to MIPEs is an important strategy to improve the mechanical performance of macroporous polymers. The objective of this work was to study the influence of emulsion components on the morphological aspects and physical properties of the resulting macroporous polymers in order to find the optimal formulation of the MIPEs with the organic phase containing styrene and DVB. Three initiator types including AIBN, KPS and a redox initiator system were adopted. Furthermore, four different surfactants (surfactant mixtures) containing Hypermer 2296, Span 80 and even surfactant combination such as Hypermer 2296/Span 80 mixture and Hypermer 2296/ Hypermer B246sf mixture were used to stabilise the emulsion templates.

The high degree of crosslinking of the final macroporous polymers led to the absence of a glass transition in the temperature range of 25-250 ℃. The macroporous polymers produced from the emulsion templates containing the oil soluble initiator AIBN showed desired interconnected open porous structures no matter which surfactant (surfactant mixture) was used. Another widely used water soluble initiator KPS was used to produce polyMIPEs **5**-**8** from emulsion templates with the same composition but the resulting polyMIPEs had an effectively closed cell microstructure because of the high radical concentration produced by KPS which might lead to the fast formation of a solid closed cell skin (shell) surrounding the water droplets suppressing pore throat formation. Furthermore, polyMIPEs **6** and **8** shrunk after drying and the pores were deformed. This might be caused by residual surfactant which could not be removed during purification due to the completely closed cell structure of polyMIPEs **6** and **8**. In this case, the residual surfactant acted as plastizer during drying at temperatures between 70 ℃ and 120 ℃. A redox initiator system was introduced into emulsion templates in order to trigger the polymerisation

at ambient temperatures. PolyMIPEs **9-12** exhibited interconnected pore structures but thick walls were found in the resulting the polyMIPEs. The usage of different surfactants depends on the different purpose. If the objective is keeping the degree of interconnectivity of the resulting polyMIPEs, Span80 seems the most suitable surfactant to stabilise MIPEs containing the used redox initiator system. However, if the aim is obtaining best pore structure of the resulting polyMIPEs, it appears Hypermer B246sf is the best candidate to stabilise a MIPE containing the used redox initiator system.

5 Tough interconnected polymerised medium and high internal phase emulsions reinforced by silica particles

5.1 Introduction

In order to explore real industrial applications of conventional polyHIPEs, Menner et al. [8, 9] successfully developed low density but tough macroporous polymers via emulsion templating. Poly(ethylene glycol) dimethacrylate (PEGDMA) was used as a crosslinker [8] to reduce brittleness and copolymerised with methoxysilyl propyl-methacrylate (MPS) and styrene. MIPEs, which increase the resulting macroporous polymer foam density, were used as templates to improve the overall mechanical performance [8, 9]. A further improvement of mechanical performance was obtained by the incorporation of silica particles into the polymer network [8, 9]. However, the final macroporous polymers did not possess an open porous network structure. Furthermore, approximately 20 μm thick walls with a porous microstructure surrounded the pores (Figure 2-5). The formation of methanol during the polycondensation of MPS and the reaction with the surface of silica particles caused the emulsion template to destabilise rapidly (Scheme 5-1).

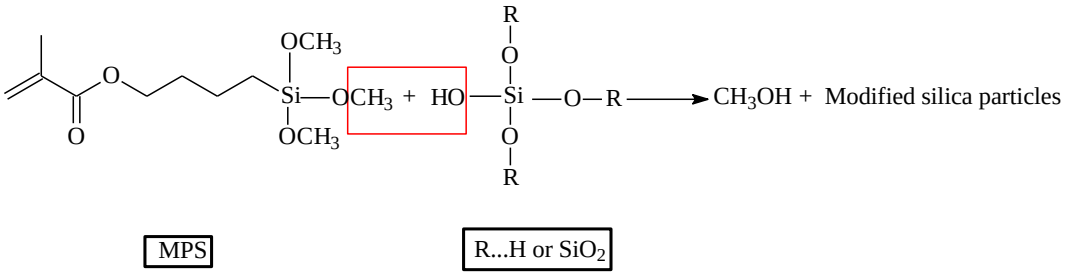

Scheme 5-1 Schematic illustration of the reaction involved in grafting particles

Since then, various open celled and tough macroporous polymer nanocomposites have been produced using carbon nanotubes, titania nanorods [68] and clay [131] as reinforcement for the pore walls. The aim of present research is to enhance the mechanical properties of high porosity macroporous polymers without affecting the open and interconnected pore structure. In order to achieve this objective, the more flexible crosslinker PEGDMA was used instead of conventional DVB. A silica particulate reinforcement was introduced and the continuous phase volume was increased to 40 vol.%. Before preparing emulsion templates and to avoid the formation of methanol during emulsification and subsequent polymerisation, the "as received" silica particles were silylated using MPS. The MPS modified silica particles possess polymerisable double bonds and can, therefore, be incorporated into the polymer acting as crosslinker during the radical polymerisation of the continuous phase of emulsion templates. Both polyHIPEs and polyMIPEs containing increasing loading fractions of silylated silica particles were made to study the relationship between the continuous phase volume of the emulsion templates and the physical and mechanical properties of the resulting macroporous polymers.

5.2 Summary of the composition of emulsion templates

Both HIPEs and MIPEs were prepared to investigate the influence of the porosity of macroporous polymers on their mechanical performance. Various amounts from 0 to 60 wt.% of MPS silylated silica particles were added to the continuous phase to determine the optimal concentration of the reinforcement which leads to a type of macroporous polymer with outstanding mechanical properties. The compositions of the emulsion templates are summarised in Table 5-1. After polymerisation of these emulsions, the macroporous polymers **1**-**14** were produced. The sample preparation procedure was presented in Chapter 3.3 and 3.4.

Table 5-1 Composition of the emulsion templates

Sample ID	Organic phase volume [a]	Organic phase composition Styrene/PEGDMA/Surf. (vol.%)[b]	Silylated silica particles (wt.%) [c]
1	20	40/40/20	0
2	20	40/40/20	1
3	20	40/40/20	5
4	20	40/40/20	10
5	20	40/40/20	20
6	20	40/40/20	40
7	20	40/40/20	60
8	40	40/40/20	0
9	40	40/40/20	1
10	40	40/40/20	5
11	40	40/40/20	10
12	40	40/40/20	20
13	40	40/40/20	40
14	40	40/40/20	60

[a] Volume of the organic phase relative to the total volume of the emulsion

[b] Ratio of styrene, PEGDMA and Hypermer B246sf in the organic phase

[c] wt.% filler relative to the monomers

5.3 Results and discussion of macroporous polymers produced from high and medium internal phase emulsion (HIPE or MIPE) templates

HIPEs **1**-**7** contained 20 vol.% continuous phase while the continuous phase of MIPEs **8**-**14** occupied 40 vol.% of the emulsion volume (Table 5-1). All emulsions were stabilised by the nonionic, polymeric surfactant Hypermer B246sf. Hypermer B246sf is a block copolymer of a polyhydroxy fatty acid and polyethylene glycol with a hydrophilic-lipophilic balance (HLB value) of 6 [8]. The continuous phase of the emulsions contained PEGDMA as crosslinker, to reduce the chalkiness and brittleness of the produced macroporous polymers in comparison to conventional polyHIPEs using DVB as a crosslinker [8]. In addition, varying amounts of MPS silylated silica particles were added into the continuous phase of HIPEs **2**-**7** and MIPEs **9**-**14** whereas HIPE **1** and MIPE **8** without modified silica particles were prepared as reference to study the effect of silylated silica filler on the mechanical properties of the resulting macroporous polymers. The degree of MPS functionalisation of the surface of the silica particles was 3 wt.% as determined by TGA.

Compared to MIPEs **8**-**14** with an organic phase of 40 vol.%, the HIPEs **1**-**7** with an organic phase content of 20 vol.% were much more viscous because of the increased dispersed phase volume which leads to a higher and denser droplet packing [18]. The polymerisation of HIPEs **1**-**7** produces non-chalky porous polymers. The macroporous polymers possess an open porous interconnected pore structure as can be seen in the SEM images (Figure 5-1); the incorporation of nanometre sized

silylated silica particles did not affect the interconnected open porous structure of the polyHIPEs **2**-**7** when compared to polyHIPE **1** (Figure 5-1). The silylated particles were covalently incorporated into the growing polymer by copolymerisation of MPS grafted to SiO_2 with the monomers. With increasing concentration of silylated silica particles, the average pore diameter of polyHIPEs **1**-**7** decreases from 11 μm (polyHIPE **1**) to only 4 μm (polyHIPE **7**). Furthermore, the average pore throat sizes decreased from 2.2 μm (polyHIPE **1**) to 0.8 μm (polyHIPE **7**) (Table 5-2). The analysis of pore and pore throats diameters was using the UTHSCSA Image tool software and at least 50 pores (pore throats) were measured. The SEM images of polyHIPEs **1**-**7** with different magnification is because the SEM image not only should show the structure of single pore but also need exhibit enough numbers of pores to ensure the interconnected microstructure of the fractured surface. As a result, the SEM images of polyHIPEs **5**-**7** with lower magnification because of the smaller pore size. The reduction of pore size with increasing silica particle content indicates that the droplet size of emulsion templates decreased with increasing amount of silica particles since the porous structure of polyHIPEs is a replica of the emulsion structure at the gel point of the polymerisation [13, 19]. The silylated hydrophobised silica might have acted as co-emulsifier of the emulsion template [79, 80, 87] which lead to an increased emulsion stability and, therefore, smaller average droplet diameters [16, 20].

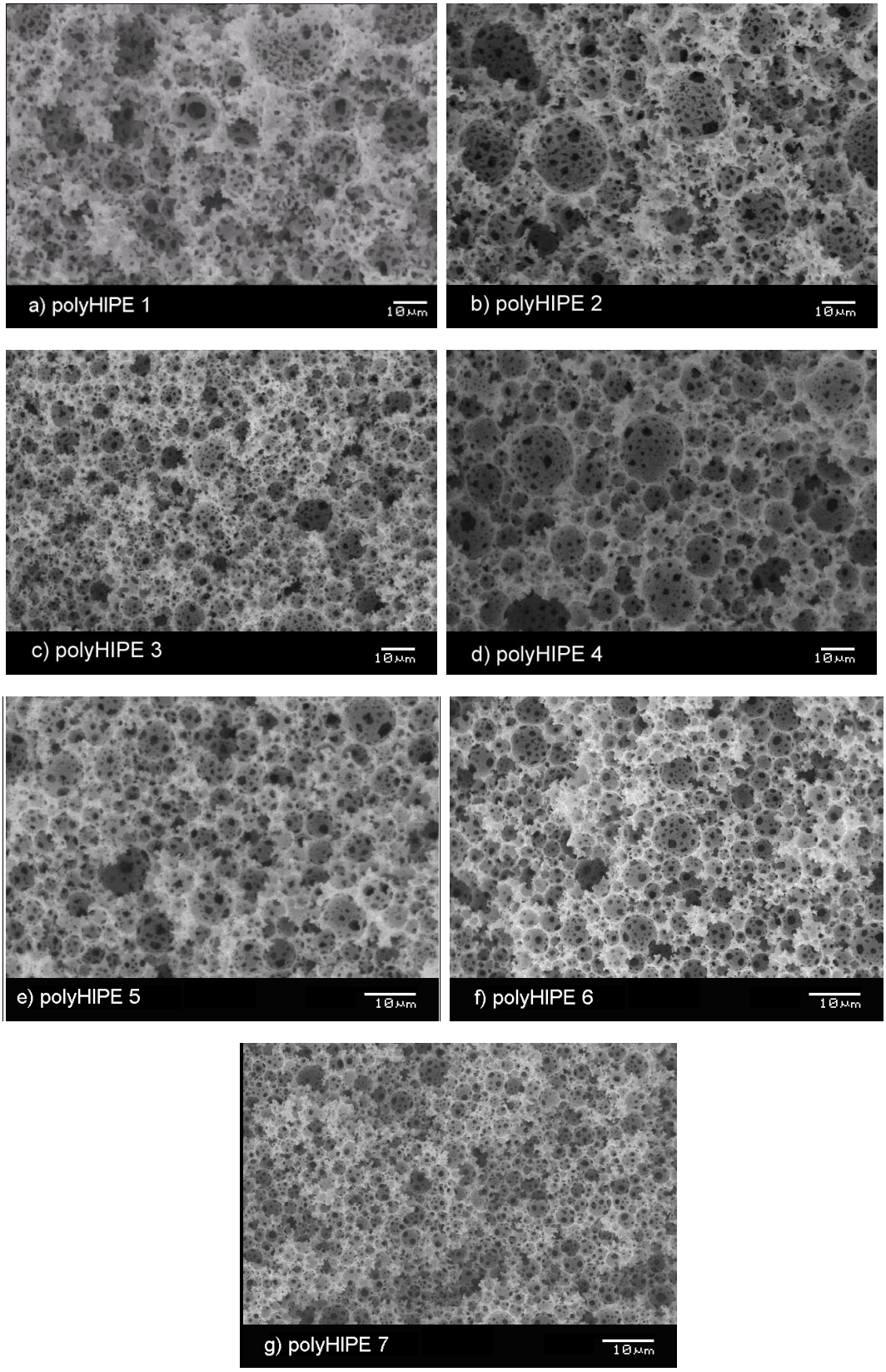

Figure 5-1 SEM images of polyHIPEs 1-7

The skeleton density ρ_m of the synthesised macroporous polymers increased from 1.128 g/cm^3 (polyHIPE **1**) to 1.418 g/cm^3 (polyHIPE **7**) (Table 5-2) due to the increasing concentration of silica particles within the polymer. Although the matrix density of resulting polymer increased with increasing silica filler concentration, the foam density and porosity of all polyHIPEs **1-7** were similar since all emulsion templates contained the same amount of internal phase volume. The foam density ρ_e and porosity P remained constant at about 0.194 g/cm^3 and about 84 % (Table 5-2). PolyHIPEs **1-7** possess surface areas of approx. 5 m²/g, which are within the range of surface areas commonly reported for polyHIPEs [16, 17, 46].

Table 5-2 Physical properties of polyHIPEs 1-7

Sample ID	ρ_m (g/cm^3)	ρ_e (g/cm^3)	P (%)	A_s (m^2/g)	Pore size (μm)	Pore throat size (μm)	k (mD)
1	1.128 ±0.003	0.203 ±0.003	82 ±1	5.58 ±0.01	11 ±3	2.2 ±0.6	185 ±2
2	1.139 ±0.002	0.183 ±0.005	84 ±2	3.74 ±0.01	10 ±4	1.8 ±0.6	190 ±10
3	1.168 ±0.003	0.178 ±0.003	85 ±1	3.059 ±0.007	5 ±2	1.2 ±0.4	186 ±2
4	1.194 ±0.002	0.178 ±0.004	85 ±2	4.84 ±0.02	6 ±3	1.3 ±0.5	200 ±10
5	1.250 ±0.001	0.216 ±0.005	83 ±2	5.23 ±0.02	6 ±1	1.2 ±0.4	230 ±10
6	1.396 ±0.001	0.217 ±0.004	85 ±2	4.89 ±0.02	5 ±1	1.1 ±0.3	230 ±10
7	1.418 ±0.001	0.186 ±0.003	84 ±3	6.64 ±0.01	4 ±1	0.8 ±0.2	143 ±7

The gas permeability coefficient *K*, which accounts for the contributions of viscous and Knudsen flow, was calculated from the measured rate of pressure rise as function of applied mean pressure p_m. The viscous permeability is derived from the gradient of the K vs p_m curves (Figure 5-2) [6, 132]. The viscous permeability of polyHIPEs **1**-**7** are summarised in Table 5-2. PolyHIPEs **1-6** were found to have similar viscous permeabilities of around 200 mD (1mD = 10^{-12} m^2). However, polyHIPE **7**, which contained the highest concentration of silylated silica particles in the emulsion template, showed a dramatic decrease in viscous permeability to 143 mD. This decrease of permeability was caused by the reduction in the average pore throat size (Table 5-2, Figure.5-1). Although the pore throat diameters of polyHIPEs **1** and **2** are larger than those of polyHIPEs **3-6** (see SEM images Figure. 5-1(c-f)), the permeabilities of these macroporous polymers are similar. SEM analysis only provided the average pore throat diameter but not the flow limiting pore throat diameter, which controls the gas flow rate [6]. In addition, polyHIPE **7** seems to have smaller flow limiting pore throats than the other polyHIPEs since a higher applied pressure is required to initiate the gas flow through polyHIPE **7** than for the other samples.

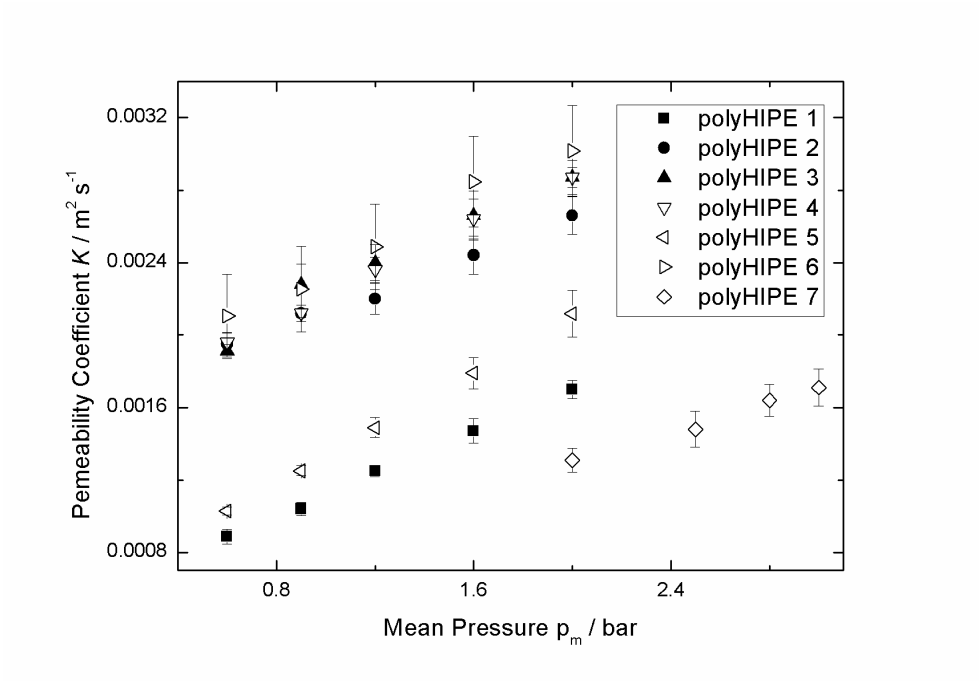

Figure 5-2 Permeability coefficient as a function of applied mean pressure for polyHIPEs 1-7

The mechanical properties of all macroporous polymer monoliths were measured at room temperature determined from the stress-strain curves. The mechanical properties are summarised in Table 5-3; Figure 5-3 shows representative compressive stress-strain curves for polyHIPEs **1**-**7**. Three typical regions commonly observed for polymer foams can be identified: the initial linear elastic region, plateau region and bulk compression region [25, 158].

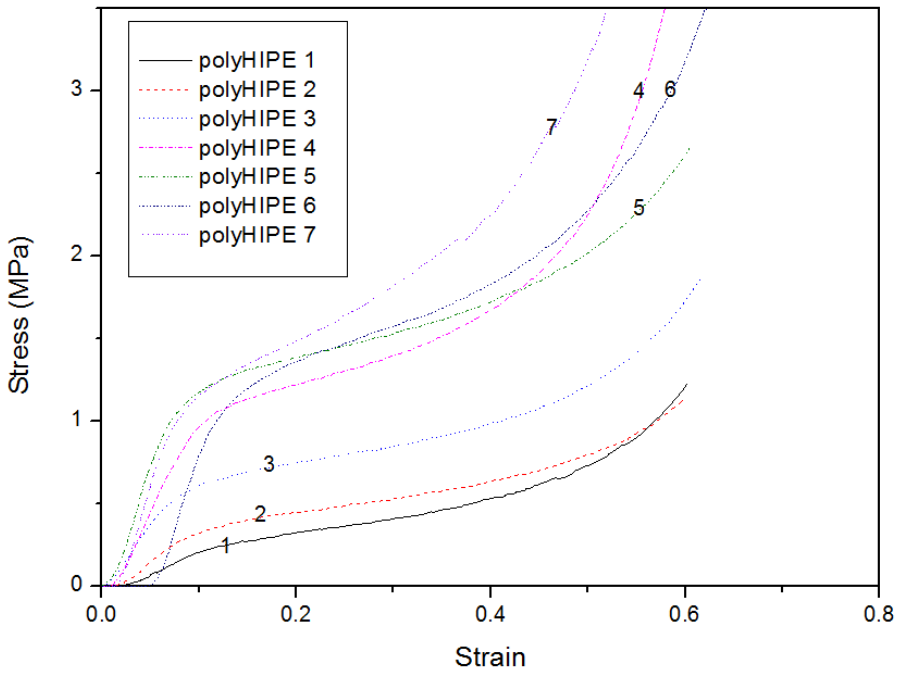

Figure 5-3 Typical stress-strain curves of polyHIPEs 1-7 materials under compressive loads

The compression modulus (Table 5-3) of polyHIPE **1** is 3 MPa and the crush strength is 0.2 MPa, which are relatively low in comparison to other macroporous nanocomposites but typical for polyHIPEs [10, 140]. The compression modulus and crush strength of polyHIPE **2** were already slightly improved by the introduction of only 1 wt.% of silylated silica particles. A further increase in the loading fraction of modified silica particles from 1 wt.% to 20 wt.% led to a steady improvement of the compression modulus as well as crush strength (Table 5-3). The compression modulus increased to 16 MPa and the crush strength to 1.2 MPa for polyHIPE **5**. This significant improvement was the result of the covalent incorporation of silylated silica particles into the pore walls of these macroporous polymers. It is worth noting that the particle size plays a crucial role. Only particles, which are smaller than the width of the pore walls, such as the nano-sized particles used in this study are suited to reinforce the polymer skeleton of macroporous polymers made by emulsion

templating. The particles would be "polyHIPE grafted" rather than incorporated into the pore walls if the particle size would exceed the dimensions of the pore walls, which leads to stress points and, therefore, a reduction in mechanical strength. However, polyHIPEs **6** and **7**, which contained higher silylated silica particle loadings, did not exhibit any significant improvement of mechanical performance compared to polyHIPE **5**. The compression modulus increased slightly from 16 MPa (polyHIPE **5**) to 22 MPa (polyHIPE **7**), but the crush strength of polyHIPEs **6** and **7** remained constant within the errors. However, its average values decreased slightly, which might be caused by the uneven distribution of the silica filler within the polymer walls of the macroporous polymers. With increasing content of silylated silica particles, it became more and more difficult to evenly distribute the silica filler within the continuous phase of the HIPEs since the particles tend to aggregate. Areas within the polyHIPEs, which contain rather large aggregates, may lead to higher compression moduli within the sample while areas lacking particles have lower compression moduli, which may cause premature failure of the sample. Specific compression moduli (Table 5-3) constantly increased with increasing silica content but the error became large for the samples with high concentration of particles because of the uneven distribution of silica fillers within the walls of macroporous polymers. The specific crush strength at first steadily increased until a silica content of 20 wt.% was reached and then remained constant within errors.

Table 5-3 Mechanical properties of the polyHIPEs 1-7

Sample ID	Compression modulus (MPa)	Specific compression modulus (kPa $kg^{-1}m^3$)	Crush strength (MPa)	Specific crush strength (kPa $kg^{-1}m^3$)
1	3 ±1	18 ±5	0.2 ±0.1	0.9 ±0.2
2	5 ±1	26 ±2	0.3 ±0.1	1.8 ±0.1
3	8 ±1	47 ±8	0.5 ±0.1	2.6 ±0.7
4	10 ±2	60 ±10	0.8 ±0.2	4 ±1
5	16 ±1	75 ±6	1.2 ±0.1	5.6 ±0.3
6	19 ±1	89 ±5	1.1 ±0.1	5.0 ±0.2
7	22 ±5	120 ±30	1.0 ±0.1	5.5 ±0.5

In summary, the significant improvement of the (specific) compression modulus and (specific) crush strength of silica reinforced polyHIPEs demonstrates that the particles were successfully integrated into the polymer network without damaging the open porous interconnected structure of the macroporous polymers. The optimal content of reinforcement is about 20 wt.% since the produced polyHIPEs still had a typical polyHIPE structure and outstanding mechanical properties equivalent to polyHIPEs containing a higher silica filler content.

In order to increase further the mechanical properties of macroporous polymer nanocomposites, the continuous phase volume of the emulsion templates was increased to 40 vol.% in order to increase the foam density. It has already been shown [7, 8, 132] that the polymerised products of less concentrated medium internal phase emulsions (MIPE, 60 vol.% of internal phase) also exhibit low densities and

highly interconnected structures, which are considered as the most important characteristics of polyHIPEs but have much improved mechanical properties. MIPEs **8**-**14** have the same composition as HIPEs **1**-**7** but contain 40 vol.% of organic phase (Table 5-1).

Compared to HIPEs **1**-**7**, MIPEs **8**-**14** were less viscous and easier to transfer into the Falcon® tubes. MIPEs **8**-**14** were also polymerised resulting in polyMIPEs. Similar to polyHIPEs **1**-**7**, all macroporous polymers were non-chalky and porous materials. The SEM images of polyMIPEs **8**-**14** reveal that they all possess an open porous interconnected pore structure (Figure 5-4). The pore diameters of polyMIPE **8**, which does not contain any silica filler, ranged from 6 μm to 12 μm and the pores are interconnected via pore throats of 1.6 μm in diameter (Table 5-4). The average pore and pore throat diameters of the polyMIPEs decreased with the addition of increasing amounts of silylated silica particles. The pore diameters of polyMIPE **14** containing 60 wt.% silylated silica particles decreased to only 4 μm and the pore throat size decreased to only 0.7 μm for the reason discussed above (Figure 5-4(g)).

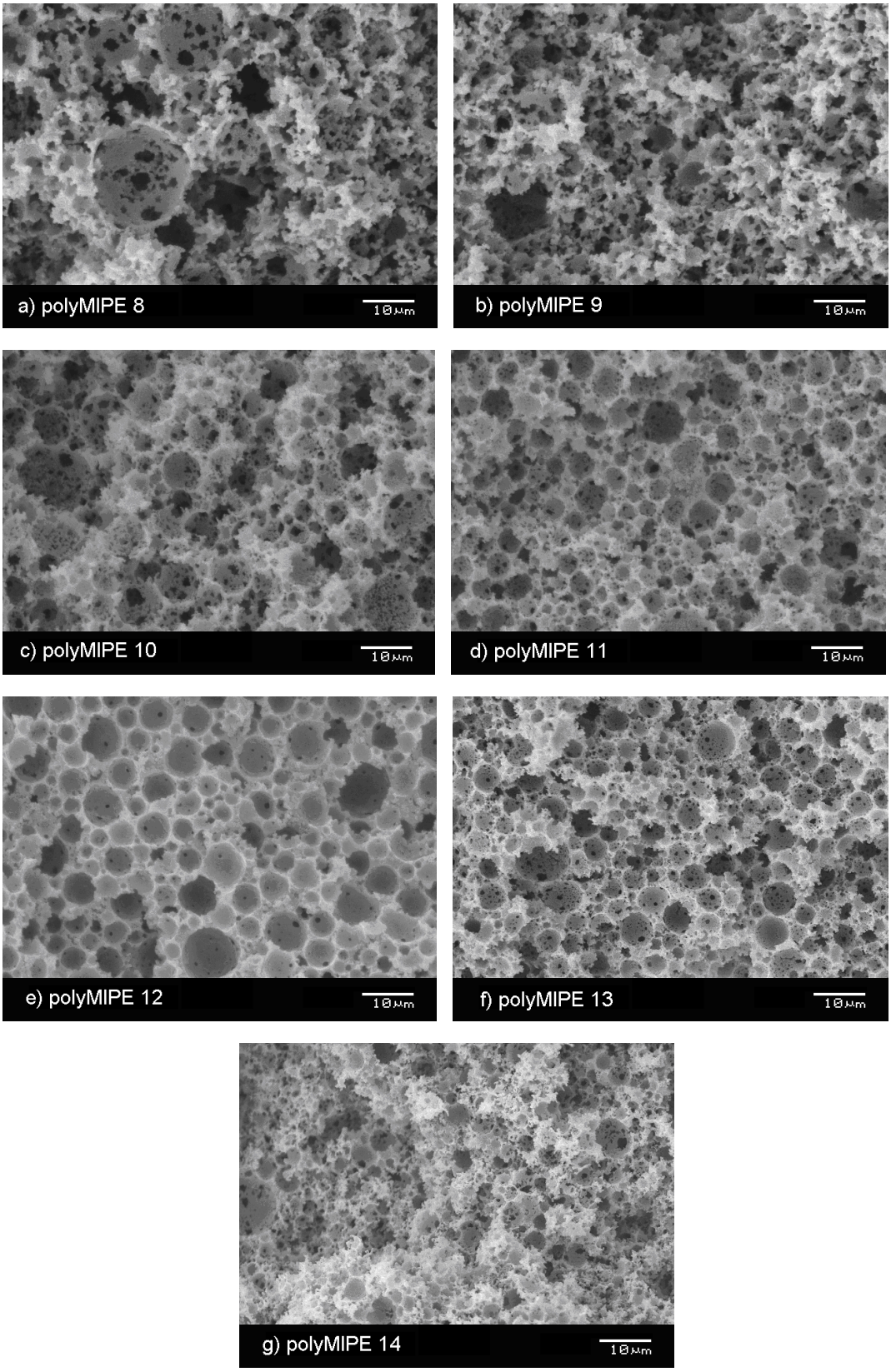

Figure 5-4 SEM images of polyMIPEs 8-14

The skeleton density ρ_m of polyMIPEs **8**-**14** increased steadily from 1.131 g/cm^3 (polyMIPE **8**) to 1.387 g/cm^3 (polyMIPE **14**) upon the incorporation of more and more silica particles. The skeleton density of both polyHIPEs and polyMIPEs composites should be identical because the skeleton density is the density of final composite and, therefore, only depends on the composition of the organic phase in emulsion templates. In the fact, the skeleton densities of both polyHIPEs and polyMIPEs with the same composition of the organic phase in emulsion templates are almost identical within the errors.

Table 5-4 Physical properties of polyMIPEs 8-14

Sample ID	ρ_m (g/cm^3)	ρ_e (g/cm^3)	P (%)	A_s (m^2/g)	Pore size (μm)	Pore throat size (μm)	k (mD)
8	1.131±0.002	0.369±0.007	67±2	2.574±0.005	9±3	1.6±0.6	47±4
9	1.139±0.001	0.368±0.008	68±1	3.08±0.01	6±1	1.2±0.4	59±5
10	1.171±0.002	0.378±0.006	68±2	3.81±0.02	7±1	1.0±0.4	20±1
11	1.195±0.003	0.395±0.005	67±2	4.30±0.01	5±1	0.7±0.2	22±8
12	1.223±0.003	0.42±0.01	66±1	4.258±0.004	6±1	0.7±0.2	24±2
13	1.336±0.004	0.4±0.1	68±3	3.122±0.006	6±1	0.6±0.2	8±1
14	1.387±0.003	0.5±0.1	68±3	3.027±0.009	4±2	0.7±0.2	13±3

As expected, the foam densities ρ_e of polyMIPEs **8**-**14** are much higher than those of polyHIPEs **1**-**7** due to the increase of the organic phase level in the emulsion templates. The foam densities of polyMIPEs **8**-**14** increased slightly from

0.369 g/cm^3 (polyMIPE **8**) to 0.5 g/cm^3 (polyMIPE **14**). The porosities *P* of all samples were similar since all MIPE templates contained the same internal phase volume (Table 5-4). The slight increase in porosities (67%) of polyMIPEs compared to the internal phase volume of emulsion templates (60%) is caused by the removal of non-converted monomers and the surfactant. As expected, all polyMIPEs **8-14** had a surface area of about 4 m^2/g, which is slightly lower than those of polyHIPEs **1-7**.

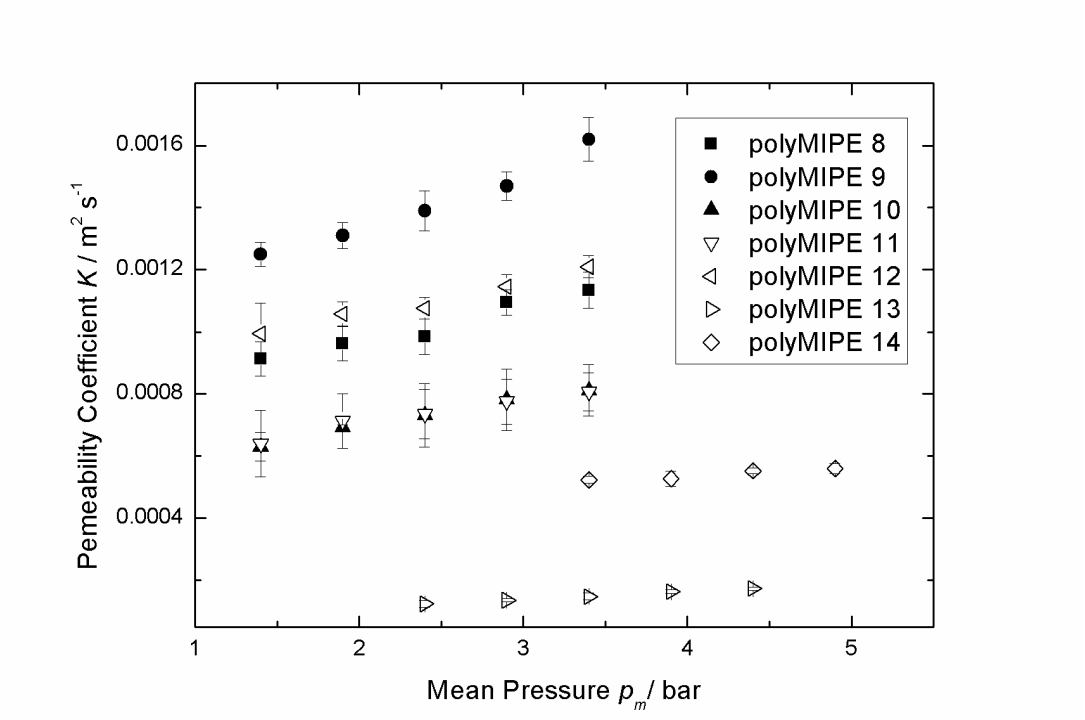

Figure 5-5 The permeability coefficient as a function of mean pressure for polyMIPEs 8-14

As discussed above, the viscous permeability *k* is derived from the gradient of the K vs p_m curves (Figure 5-5). Compared to polyHIPEs **1-7**, the viscous permeability of polyMIPEs **8-14** was much lower because of their reduced porosity (Table 5-4). Furthermore, the viscous permeabilities of polyMIPEs **8-14** decreased with increasing content of silylated silica particles from 47 to 13 mD (Table 5-4). The

reduced permeabilities can be explained by the reduction of the pore and more importantly the pore throat diameters caused by the addition of increasing amounts of silylated silica particles. The average pore diameter decreases from 9 μm (polyMIPE **8**) to only 4 μm (polyMIPE **14**) and the pore throat diameter decreased from 1.6 μm (polyMIPE **8**) to only 0.7 μm (polyMIPE **14**). The smallest pore throat diameter of a series of interconnected pores determines the resistance to gas flow through a porous media. PolyMIPEs **13** and **14** seem to have smaller flow limiting pore throats than the other samples since higher applied pressures were required to initiate the gas flow through polyMIPEs **13** and **14** than polyMIPEs **8-12**. According to the analysis of all the SEM images (Figure 5-4), polyMIPEs **11-14** have similar pore throat diameters; again the analysis of SEM images only provides the average pore throat diameters and not necessarily the smallest diameters of the biggest interconnecting pores throughout the sample which limit the gas flow [6].

The compression moduli and crush strengths of polyMIPEs **8-14** (Table 5-5) were significantly higher than those of polyHIPEs **1-7** because of the increase of the foam density. Even polyMIPE **8** without reinforcement had a similar compression modulus (14 MPa) to polyHIPE **5** (16 MPa) containing 20 wt.% of sylilated silica. Furthermore, the crush strength of polyMIPE **8** (1.7 MPa) was higher than that of polyHIPE **5** (1.2 MPa), which was the maximum value of polyHIPEs **1-7**. The addition of silylated silica particles and their incorporation into the polymer walls of the macroporous polymers led to a persistent improvement of the compression modului of polyMIPEs **9-14** to up to 110 MPa. However, the maximum crush strength is 4.3 MPa; it does not increase any further when the silica loading exceeds 10 wt.%. PolyMIPE **14** has the highest average compression modulus but the standard error became larger because of the heterogeneous distribution of silica

particles within the polymer walls of polyMIPE **14**. In addition, the inhomogeneous distribution of the filler resulted in a decrease of the crush strength from 4.3 MPa (polyMIPEs **11** and **12**) to 3.7 MPa (polyMIPE **13**) and 3.9 MPa (polyMIPE **14**), respectively.

Specific compression moduli (Table 5-5) steadily increased with increasing silica filler content. However, the specific crush strength at first continuously increased until the silica filler content reached 10 wt.% but remained constant for a silica content of 20 wt.% and then decreased. Although polyMIPEs **11** and **12** possessed the same crush strength values, the slightly lower foam density of polyMIPE **11** led to a higher specific crush strength.

Table 5-5 Mechanical properties of polyMIPEs 8-14

Sample ID	Young's modulus (MPa)	Specific compression modulus (kPa $kg^{-1}m^3$)	Crush strength (MPa)	Specific crush strength (kPa $kg^{-1}m^3$)
8	14 ±3	38 ±7	1.7 ±0.2	4.6 ±0.4
9	20 ±3	54 ±9	2.2 ±0.5	5.9 ±0.3
10	50 ±7	130 ±20	2.9 ±0.2	7.8 ±0.6
11	70 ±7	180 ±20	4.3 ±0.1	10.8 ±0.1
12	80 ±5	190 ±10	4.3 ±0.2	10.3 ±0.4
13	100 ±20	220 ±30	3.7 ±0.2	8.4 ±0.4
14	110 ±20	220 ±30	3.9 ±0.1	8.0 ±0.3

In summary, significant improvements in the (specific) compression moduli and (specific) crush strengths of macroporous polymers were achieved by raising the organic phase volume of the emulsion templates used to produce them. Further improvement was obtained by the incorporation of silylated silica particles into the walls of the macroporous polymers. The silylated silica was successfully integrated into the polymer network without affecting the open porous interconnected nature of the structure. However, the pore and pore throat sizes of the macroporous polymer composites decreased significantly in comparison to their non-reinforced counterpart. The viscous permeability decreased with increasing the organic phase volume and the content of silylated silica particles in emulsion templates. The optimal content of reinforcement seems to be between 10 and 20 wt.% as the

resulting macroporous polymers had homogeneous and impressive mechanical properties compared to polyMIPEs with lower silica content.

5.4 Summary

Emulsion templating using high internal phase emulsions is an effective route to prepare low density, high porosity macroporous polymers known as polyHIPEs. Conventional polyHIPEs, synthesised from surfactant stabilised w/o emulsions, have low permeabilities and poor mechanical properties. Here interconnected open macroporous low density nanocomposites have been produced by polymerising the continuous phase of emulsion templates, which contained styrene, PEGDMA and silylated silica particles. PEGDMA and the silylated silica particles acted as crosslinker. The functionalised silica particles were incorporated into the polymer, which resulted in a significant improvement of the mechanical properties of the polyHIPEs without affecting the interconnected and permeable pore structures. The polyHIPEs contained up to 60 wt.% silylated silica particles. Compression modulus of the reinforced macroporous polymers increased up to 600% compared to non-reinforced macroporous polymers. The mechanical performance was further increased by increasing the foam density of the macroporous nanocomposites from around 200 g/cm^3 to 370 g/cm^3 by raising the organic phase volume of the emulsion templates from 20 vol.% to 40 vol.%. The macroporous polymers synthesised from less concentrated emulsions also possessed interconnected open porous although less permeable structures. The polyHIPE nanocomposites have a permeability of about 200 mD while the polyMIPE nanocomposites still have permeabilities of around 50 mD for polyMIPEs **8** and **9**.

6 Shear/tensile and fracture mechanics of tough permeable macroporous polymers determined using the Arcan test

6.1 Introduction

It is well known that most conventional polyHIPEs are very brittle and chalky, which translate into the poor shear properties of these macroporous polymers. However, until now no investigation has done to research the shear properties of these macroporous polymers. Therefore, it is necessary to carry out the evaluation of the shear properties of such macroporous polymers. The present research aimed to investigate both the shear and tensile properties and fracture toughness of silylated silica particle reinforced macroporous polymers. Both polyHIPE and polyMIPEs were prepared to study the relationship between the continuous phase volume of the emulsion templates and the mechanical properties of the resulting macroporous polymers. Furthermore, polyMIPEs with varying amounts of MPS silylated silica particles were prepared to investigate the influence of silica reinforcement on mechanical properties of the resulting macroporous polymers.

6.2 Summary of sample recipes

Both polyHIPE and polyMIPEs were prepared to investigate the influence of the continuous phase volume of the emulsion templates on the mechanical performance of the resulting macroporous polymers. Following on the previous work (Chapter 5),

the optimal concentration of MPS silylated silica particles, which were used as reinforcement in emulsion templates, is 20 wt.% with respect to the monomers. Therefore, various amount up to 20 wt.% of MPS silylated silica particles were added into the continuous phase of emulsion templates. Although the recipes were same as part of samples in Chapter 5, larger volume of emulsion templates were prepared and these emulsion were placed into a PTFE rectangular shaped mould with the following dimensions: length, 300 mm; width, 75 mm; thickness, 25 mm mould instead of free standing centrifuge Falcon® tubes. After polymerisation of these emulsions, the macroporous polymers **1**-**5** were produced. The sample preparation procedure was described in Chapter 3.3 and 3.4. The composition of the emulsion templates is summarised in Table 6-1.

Table 6-1 Composition of the emulsion templates

Sample ID	Organic phase volume [a]	Organic phase composition Styrene/PEGDMA/Surf. (vol.%)[b]	Silylated silica particles (wt.%) [c]
1	20	40/40/20	0
2	40	40/40/20	0
3	40	40/40/20	5
4	40	40/40/20	10
5	40	40/40/20	20

[a] Volume of the organic phase relative to the total volume of the emulsion

[b] Ratio of styrene, PEGDMA and Hypermer B246sf in the organic phase

[c] wt.% filler relative to the monomers

The continuous phase of HIPE **1** made up 20 vol.% of the emulsion volume whereas the continuous phase of the MIPEs **2**-**5** occupied 40 vol.% of the emulsion volume

(Table 6-1). All emulsions were stabilised by the nonionic, polymeric surfactant Hypermer B246sf with a hydrophilic-lipophilic balance (HLB value) of 6. The continuous phase of the emulsions contained PEGDMA as crosslinker in order to reduce the chalkiness and brittleness of the produced macroporous polymers in comparison to conventional polyHIPEs using DVB as a crosslinker [8, 70]. In addition, 5,10 and 20 wt.% of MPS silylated silica particles, were added into the continuous phase of MIPEs **3-5** while MIPE **2** without modified silica particles was prepared as reference to study the effect of silylated silica filler on the mechanical properties of the resulting macroporous polymers. At the same time, HIPE **1** with only 20 vol.% of the continuous phase was prepared to investigate the effect of increasing foam density on the mechanical performance of resulting polyMIPEs.

6.3 Morphology and physical properties of macroporous polymers

The polymerisation of emulsion templates **1-5** produced non-chalky open porous interconnected polymers and the pore structure as can be seen in the SEM images (Figure 6-1). The incorporation of nanometre sized silylated silica particles into MIPEs **3-5** did not affect the interconnected open porous structure of the resulting macroporous polymers because the silylated particles were covalently incorporated into the polymer by copolymerisation of the grafted acrylate groups with the monomers [70]. The average values of pore and pore throat are summarised in Table 6-2. Increasing the organic phase volume from 20% to 40%, the average pore and pore throat size of polyMIPE **2** were slightly decreased. In analogy to the samples used in Chapter 5, the addition of higher concentration of silylated silica particles led

to the decrease of average pore diameter of polyMIPEs **2-5** from 8 μm (polyMIPE **2**) to 5 μm (polyMIPE **5**). In addition, the average pore throat size decreased from 1.6 μm (polyMIPE **2**) to 0.6 μm (polyMIPE **5**) (Table 6-2). Compared to the samples with identical recipes and prepared in Chapter 5, the pore and pore throat size of macroporous polymers **1-5** were same with considering error.

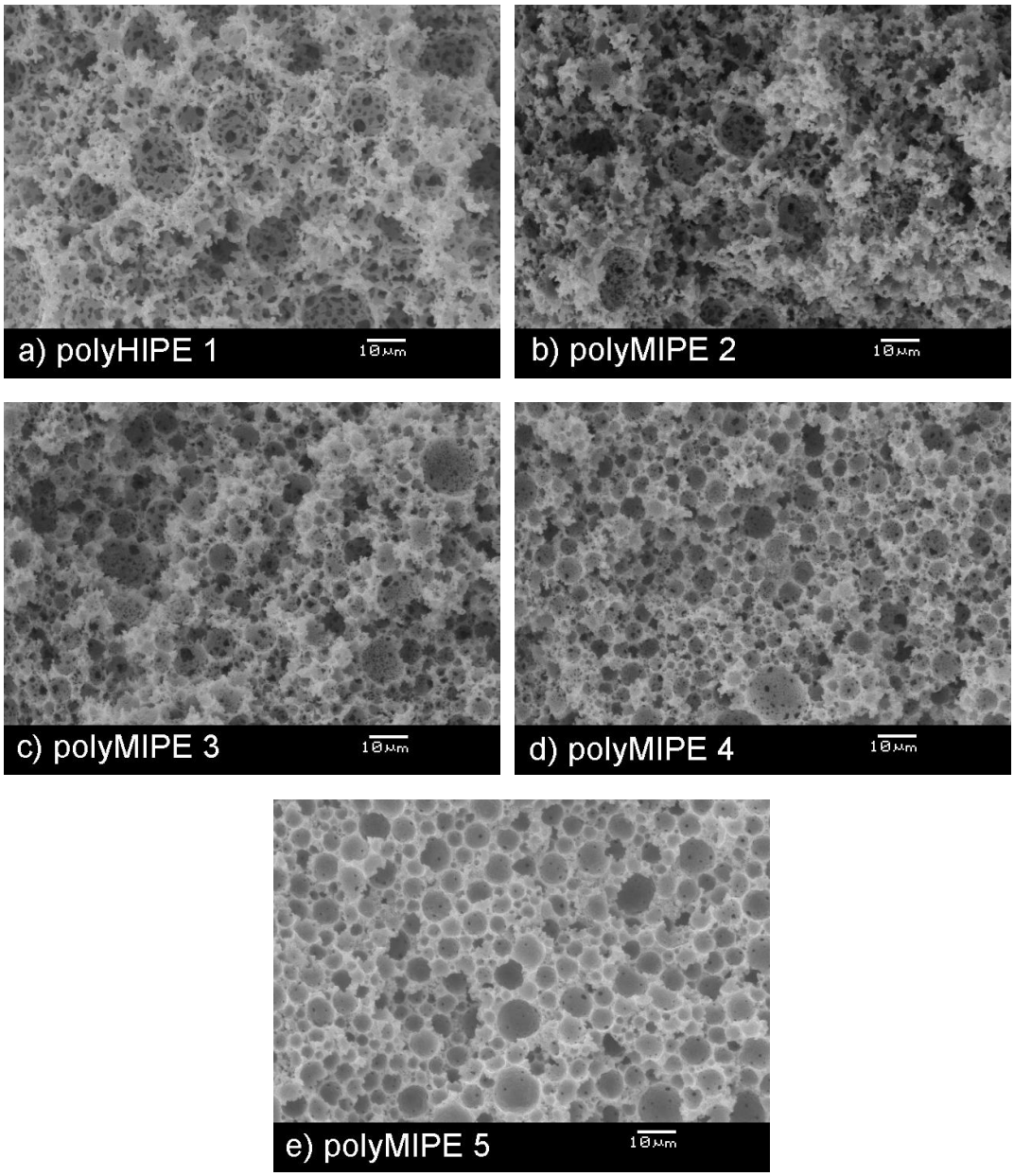

Figure 6-1 SEM pictures of poly(H)MIPEs

The density and porosity of these macroporous polymers are summerised in Table 6-2. The skeleton density of both polyHIPE **1** and polyMIPE **2** are almost identical within the errors since the skeleton density is the density of final polymer and, therefore, only depends on the composition of the organic phase in emulsion templates. However, the foam density of polyMIPE **2** was much higher than that of polyHIPE **1** due to the increase of organic phase level in the emulsion templates.

Table 6-2 Density and porosity results of macroporous polymers

Sample ID	Skeleton density (g/cm^3)	Foam density (g/cm^3)	Porosity (%)	Pore size (μm)	Pore throat size (μm)
1	1.086 ±0.003	0.183 ±0.003	83 ±1	10 ±4	2.0 ±0.7
2	1.101 ±0.002	0.346 ±0.005	69 ±1	8 ±3	1.6 ±0.6
3	1.147 ±0.001	0.353 ±0.007	69 ±2	6 ±2	1.0 ±0.4
4	1.167 ±0.001	0.385 ±0.006	67 ±2	5 ±2	0.8 ±0.3
5	1.216 ±0.001	0.402 ±0.009	67 ±1	5 ±2	0.6 ±0.2

The skeleton density of the synthesised macroporous polymers increased steadily from 1.101 g/cm^3 (polyMIPE **2**) to 1.216 g/cm^3 (polyMIPE **5**) (Table 6-2) due to the increasing concentration of silica particles within the polymer. The foam densities of polyMIPEs **2-5** increased slightly from 0.346 g/cm^3 (polyMIPE **2**) to 0.402 g/cm^3 (polyMIPE **5**). The porosities of polyMIPEs **2-5** were similar since all MIPE templates contained the same internal phase volume (Table 6-1, 6-2). The slight increase in porosities (68%) of polyMIPEs compared to the internal phase volume of emulsion templates (60%) is caused by the removal of non-converted monomers and the surfactant. Compared to the samples with identical recipes and prepared in Chapter 5, the porosities of macroporous polymers **1-5** were same with considering

error while the skeleton density and foam density of these synthesised macroporous polymers were similar but slightly lower.

6.4 Fractography of macroporous polymers

During failure, a crack propagates through the material, creating fracture features known as the mirror, mist, and hackle (Figure 6-2). The crack initially produces the smooth mirror region. However, as the crack accelerates it becomes more unstable, creating a surface known as mist. This instability eventually causes the crack to branch out, producing the rough hackle region [159].

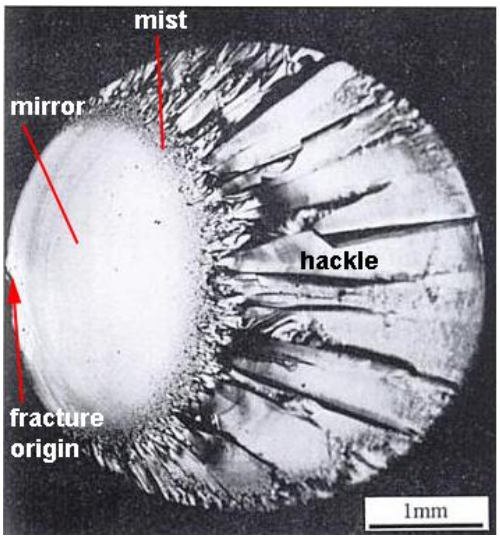

Figure 6-1 Typical mirror, mist and hackle regions on a fractured glass surface [159]

The hackle region is characterised by elongated markings that proceed in the direction of crack propagation and can often indicate the direction of loading and consequent movement of the matching fracture surface since the hackle markings point back to the fracture origin [160]. In addition, the hackle tilt angle also indicates the proportion of mode I (tensile mode) loading in a system. As the percentage of mode I decreases with respect to mode II (shear mode) the hackle tilt angle increases, from zero, in pure mode I to more than 45 °in pure mode II [161, 162].

Figure 6-3 shows the photos of the fracture surface of a macroporous polymer specimen under shear loading (Figure 6-3 (a)) tested using the Arcan jig (loading angle is 0°). The nearly 45° hackle tilt angle reflects the shear loading is the dominate loading and the fracture originates from the middle of specimen. However, some cracks with the tilt angle about 45° (Figure 6-3 (b)) can been seen from the fracture surface of a macroporous polymer specimen under tensile loading generated using the Arcan jig as well (loading angle is 90°), which indicates that not only pure tensile loading but also the shear loading was acting on the specimen using this loading condition in the Arcan jig.

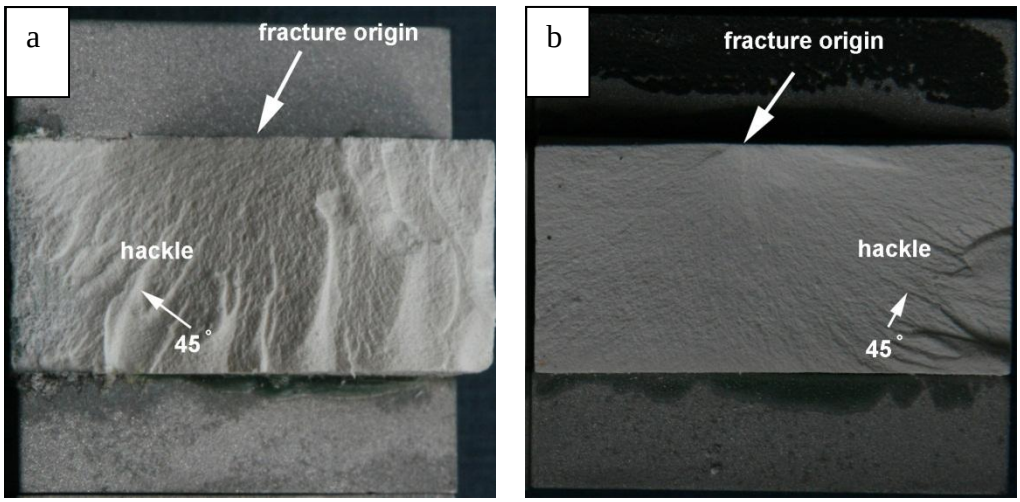

Figure 6-3 A typical fracture surface of macroporous polymers tested using the Arcan jig
(a) A typical fracture surface of a macroporous polymer under shear loading
(b) A typical fracture surface of a macroporous polymer under tensile loading

6.5 Shear and tensile properties of macroporous polymers

The investigation of shear properties of macroporous polymers was performed following the ASTM standard C-273 [142]. The specimen was firstly bonded between the steel loading plates. Then, the loading plates and bonded specimen were attached to the test machine and secured. During testing a linear variable

displacement transducer (LVDT) was used to measure the vertical specimen deflection, by measuring the difference in displacement along the length of the loading plates. Shear modulus can be calculated afterwards. However, the specimens were failed prematurely and no data can be obtained.

Therefore, the shear and tensile properties of all macroporous polymer monoliths were measured at room temperature under shear or tensile loads using the Arcan jig since the very heavy loading plates are not needed in this method. Pure shear was produced in the test region of the test specimen when load in the direction $\theta = 0°$ is applied while the specimen should have been loaded in tensile loading when load was applied in the direction of $\theta = 90°$ of the Arcan fixture. Both shear (tensile) moduli and strength were determined from the stress-strain curves (Figure 6-4, 6-5). The shear and tensile properties of polyH(M)HIPEs **1**-**5** are summarised in Table 6-3 and 6-4. All results were after compliance, which means displacement used to calculate the strain here was the displacement recorded minus the displacement caused by the test system.

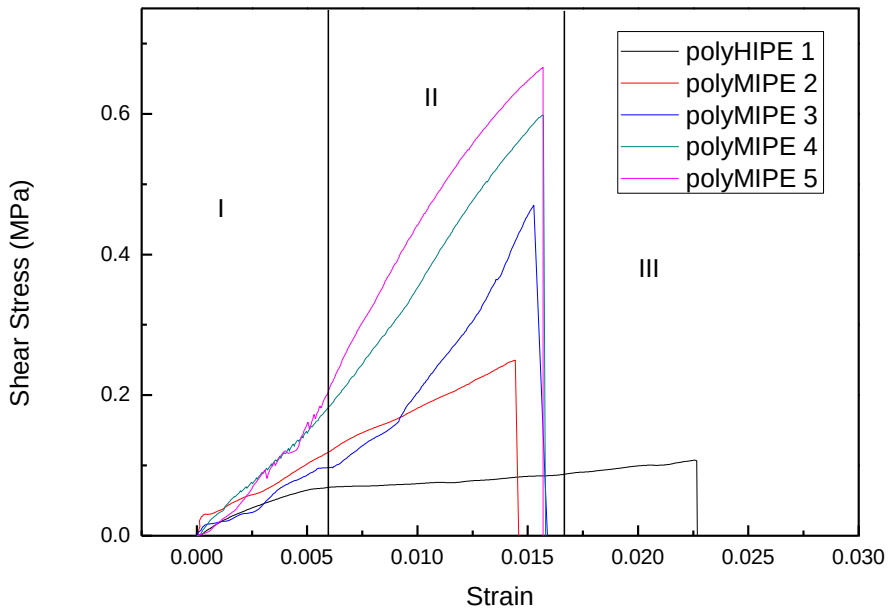

Figure 6-4 Typical stress-strain plot of polyH(M)IPEs 1-5 under shear load

Figure 6-4 shows representative shear stress-strain plot for polyH(M)IPEs **1-5**. Generally, there are three regions; the first is a fluctuant region which indicated the test instrument was undergoing some sort of adjustment. The second region is the linear region. The shear modulus is defined as the linear slope of the stress–strain plot and the shear strength is the maximum value of the shear stress–strain plot at the end of the linear region. After the peak of shear stress, the specimen completely broke and the shear stress suddenly dropped to zero.

Table 6-3 Shear properties of polyH(M)IPEs 1-5

Sample ID	Shear modulus (MPa)	Shear strength (MPa)	Specific shear modulus ($kPa\ kg^{-1}m^3$)	Specific shear strength ($kPa\ kg^{-1}m^3$)
1	3.14±0.37	0.10±0.02	19±2	0.55±0.06
2	18.47±1.3	0.25±0.05	54±6	0.72±0.1
3	45.36±3.4	0.51±0.10	128±10	1.44±0.3
4	49.75±3.4	0.59±0.10	129±12	1.53±0.3
5	52.37±4.6	0.65±0.12	129±24	1.62±0.5

The shear modulus of polyHIPE **1** was 3 MPa and its shear strength was only 0.10 MPa, which are much lower in comparison to polyMIPEs **2-5** due to the lower foam density. Increasing the foam density from 0.183 $g/cm^3$to 0.346 g/cm^3 or reducing the porosity from 83% to 69% resulted in a much increased shear modulus and shear strength of polyMIPE **2** compared to polyHIPE **1** (Table 6-2, 6-3). The shear modulus of polyMIPE **2** without any reinforcement increased by 600% to 18 MPa and the shear strength almost tripled to 0.25 MPa. Further improvement of shear properties was obtained by incorporating silylated silica particles into the polymer matrix of these polymers. It was shown [70] that the optimal concentration of the reinforcement was 20 wt.% relative to organic phase which can result in an improvement of the mechanical performance. Above this filler loading, it was more and more difficult to evenly distribute the silica filler within the resulting polymer foams. Both shear modulus and shear strength of polyMIPE **3** containing 5 wt.% of modified silica particles increased to 45 MPa and 0.51 MPa, respectively, due to the covalent incorporation of silylated silica particles into the pore walls. A further

increase in the loading fraction of modified silica particles from 5 wt.% to 20 wt.% led to a steady improvement of the shear moduli as well as shear strengths. However, the rate of increase in both shear modulus and shear strength significantly decreased with further increase of the silica content. PolyMIPE **4** which contains 10 wt.% of silylated particles exhibited slightly increased shear modulus (50 MPa) and similar shear strength (0.59 MPa) in comparison to polyMIPE **3**. PolyMIPE **5** with the highest silylated silica particle loading possessed a shear strength of 0.65 MPa. However, the shear modulus of polyMIPE **5** remained constant within the error compared to polyMIPE **4**. Specific shear moduli and specific shear strength (Table 6-3) were significantly increased firstly by increasing the organic phase volume from 20% to 40% and further improved by adding silylated silica reinforcement. However, the specific shear moduli and specific shear strength of polyMIPEs **3**-**5** remained similar within errors because the addition of more silylated silica reinforcement not only improved the shear properties but also increased the foam density of resulting macroporous polymers.

The significant enhancement of shear performance of these macroporous polymers followed the same trend to polyMIPEs made from the same formulation characterised under compressive load [70]. The observed improvement of the mechanical properties was a result of the covalent incorporation of silylated silica particles into the polymer matrix by copolymerisation of grafted MPS with the monomers.

Comparing to another foam material, which is widely used as core material in sandwich composites, PVC foams (Divinycell® H), polyMIPE **5** (52 MPa, 0.65MPa) exhibited similar shear modulus to Divinycell® H130 (50 MPa, 2.2MPa) but much

lower shear strength [163]. Furthermore, the foam density of Divinycell® H130 (0.13 g/cm$^{3)}$ is than that of polyMIPE **5** (0.40 g/cm^3) because the Divinycell® H130 is one type of close cell PVC foam while polyMIPE **5** is a type of open porous material.

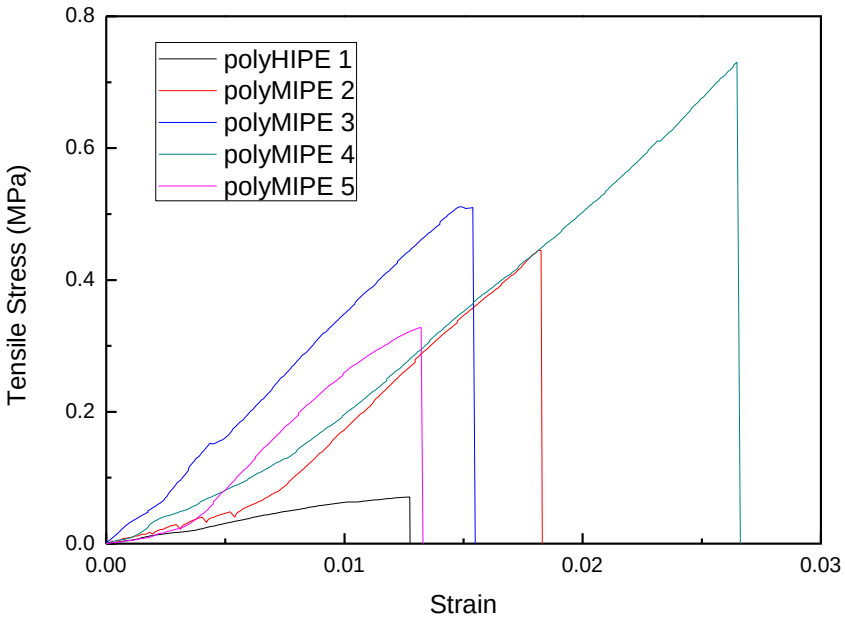

Figure 6-5 Typical stress-strain plot of polyH (M)IPEs 1-5 under tensile load

The mechanical performance of macroporous polymers under tensile loading was also studied and the results are summarised in Table 6-4. Figure 6-5 shows representative tensile stress-strain plots for polyH(M)IPEs **1**-**5**. In analogy to the shear stress-strain curves, there are three regions; the self-adjustment region of the test jig, the linear region and the specimen failure region. The tensile modulus is defined as the linear slope of the stress–strain plot and the tensile strength is the maximum value of the stress–strain plot at the end of the linear region.

Table 6-4 Tensile properties of polyH(M)IPEs 1-5

Sample ID	Tensile modulus (MPa)	Tensile strength (MPa)	Specific tensile modulus (kPa $kg^{-1}m^3$)	Specific tensile strength (kPa $kg^{-1}m^3$)
1	5.46 ±0.25	0.11 ±0.01	30 ±2	0.60 ±0.05
2	36.88 ±2.62	0.44 ±0.10	107 ±10	1.27 ±0.2
3	35.19 ±2.19	0.51 ±0.03	100 ±8	1.44 ±0.1
4	34.20 ±3.83	0.72 ±0.10	89 ±14	1.87 ±0.3
5	32.62 ±4.06	0.33 ±0.05	82 ±18	0.82 ±0.2

PolyHIPE **1** had a very low tensile modulus of only 5.46 MPa and tensile strength of only 0.11 MPa. Increasing the foam density, i.e. reducing the porosity of a polyHIPE to polyMIPEs resulted in a significant improvement of the tensile modulus and tension strength. The tensile modulus of polyMIPE **2** without reinforcement increased to 37 MPa and tensile strength to 0.44 MPa. However, the addition of silylated silica reinforcement seems did not lead to a further improvement of the tensile moduli or the strengths. Although the silica filler concentration increased from 0 to 20 wt. %, the tensile moduli of polyMIPEs **2-5** were similar within error. Furthermore, the tensile strengths of polyMIPE **2-5** fluctuated between 0.3 MPa and 0.7 MPa and did not follow a clear trend. Specific tensile moduli and specific tensile strength of macroporous polymers **1-5** (Table 6-4) increased by increasing the foam density. However, the introduction of silylated silica particles did not further improve the specific tensile moduli or specific tensile strength of polyMIPEs **2-5**. In principle, the Arcan jig should produce pure tension loading in the direction $\theta = 90°$. However, in practice, as indicated by the fractography, some shear component was also observed in the test. The real loading is mixed-mode loading and may cause

premature failure of the specimen. As a result, the tensile properties of polyMIPEs **2-5** did not exhibit a clear trend.

6.6 Fracture toughness of macroporous polymers

Another objective of this study was to investigate the fracture toughness of macroporous polymers. Fracture toughness is a property which describes the ability of a material containing a crack to resist fracture and is one of the most important properties of any material for virtually all design applications. In this study, the fracture toughness was assessed by determining the stress intensity factor (K_{II}) at fracture under shear mode.

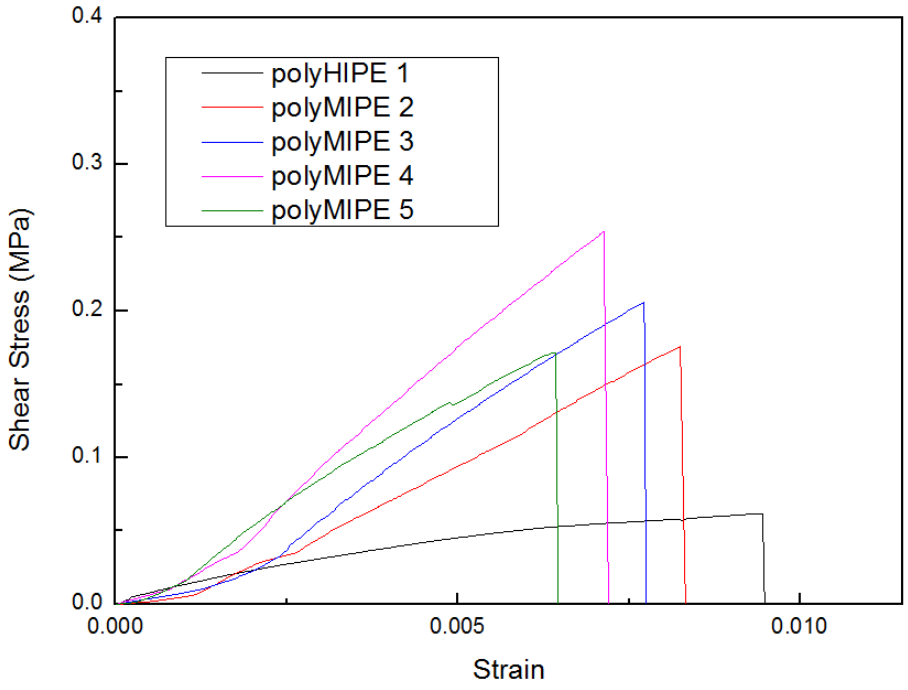

Figure 6-6 Typical stress-strain plot of polyH (M)IPEs 1-5 in fracture toughness tests

Figure 6-6 shows representation shear stress-strain polts for polyH(M)IPEs under the shear fracture toughness measurements. Similar to the stress-strain plots for polyH(M)IPEs in shear and tensile loads (Figure 6-4, 6-5). There are three regions;

the self-adjustment region of the test jig, the linear region and the specimen failure region.

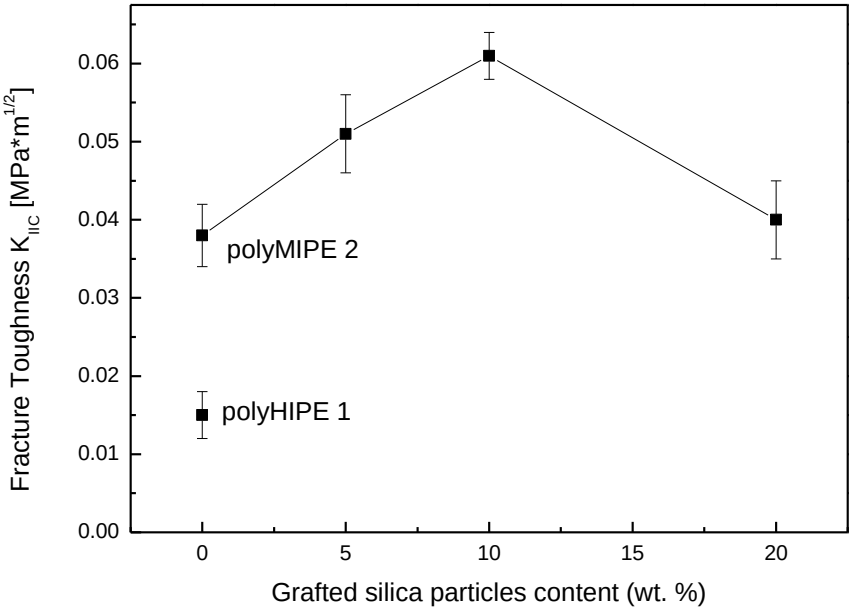

Figure 6-2 The fracture toughness of polyH(M)IPEs 1-5

Due to the increase of the foam density, the fracture toughness of polyMIPEs **2-5** was higher than that of polyHIPE **1** (Figure 6-7). Even the fracture toughness of polyMIPE **2** without reinforcement was increased in comparison to polyHIPE **1** from 0.015 MPa*m$^{1/2}$ to 0.038 MPa*m$^{1/2}$. The incorporation of silylated silica particles and their incorporation into the polymer walls of the macroporous polymers led to a further improvement of the fracture toughness of these macroporous composites. Even the introduction of 5 wt.% of silylated silica particles resulted in the fracture toughness of polyMIPE **3** to increase to 0.051 MPa*m$^{1/2}$. PolyMIPE **4** (0.061 MPa*m$^{1/2}$) which containing 10 wt.% of reinforcement showed a slight increase in fracture toughness in comparison to polyMIPE **3**. However, continuous increasing of silica filler up to 20 wt. % did not lead the further a increase in fracture toughness

and it slightly decreased to 0.040 MPa*$m^{1/2}$. According to these results, the optimal content of the reinforcement seems to be between 10 and 20 wt.%, which followed the same trend obtained from compression tests of the same formulation macroporous polymers [70], as the resulting macroporous polymers showed impressive fracture properties in comparison to other concentrations of the reinforcement.

Comparing to the closed cell PVC foams, poly(H)MIPEs **1**-**5** possessed much lower mode II fracture toughness due to the open porous microstructure. Noury et. al. [164] found that the mode II fracture toughness for C70.200 foam was 0.236 MPa*$m^{1/2}$ average and Grenestedt et. al. [165] found that the mode II fracture toughness of H100 PVC foam was 0.206 MPa*$m^{1/2}$.

6.7 Summary

In summary, significant improvements of both shear and tensile properties of macroporous polymers are achieved by raising the organic phase volume of the emulsion templates and therefore the foam densities. Further improvement of shear properties was obtained by the incorporation of silylated silica particles into the walls of the macroporous polymers without affecting the interconnected microstructure. However, the tensile properties of polyMIPEs **2**-**5** determined using the Arcan test showed that the addition of modified silica particles did not result in further improvements of both tensile modulus and tensile strength, which is different from the trend obtained in both compressive and shear properties of these macroporous polymers with the same formulation. These results demonstrate the Arcan test is suitable to investigate the shear properties of macroporous polymers but

is not reliable to determine the tensile properties of these macroporous polymers as no pure tensile load can be introduced into the specimen. The fracture toughness in shear mode was also investigated. Increasing the foam density resulted in a significant increase of the fracture toughness and the introduction of silylated silica particles in the polymer matrix led to further improvements of the fracture toughness.

7 Investigation of the wetting properties of styrene and DVB based macroporous polymers

7.1 Introduction

The macroporous polymers produced from HIPEs, especially using the water-in-styrene/DVB HIPEs are usually hydrophobic and are impeded in some applications such as bioengineering. In order to solve the problem, three routes are commonly used to synthesise hydrophilic polyHIPEs. The first route is post modifying hydrophobic polyHIPEs based on styrene/DVB after polymerisation using a second synthesis stage. For example, the poly(St-DVB)HIPEs have been modified by electrophilic aromatic substitution to yield nitro-, bromo- and sulfonic acid substituted materials [16] or plasma treatment [166]. Comparing to the two-step process, synthesising hydrophilic monomers within o/w I-HIPEs produces hydrophilic polyHIPEs directly. However, I-HIPEs are often more difficult to stabilise than w/o HIPEs [39] and uneconomic since the procedure is extremely solvent intensive. The oil template phase is difficult to remove after polymerisation. Furthermore, limited amount of monomers can be dissolved in the aqueous phase and the method to avoid portioning of the monomer into the oil phase needs to be explored. The third route is synthesising hydrophilic polymer/polymer composites within w/o HIPEs using a single synthesis stage [50-55]. In this route, the continuous organic phase normally contains hydrophobic monomers while the dispersed aqueous phase consists of hydrophilic monomers, N,N-methylenebisacrylamide (MBA) and acrylamid (AM). Hydrophobic and hydrophilic monomers within the

external phase and the internal phase are simultaneously polymerised to produce hydrophilic polyHIPEs. The aim of present research is to develop hydrophilic macroporous polymers based on styrene and DVB using a single synthesis stage. In order to achieve the objective, methacrylic acid (MA) and dimethylaminoethyl methacrylate (DMAEMA) were introduced into the aqueous phase of emulsion templates to manufacture polymer/polymer composites. Furthermore, MPS modified silica particles, which were proven can improve the mechanical performance of resulting macroporous polymers (Chapter 5 and 6), were also added in the continuous phase to investigate their influence on the surface properties of resulting macroporous polymers.

7.2 Summary of sample formulations

Both MIPEs and HIPEs were prepared and they all contained styrene and DVB as monomers. The continuous phase of all emulsion templates consisted of 80 vol. % of monomers, 20 vol. % of Hypermer 2296 as surfactant and 2 mol.% of AIBN as initiator. Furthermore, MIPE **2** contained 40 wt. % silylated silica particles in the continuous phase with respect to the monomers while MIPE **1** did not contain any silylated silica particles. MA or DMAEMA as additional monomers were added to the aqueous phase of HIPE **4** and **5**, respectively while HIPE **3** contained nothing in the aqueous phase as reference. In order to transfer these monomers from the aqueous phase to the organic phase, a suitable pH value of the aqueous phase was chosen to form the corresponding monomer salts (pH 11 and pH 1 respectively). After polymerisation of these emulsions, the macroporous polymers **1-5** were produced. The sample preparation procedure was presented in Chapter 3.3 and 3.4. The compositions of the emulsion templates are summarised in Table 7-1.

Table 7-1 Composition of the emulsion templates

Sample ID	Organic phase volume [a]	Organic phase composition Styrene/DVB/Surf. (vol.%)[b]	Aqueous phase composition MA/DEAEMA (vol.%)[c]	Silylated silica particles (wt.%) [d]
1	40	60/20/20	0/0	0
2	40	60/20/20	0/0	40
3	20	40/40/20	0/0	0
4	20	40/40/20	6/0	0
5	20	40/40/20	0/6	0

[a] Volume of the organic phase relative to the total volume of the emulsion

[b] Composition of the organic phase, DVB, styrene and surfactant ratio

[c] Content of MA, DMAEMA in the aqueous phase

[d] wt. % filter relative to the monomers

7.3 Result and Discussion

MIPEs **1** and **2** contained 40 vol.% of the continuous phase while the continuous phase of HIPEs **3-5** occupied 20 vol.% of the emulsion volume. The HIPEs **3-5** were much more viscous compared to MIPEs **1** and **2** because of the increased dispersed phase volume which leads to a denser droplet packing [18]. All emulsions were stabilised by the nonionic, polymeric surfactant Hypermer 2296 containing ethoxylated ester with a HLB value of 4.9.

After polymerisation, all resulting polymer foams were white porous monoliths. The macroporous polymers possessed an open porous interconnected pore structure as can be seen in the SEM images (Figure 7-1). The different magnification of each image is because the image should provide the information about the single pore and

enough numbers of pores in order to prove the interconnected microstructure of these macroporous polymers. The average values of pore and pore throat sizes were analysed by UTHSCSA Image tool software and at least 50 pores (pore throats) were measured and summarised in Table 7-2. The pore diameters of polyMIPE **1** ranged from 2 to 4 μm and the pore throat diameter was approximately 1 μm. The incorporation of silylated silica particles did not affect the interconnected open porous structure of the polyMIPEs **2,** the silylated particles were covalently incorporated into the growing polymer by copolymerisation of silylated silica particles with the monomers. Comparing to polyMIPE **1**, the average pore size of polyMIPE **2** significantly increased from 3 μm to 6 μm. Furthermore, the average pore throat size increased from 0.9 μm to 1.3 μm. The pore size distribution of polyMIPE **2** was much wider than that of polyMIPE **1** (Table 7-2). Due to the addition of 40 wt.% silylated silica particles in the continuous phase of MIPE **2**, MIPE **2** was observed to be more viscous than MIPE **1.** The high viscosity of MIPE **2** may be a result from particle flocculation in the organic phase of MIPE **2**. When stirring emulsions during the preparation process; the same shear stress of mixing was insufficient to separate all large droplets in MIPE **2** because of the high viscosity. As a result, it is difficult to generate a uniform, fine dispersion of the droplets in highly viscous emulsion templates. Since the porous structure of polyHIPEs is a replica of the emulsion structure at the gel point of the polymerisation [13, 131], polyMIPE **2** showed larger pore size and wider pore size distribution.

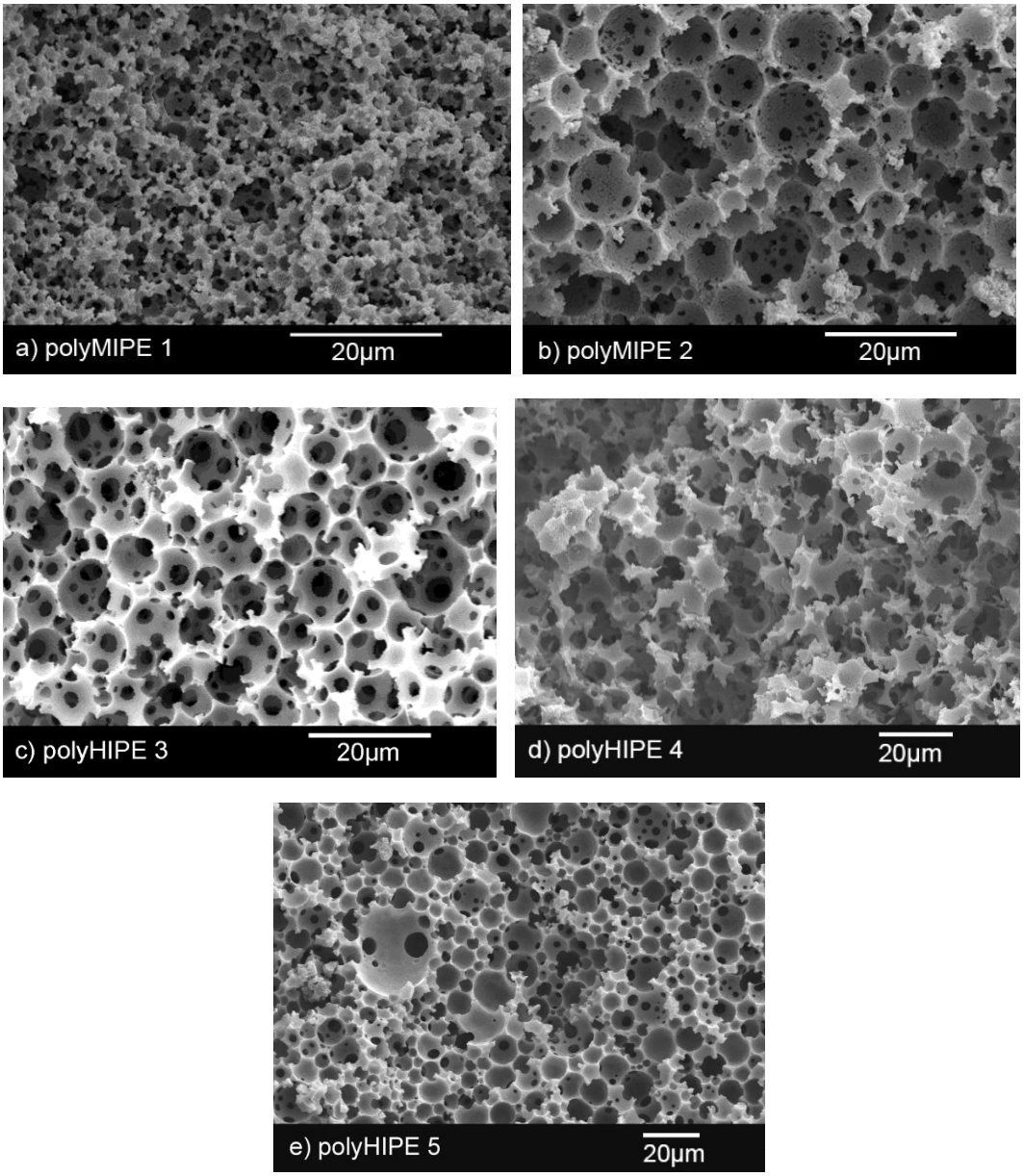

Figure 7-1 SEM images of macroporous polymer foams 1-5

HIPE **3** did not contain silica particles or other additional monomers except styrene and DVB to polymerise while HIPE **4** contained MA in the aqueous phase as additional monomer to copolymerise with styrene and DVB and HIPE **5** contained DEAEMA in the aqueous phase as an additional monomer. The resulting polyHIPE **3** and polyHIPE **4** possessed an interconnected pore network structure. PolyHIPE **3** had pores with diameters ranged from 6 to 9 µm and the pores interconnected via pore throats of approximately 3.0 µm in diameter. The pore size of polyHIPE **4**

ranged from 7 to 11 μm and the pores interconnected via pore throats of approximately 3.7 μm in diameter (Table 7-2). The resulting polyHIPE **5** again had an open porous structure. The pore diameter of polyHIPE **5** varied between 4 μm and 12 μm and the pore throat size ranged from 1.3 μm to 3.7 μm. The high viscosity of HIPEs **3-5** led to the lager pore sizes of resulting macroporous polymers compared to polyMIPE **1** and **2**.

In contrast to the highly interconnected structure of polyHIPE **3** and **4**, some pore throats of polyHIPE **5** seemed to be covered by a polymer film since the polymerisation of HIPE **5** led to a formation of polymer/polymer composite. The polymerisation first started in the organic phase and produced free radicals. Afterwards, some free radicals near the interface between the organic phase and the aqueous phase triggered the polymerisation of DMAEMA. The polyDMAEMA hydrogel was grafted to the poly(St-DVB)HIPE "scaffold" and produced the polymer/polymer composite. HIPE **4** also contained MA as additional monomer but exhibited highly interconnected structure. The difference in morphology revealed the different polymerisation principles. In copolymersation systems, containing at least two different monomers (M_1 and M_2) and each monomer has the possibility to homopolymerise with itself and the possibility to copolymerise with other monomers (Scheme 7-1). These possibilities are described by copolymerisation reactivity ratios r_1 (defined as the ratio of k_{11} / k_{12}) and r_2 (defined as the ratio of k_{22} / k_{21}), which are important quantitative parameters in the prediction of copolymer composition.

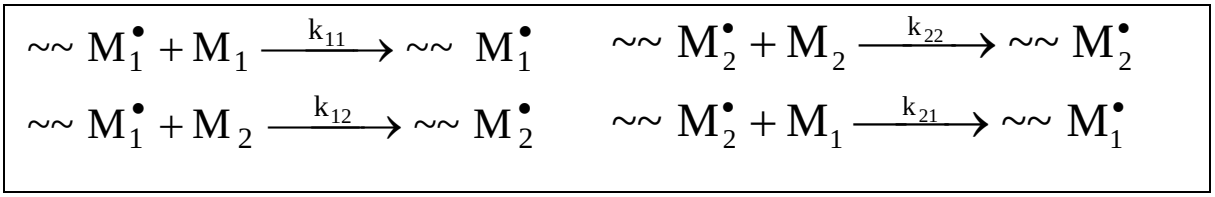

Scheme 7-1 Definition of copolymerisation reactivity ratios

In this case, the continuous phase consists of styrene and DVB as monomers and the the aquous phase contains MA or DMAEMA as additional monomer. For the styrene/DVB system, r_1 =0.26 and r_2 =1.18 [151], which means both styrene and DVB are prone to polymerise with DVB. At the same time, for the styrene/MA system, r_1 = 0.21 and r_2 = 0.55 [151]. This indicates both styrene and MA are prone to polymerise with others and led to a formation of styrene/MA network. Therefore, the residual styrene copolymerises with MA. Consequently, polyHIPE **4** possesses a highly interconnected structure. Turn to the styrene/DMAEMA system, r_1 = 1.74 and r_2 = 0.43 [167]. This means both styrene and DMAEMA are prone to polymerise with styrene. Styrene is consumed first and the residual DMAEMA can only polymerise with itself forming the DMAEMA hydrogel to cover part of the pores of polyHIPE **5**. Consequently, part of pore throats of polyHIPE **5** were covered by a polyDMAEMA film.

Table 7-2 Physical properties of macroporous polymer foams 1-5

Sample ID	Pore size (μm)	Pore throat size (μm)	Skeleton density (g/cm^3)	Foam density (g/cm^3)	Porosity (%)	Surface area (m^2/g)
1	3±1	0.9±0.2	1.010±0.002	0.307±0.002	70	4.103±0.011
2	6±3	1.3±0.3	1.326±0.007	0.379±0.002	71	3.055±0.006
3	9±3	3.0±1.0	1.160±0.006	0.144 ±0.003	87	4.700±0.100
4	9±2	3.7±1.4	1.250±0.002	0.165±0.005	86	2.410±0.013
5	8±4	2.5±1.2	1.216±0.002	0.225±0.002	82	3.190±0.016

The addition of silylated silica particles into the continuous phase of MIPE **2** led to the skeleton density increase from 1.010 g/cm^3 (polyMIPE **1**) to 1.326 g/cm^3 (polyMIPE **2**) (Table 7-2). Furthermore, the foam density was increased from 0.307 g/cm^3(polyMIPE **1**) to 0.379 g/cm^3(polyMIPE **2**). However, the porosities of these

two macroporous polymers were similar since both emulsion templates contained the same volume of internal phase, which was the same in both formulations (70%). The slight increase in porosities (70%) of polyMIPEs **1** and **2** compared to the internal phase volume of the emulsion templates (60%) is caused by the removal of non-converted monomers and the surfactant. PolyHIPE **3** possessed a lower skeleton density of 1.160 g/cm^3 compared to polyHIPEs **4** (1.250 g/cm^3) and polyHIPEs **5** (1.216 g/cm^3). The increase of the internal phase level from 60 vol.% to 80 vol.% led to a decrease of foam density of polyHIPEs 3 (0.144 g/cm^3), **4** (0.165 g/cm^3) and **5** (0.225 g/cm^3) and an increase of the porosity of polyHIPEs **3** (87%), **4** (86%) and **5** (82%) in comparison to polyMIPEs **1** and **2.** The surface area of macroporous polymers **1-5** ranged from approximately 2 to 5 m^2/g, which are within the range of surface areas commonly reported for polyHIPEs [16, 167].

The wetting behaviour of macroporous polymers was investigated using both water contact angle and Dynamic Vapour Sorption (DVS) measurements. The static contact angle was measured in the static mode, 10s after placing a water droplet into the surface of macroporous polymers at room temperature. The results were summerised in Table 7-3. The nearly spherical water droplet on polyMIPE **1** in Figure 7-2 (a) (a contact angle of around 140 °) reflected the hydrophobicity of polyMIPE **1**. The water droplet did not wet the walls of the hydrophobic styrene/DVB polyMIPE **1** and, therefore, water was not being absorbed into it through capillarity. In this case, the Cassie–Baxter equation describes the effective contact angle θ_c for a liquid on a composite surface and the effective contact angle (θ_c) is related to the contact angles (θ_1, θ_2) and fractions (f_1, f_2) of exposed components on the solid surface of the composite.

$$\cos\theta_c = f_1 \cos\theta_1 + f_2 \cos\theta_2$$

In this case, the surface of polyMIPE **1** consisted of air, which the contact angle of water in air (θ_1) is 180 °, and poly(St-DVB), whose contact angle of water is 103 ° [168]. The fractions of the both component were determined by the porosity test. The expected contact angle is 140 °, which is similar as the experimental values of polyMIPE **1**. However, the water droplet on the polyMIPE **2** in Figure 7-2 (b) spread extensively on the polyMIPE **2** surface and most of its volume had penetrated into the macroporous polymers (a contact angle of around 26 °). The wettability of pore walls of the macroporous polymer was enhanced by the addition of silylated silica particles in the continuous phase of MIPE **2** and the water droplet was drawn into polyMIPE 2 by capillarity.

Table 7-3 Wetting behaviour of macroporous polymer foams 1-5

Sample ID	Water Contact angle (°)	Equilibrium moisture content (%)
1	142±2	2.2
2	26±4	1.5
3	144±2	1.7
4	137±2	57
5	19±5	37

As discussed previously, MA and DMAEMA were introduced into the aqueous phase of HIPEs **4** and **5** to produce polymer/polymer composites while HIPE **3** did not contain the additional monomers. Similar to polyMIPE **1**, the water droplet did not wet the walls of the hydrophobic styrene/DVB polyHIPE **3** and average contact angle is 144 ° (Figure 7-2(c)). The resulting macroporous polymers from HIPEs **4** and **5** should be hydrophilic since the pore walls contain hydrophilic monomers. The water droplet spread extensively on the surface of polyHIPE **5** and the average contact angle is around 20 °(Figure 7-2(e)) due to the introduction of DMAEMA.

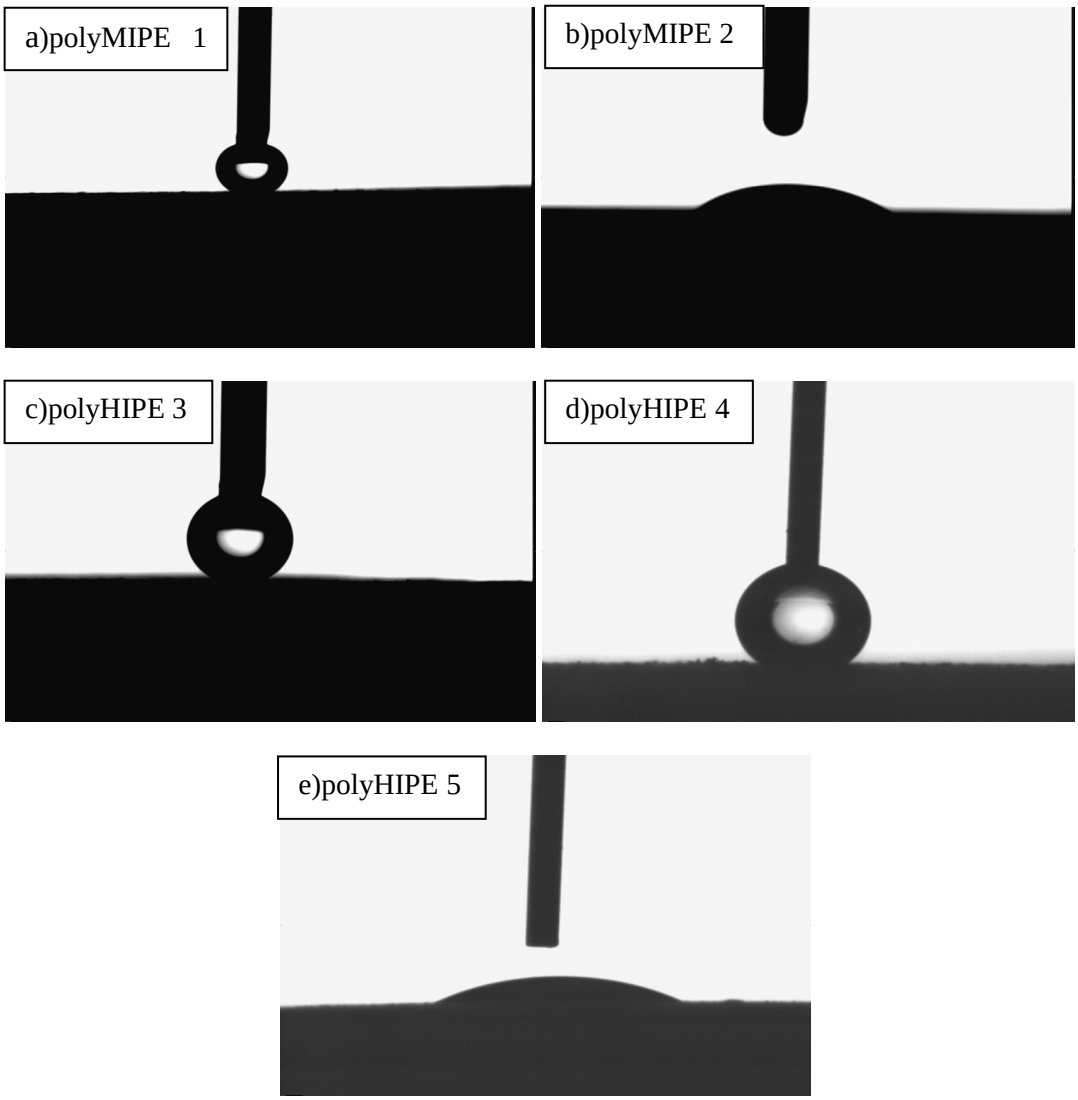

Figure 7-2 Pictures of water droplet on the surface of polyfoams 1-5

However, the introduction of MA did not appear to promote the spreading of the water droplet into the surface of polyHIPE **4** and the contact angle is still around 140 ° (Figure 7-2 (d)). As discussed previously, styrene, DVB and MA are prone to copolymerise and the surface of polyHIPE **4** consists of air and poly(St-DVB-MA). However, polyHIPE **5** it seems did not form poly(St-DVB- DMAEMA)HIPE since part of the pores were covered by poly(DMAEMA) film. Wetting is determined by the surface composition. MA formed intra/intermolecular hydrogen bonds between the methacrylic acid moieties and so exposed a hydrophobic polymer backbone in air, which means a higher initial contact angle of polyHIPE **4**. In contrast, no

hydrogen bonds formed for polyHIPE **5** and the hydrophilic hydrogel was exposed and resulted in the low values of the average contact angle of polyHIPE **5**.

Besides the contact angle measurements, DVS studies were carried out to investigate the water absorption of macroporous polymers **1**-**5** at 95% RH. The completely dried sample was put into 95% RH for 24h. The mass change was monitored until constant. The mass change was recorded and is summarised in Table 7-3. The water uptake of the silylated silica particle was also determined and the equilibrium moisture content after conditioning is only about 1.3 wt.%. The 2 wt.% of equilibrium moisture content reflected the hydrophobility of polyMIPE **1**, which is in accordance with the result obtained from water contact angle measurements. However, polyMIPE **2**, which had a water contact angle of only 26 °, did not absorb much water and only around 1.5 wt.% of equilibrium moisture content was detected. Comparing to polyMIPE **1**, the decrease of water contact angle value of polyMIPE **2** was caused by the addition of silylated silica particles, which promoted the spreading of water droplet on the surface of polyMIPE **2**. Consequently, the water droplets penetrated into polymer walls by capillarity. In other words, the addition of silylated silica particles into the emulsion templates improved the wettability but the resulting macroporous polymers still cannot absorb much water since the silylated silica particles are not adsorbing water.

PolyHIPE **3** only possessed 1.7 wt.% of equilibrium moisture content but polyHIPEs **4** and **5** exhibited significant water absorption due to the addition of hydrophilic monomers into the aqueous phase of HIPEs **4** and **5**. The equilibrium moisture content reached 57 wt.% (polyHIPE **4**) and 37 wt.% (polyHIPE **5**), respectively. Comparing to the water contact angle measurements of polyHIPEs **4** and **5**,

polyHIPE **5** possessed a contact angle around 20 ° and reflected the hydrophilicity of the macroporous polymer, which was confirmed in the DVS study. On the other hand, the equilibrium moisture content of polyHIPE **4**, which showed a contact angle of around 140 °, reached 57 wt.%. The high initial values of contact angle of polyHIPE **4** is because MA formed hydrogen bonds and exposed a hydrophobic backbone to the composite surface, which determines the wetting. The formation of composite surface, which includes mostly air does not allow for fast swelling but the water vapour does interact with MA and lead to the high water uptake.

7.4 Summary

Generally, the macroporous polymers based on styrene and DVB resulted from w/o emulsions are hydrophobic and need modification after polymerisation to improve the surface hydrophilicity. The objective of the present research was to synthesise hydrophilic macroporous polymers based on styrene and DVB directly via emulsion templating. Silylated silica particles and hydrophilic monomers were introduced in the emulsion templates. The incorporation of silylated silica particles did not affect the interconnected microstructure but enhanced the wettability and mechanical performance of resulting macroporous polymers (polyMIPE **2**). Water droplets are drawn into the polymer walls by capillarity. However, the water absorption of the resulting macroporous polymer did not increase by the introduction of silylated silica particles because the silylated silica particles do not absorb water. MA and DMADMA were introduced into the aqueous phase of emulsion templates as additional monomers in order to produce hydrophilic polymer/polymer macroporous composites. MA was successfully incorporated into the polymer by the copolymerisation with styrene and DVB and the resulting macroporous polymer

(polyHIPE **4**) showed highly interconnected microstructure. The nearly 60 wt.% of equilibrium moisture content of polyHIPE **4** reflected the improved hydrophilicity. However, the spherical shape of water droplets on the polyHIPE 4 surface according to contact angle measurement indicated the poor wettability due to the formation of MA hydrogen bonds, which caused the surface in air to appear hydrophobic. The formation of a composite surface (including air) on the polyHIPE **4** prevents sufficient contact with water, which does hinder water uptake if the macroporous polymer is in contact with liquid water. The introduction of DMAEMA resulted in hydrophilic macroporous polymer (polyHIPE **5**) with low contact angle value (around 20) and high water adsorption (about 37 wt.% equilibrium moisture content) due to no formation of hydrogen bonds. PolyHIPE **5** showed an open porous structure but part of the pore throats were covered by polyDMAEMA film.

8 Conclusion and recommendation for future work

8.1 Conclusions

This thesis describes the development and characterisation of tough and permeable macroporous nanocomposites via emulsion templating. The influence of different initiators and surfactants used in MIPE formulations on the morphology and physical properties of the resulting macroporous polyMIPEs was initially investigated to optimise the formulation of MIPEs based on styrene and DVB. Three types of initiator including AIBN, KPS and redox initiator system and four different surfactants (surfactant mixture) containing Hypermer 2296, Span 80 and even surfactant combination such as Hypermer 2296/Span 80 mixture and Hypermer 2296/ Hypermer B246sf mixture were used to stabilise the emulsion templates. AIBN is a good initiator for the polymerisation of MIPEs consisting of styrene and DVB to produce macroporous polymers possessing the desired open porous interconnected microstructure no matter which surfactant (surfactant mixture) was used. The widely used water-soluble KPS was also used and produced macroporous polymers with almost closed cell microstructure no matter which surfactant (surfactant mixture) was used. This closed cell pore structure of the polyMIPEs was believed to be caused by the high radical concentration produced by the decay of KPS at 70 ℃, which results in the fast formation of a solid closed cell skin (shell) surrounding the water droplets, which suppressed the formation of pore throats. The polymerisation of MIPEs based on styrene and DVB can be initiated by a redox initiator system, which consisted of iron (II) sulfate heptahydrate, L-ascorbic acid

(reducing agent) and hydrogen peroxide (oxidising agent). Although the resulting macroporous polymers possessed an interconnected pore structure thick walls were found. Different surfactants perform differently in the stabilisation of a MIPE containing the redox initiator system. It appears that Span 80 is the most suitable surfactant solely based on the degree of interconnectivity of the resulting polyMIPEs. However, it seems Hypermer B246sf is the better surfactant based on pore structure of the resulting polyMIPEs.

Subsequently, AIBN was chosen as initiator and the Hypermer B246sf was used as surfactant for the emulsion templates in order to develop interconnected high porosity macroporous polymers with significantly improved mechanical properties compared to conventional polyHIPEs. PEGDMA was used instead of DVB as crosslinker to copolymerise with styrene in order to reduce the brittleness of the resulting macroporous polymers. Two strategies were used to improve the mechanical performance of macroporous polymers produced by the polymerisation of the continuous phase of the emulsion templates. Firstly, silica particles silylated with MPS were added into the organic phase of the emulsion templates to act as reinforcement for and additional crosslinker of the polymer matrix. Secondly, the organic phase volume of the emulsion templates was increased from 20 vol.% (HIPEs) to 40 vol.% (MIPEs) in order to increase the foam density of resulting macroporous polymer monoliths. The addition of reinforcement into the organic phase increased, rather than negatively affected, the stability of the HIPE templates. The silylated silica particles were successfully incorporated into the growing polymer and the produced macroporous polymer composites were open porous and permeable. Furthermore, the silylated silica particles acted as reinforcement and significantly improved both the compression modulus and crush strength in

comparison to the polyH/MIPEs without reinforcement. Both the compression modulus and the crush strength increased by 600% compared to non-reinforced polyHIPEs.

Increasing the foam density is another effective method to improve the mechanical properties of these macroporous polymers and so polyMIPEs were also prepared. The macroporous polymers synthesised from these less concentrated emulsion templates are also open porous and permeable. Compared to polyHIPEs, the overall mechanical performance of resulting macroporous polymers significantly increased. Further improved mechanical performance of these macroporous polymers can be achieved by the incorporation of MPS functionalised silica in the continuous phase of emulsion templates. Compared to the polyHIPE without any reinforcement, the compression modulus of polyMIPE containing 60 wt.% of silica reinforcement was increased from 3 MPa to 110 MPa and the crush strength was increased from 0.2 MPa to 4.3 MPa.

The brittleness and chalkiness of conventional polyHIPEs leads to the poor shear properties of these macroporous polymers. However, until now, no literatures discuss the investigation of the shear properties of these macroporous polymers exists. The shear properties of macroporous polymers via emulsion templating were determined using the Arcan test. Furthermore, the tensile properties and the fracture toughness in mode II (shear) loading were also investigated. Increasing the organic phase volume of the emulsion templates substantially improved both shear and tensile performance of emulsion templated macroporous polymers. The shear modulus of polyMIPE with a porosity of 69% increased by 6 times to 18 MPa and the shear strength also increased approximately 3 times to 0.25 MPa in comparison

to polyHIPEs with a porosity of 83%. The tensile modulus was also significantly improved from 5.46 MPa to 36.88 MPa as a result of increasing the foam density from 0.183g/cm^3 to 0.346g/cm^3 of resulting macroporous polymer monoliths produced from emulsion templates. The addition of silylated silica particles into the emulsion templates led to further improvements in the shear properties of the resulting macroporous polyMIPEs due to the incorporation of particles into the pore walls. The shear modulus was improved from 18 MPa to 52 MPa with increasing the silica filler up to 20 wt.%. However, the tensile properties obtained using the Arcan test showed no further improvement with the addition of modified silica reinforcement because pure tensile loading could not be introduced into the specimens. Determination of the mode II (shear) fracture toughness was another objective of this study. The values of fracture toughness determined increased significantly with increased organic volume of the emulsion templates, and, therefore reduced porosity but increased foam density of the resulting macroporous polymers and again when silica particles were added. The addition of increasing amounts of silica particles resulted in further increases in the fracture toughness. Compared to other PVC foams, the emulsion templated macroporous polymers possessed much lower mode II (shear) fracture toughness because PVC foams are closed cell foam while emulsion templated macroporous polymers are open porous.

Finally, approaches to directly synthesise hydrophilic macroporous polymers based on styrene and DVB were presented since most of macroporous polymers produced from HIPEs are hydrophobic and need modification after polymerisation to improve the surface wettability. Silylated silica particles and hydrophilic monomers, MA and DMAEMA, were introduced into the emulsion templates in order to directly synthesise hydrophilic macroporous polymers based on styrene and DVB via

emulsion templating. The incorporation of silylated silica particles did not affect the interconnected microstructure of resulting macroporous polymer. In addition, the wettability of the pore surface was enhanced so water droplets penetrated into the pore space of the macroporous polymers. MA and DMADMA were introduced into the aqueous phase of emulsion templates as additional monomers in order to synthesise hydrophilic polymer/polymer macroporous composites. MA was successfully incorporated into the polymer by copolymerisation with styrene and DVB and the resulting macroporous polymer possessed a highly interconnected microstructure. The polyHIPEs containing polyMA took up nearly 60 wt.% of moisture in equilibrium with 95% RH, which reflected the improved hydrophilicity. However, the high value of water contact angles indicated the poor wettability of the porous polyHIPE surfaces due to the formation of intra/intermolecular hydrogen bonds between the methacrylic acid moieties, which exposed the hydrophobic polymer backbone in air. Similar to incorporation of MA, the introduction of DMAEMA resulted in hydrophilic macroporous polymers with low average water contact angle (around 20) and high equilibrium moisture content (about 37 wt.%). However, part of the pores in the polyHIPEs containing polyDMAEMA were covered by polyDMAEMA films.

8.2 Recommendation for future work

Since a number of limitations need to be considered in view of extending the scope of the potential applications of emulsion templated macrorporous polymers, the following should be considered for future research.

- The using of KPS and of a redox initiator system to initiate the polymerisation of the continuous organic (monomer) phase of emulsion templates did not result in open porous macroporous polymers from MIPEs consisting of styrene and DVB. Although the emulsion templates in which the polymerisation of initiated using AIBN produced macroporous poly(styrene-co-DVB) possessing the desired open porous interconnected pore structure no matter which surfactant (surfactant mixture) was used, suitable initiator systems that enable the low temperature initiation of the polymerisation of emulsion templates to synthesise open porous macroporous polymers are still needed.
- Since it was impossible to introduce pure tensile loading using the Arcan tests during the determination of the tensile properties of emulsion templated macroporous polymers, therefore it was impossible to determine the resistance to crack growth G_{IIc}. It was suggested to carry out flexure tests and flexure tests with notches in order to determine the tensile properties of emulsion templated macroporous polymers and the fracture toughness under tensile loading (mode I) can be calculated afterwards.
- The reinforced, tough and permeable emulsion templated macroporous polymers exhibit the potential to be used as core material to develop composite sandwich structures. Generally, composite sandwich structures consist of a laminated composite skin and a core material. They are combined by an adhesive. The requirements of skin material are a high stiffness and strength since majority of stress is carried by the skin in the composites. Different from skin material, the core material does not carry much stress and only bends when a force is exerted. The primary mechanical requirement for

the core material is to avoid the movement of the skin. In other words, the shear properties are the key requirements of the core material. Since the shear properties of the reinforced tough and permeable emulsion templated macroporous polymers were proven to be significantly improved compared to conventional polyHIPEs, they possess the potential to be used as core material in sandwich structure composites. Although the shear properties of these macroporous polymers are low in comparison to other type of foams, the unique open porous and interconnected pore structure are attractive for a number of applications, in which the core for instance needs to be vacuumed or should be used to store either fuels or water. Therefore, the suitable composite skins need to be identified and a suitable method to bond both core and skin materials, without filling much of the interconnected pore space should be explored.

- The surfaces of polyHIPEs containing polyMA appear to be hydrophobic due the formation of MA hydrogen bonds, which does not allow for fast swelling in water. In order to determine the real contact angle of polyHIPEs containing polyMA and polyDMAEMA, contact angle measurements under both in the sessile drop and captive bubble modes should be performed. Before the captive bubble test, the samples should be immerged into and equilibrated with water and absorb water to break to the hydrogen bonds. Therefore, it would be expected that the water contact angle measured in captive bubble mode of a sample containing polyMA should be much smaller than the value measured by the sessile drop method while the sample containing polyDMAEMA should possess similar values under two different test conditions.

References

1 Barbetta, A.; Carnachan, R. J.; Smith, K.H.; Zhao, C.; Cameron, N.R.; Kataky, R.; Hayman, M.; Przyborski, S. A.; Swan, M. Macromol. Symp. 2005, 226, 203-211.

2 Haq, Z.; Barby; D. European Pat., 1982, 0068830.

3 Edwards, J. European Pat., 1987, 3025175C.

4 Haq Z. European Pat., 1984, 105634.

5 Lissant. K.J. Emulsions and emulsion technology, Part 1, Marcel Dekker, New York (1974) (Chap. 1).

6 Manley, S.; Graeber; N.; Grof; Z.; Menner, A.; Hewitt, G. F; Stepanek, F.; Bismarck, A. Soft matter, 2009, 5, 4780 – 4787.

7 Ikem, V. O.; Menner, A.; Bismarck, A. Soft Matter, 2011, 14, 6571-6577.

8 Menner, A.; Haibach, K.; Powell, R.; Bismarck, A. Polymer, 2006, 47, 7628-7635.

9 Haibach, K.; Menner, A.; Powell, R.; Bismarck, A. Polymer 2006, 47, 4513-4519.

10 Williams, J. M.; Wrobleski, D. A. Langmuir, 1988, 4, 656-662.

11 Bhumgara, Z. G. Filtr. Sep. 1995, 32, 245-251.

12 Wakeman, R. J.; Bhumgara, Z. G.; Akay. G. Chem. Eng. J. 1998, 70, 133-141.

13 Busby, W.; Cameron, N. R.; Jahoda, C. A. B. Biomacromolecules, 2001, 2, 154-164.

14 Stachowiak, A. N.; Bershteyn, A.; Tzatzalos, E.; Irvine, D. J. Adv. Mater. 2005, 17, 399-403.

15 Christenson, E. M.; Soofi, W.; Holm, J. L.; Cameron, N. R.; Mikos, A. G. Biomacromolecules, 2007, 8, 3806-3814.

16 Cameron, N. R. Polymer 2005, 46, 1439-1449.

17 Cameron, N. R.; Sherrington D. C. Adv. Polym. Sci. 1996, 126, 163-214.

18 Lissant. K. J. J. Colloid Interface Sci. 1966, 22, 462-468.

19 Barbetta, A.; Cameron, N. R.; Cooper, S. J. Chem. Commun. 2000, 221–222.

20 Cameron, N. R.; Barbetta, A.; J. Mater. Chem. 2000, 10, 2466-2471.

21 Cameron, N. R.; Sherrington D. C. Colloid. Polym. Sci. 1996, 274, 592-595.

22 Menner, A.; Bismarck, A. Macromol. Symp. 2006, 242, 19-24.

23 Akay, G. European Patent, 2005, 1526914.

24 Hoisington, M. A.; Duke, J. R.; Apen, P. G. Polymer 1997, 38, 3347–3357.

25 Choi, J. S.; Chun, B. C.; Lee, S. J. Macromol. Res. 2003, 11, 104–109.

26 Menner, A.; Powell, R.; Bismarck, A. Soft Matter 2006, 2, 337-342.

27 Krajnc, P.; Stefanec, D.; Brown, J. F.; Cameron, N. R. J. Polym. Sci., Part A: Polym. Chem. 2005, 43, 296–303.

28 Bokhari, M. A.; Akay, G.; Zhang, S. G.; Birch, M. A. Biomaterials 2005, 26, 5198–5208.

29 Williams, J. M. Langmuir 1991, 7, 1370-1377.

30 Kalentun, P.; Buschka, A.; Schmid, A.; Strombom, E. United States Pat. 2000, 6040494.

31 Desmarais, T. A. United States Pat. 1994, 5352711.

32 Barbetta, A.; Dentini, M.; Vecchis, M. S. D.; Filippini, P.; Formisano, G.; Caiazza, S. Adv. Funct. Mater. 2005, 15, 118-124.

33 Kulygin, O.; Silverstein, M., Soft Matter 2007, 3, 1525-1529.

34 Kovačič, S.; Štefanec, D.; Krajnc, P. Macromolecules 2007, 40, 8056-8060.

35 Krajnc, P.; Stefanec, D.; Pulko, I. Macromol. Rapid Commun. 2005, 26, 1289-1293.

36 Barbetta, A.; Massimi, M.; Di Rosario, B.; Nardecchia, S.; De Colli, M.; Devirgiliis, L. C.; Dentini, M. Biomacromolecules 2008, 9, 2844-2856.

37 Francisco, F.T.; Jan, C. M.; Jens C. T.; Thierry, M.; Ralf, W.; Cameron, N. R. Adv. Mater. 2009, 21, 55-59.

38 Zhang, H.; Cooper, A. I. Adv. Mater. 2007, 19, 2439-2444.

39 Cameron, N. R.; Krajnc, P.; Silverstein, M. S. In: Silverstein, M. S.; Cameron, N.R.; Hillmyer, M.A. Editors, Porous polymers, Wiley, Hoboken NJ (2011) [Chapter 4].

40 Shiveley, T. M.; Desmaris, T. A.; Dyer, J. C.; Stone, K. J. United States Pat. 1998, 5817704.

41 Barbetta, A.; Dentini, M.; Leandri, L.; Ferraris, G.; Coletta, A.; Bernabei, M.; React. Funct. Polym., 2009, 69, 724-736.

42 Gurevitch, I.; Silverstein; M. S.; Polym. Sci., Part A: Polym. Chem. 2010, 48, 1516–1525.

43 Tunç, Y.; Gölgelioğlu, C.; Hasirci, N.; Ulubayram, K.; Tuncel, A.; J. Chromatogr. A; 2010, 1217, 1654-1659.

44 Cameron, N. R.; Sherrington, D. C. J Mater. Chem. 1997, 7, 2209-2212.

45 Tai, H.; Sergienko, A.; Silverstein, M. S. Polym. Eng. Sci. 2001, 41, 1540-1552.

46 Sergienko, A.; Tai, H.; Narkis, M.; Silverstein, M. S. J. Appl. Polym. Sci. 2002, 84, 2018- 2027.

47 Normatov, J.; Silverstein, M. S. J. Polym. Sci., Part A: Polym. Chem. 2007, 46, 2357-2366.

48 Butler, R.; Davies, C. M.; Cooper, A. I. Adv. Mater., 2001, 13, 1459-1463.

49 Butler, R.; Hopkinson, I.; Cooper, A. I. J. Am. Chem. Soc. 2003, 125, 14473-14481.

50 Mitchell, M. A.; Tomlin, A. S. United States Pat. 1999, 5998493.

51 Gitli, T.; Silverstein, M. S. Polymer 2011, 52, 107-115.

52 Park, J. S.; Ruckenstein, E. Journal of Applied Polymer Science, 1989, 38, 453-461.

53 Ruckenstein, E.; Sun J. F. Membrane Sci. 1993, 81, 191-201.

54 Ruckenstein, E.; Park, J. S. Polym. Sci., Part C: Polym.Lett. 1988, 26, 529–536.

55 Ruckenstein, E.; Park, J. S. Journal of Applied Polymer Science 1990, 40, 213–220.

56 Collins, D. J. United States Pat. 2000, 6160028.

57 Dyer, J. C.; Hird, B.; Wong, P. K. United States Pat. 2001, 6231960.

58 Collins, D. J.; Mcchain, R. J.; Zhan, Y. United States Pat. 2002, 6365642.

59 Tan, L. S.; Thunhorst, K.L. United States Pat. 2006, 7138436.

60 Tadrosa, T.; Izquierdob, P.; Esquenab, J.; Solansb, C. Advances in Colloid and Interface Science 2004, 108, 303–318.

61 Boyd, J.; Parkinson, C.; Sherman, P. J. Colloid Interface Sci. 1972, 41, 359-370.

62 Pulko, I.; Wall, J.; Krajnc, P.; Cameron, N.R, Chem. Eur. J. 2010, 16, 2350–2354.

63 Beshouri, S. M.; United States Pat. 1994, 5334621.

64 Barby, D.; Haq, Z. United States Pat. 1985, 4522953.

65 Collins, D. J. United States Pat. 1998, 5753359.

66 Desmarais, T.A. United States Pat. 1994, 5352711.

67 Ikem, V.O.; Menner, A.; Horozov, T.S.; Bismarck, A. Adv. Mater. 2010, 22, 3588 - 3592.

68 Menner, A.; Salgueiro, M.; Shaffer, M. Polym. Sci., Part A: Polym. Chem. 2008, 46, 5708-5714.

69 Bismarck, A.; Menner, A.; Ikem, V .O. United States Pat. 2011, 0030948.

70 Wu, R.; Menner, A.; Bismarck, A. Polym. Sci., Part A: Polym. Chem. 2010, 48, 1979-1989.

71 Powell, R.; Bismarck, A.; Menner, A. United States Pat., 2007, 7267169.

72 Powell, R.; Bismarck, A.; Menner, A. Macromolecules, 2006, 39, 2034–2035.

73 Lim, H.; Kassim, A.; Huang, N.; Khiewc, P.; Chiu, W. Colloid. Surface Physicochem. Eng. Aspect. 2009, 345, 211-218.

74 Brownscombe, T. F.; Bass, R. M.; Wong, P. K.; Blytas, G. C.; Gergen, W. P.; Mores, M. United States Pat. 1991, 5061767.

75 Zhang, S.; Chen, J. Polymer, 2007, 48, 3021-3025.

76 Bass, R.M.; Brownscombe, T. F. PCT Int Appl, 1997, WO97/45479.

77 Barbetta, A.; Cameron, N. R. Macromolecules 2004, 37, 3202-321.

78 Williams, J. M.; Gray A. J.; Wilkerson, M. H. Langmuir, 6, 1990, 437-444.

79 Menner, A.; Ikem, V.; Salgueiro, M.; Shaffer, M.; Bismarck, A. Chem. Commun., 2007, 4274-4276.

80 Ikem, V. O.; Menner, A.; Bismarck, A. Angew. Chem., Int. Ed. 2008, 47, 8277-8279.

81 Akartuna, I.; Studart, A. R.; Tervoort, E.; Gauckler, L. J. Adv. Mater. 2008, 20, 4714-4718.

82 Arditty, S.; Whitby, C. P.; Binks, B. P.; Schmitt, V.; Leal-Calderon, F. Eur.Phys. J. E, 2003, 11, 273-281.

83 Menner, A.; Verdejo, R.; Shaffer, M.; Bismarck, A. Langmuir, 2007, 23, 2398-2403.

84 Hermant, M. C.; Klumperman, B.; Koning, C. E. Chem. Commun. 2009, 2738-2740.

85 Zifu, L.; Tian, M.; Jianfang, W.; To, N. Angew. Chem., 2009, 121, 8642-8645.

86 Li, Z. F.; Ngai, T. Colloid and Polymer Sci. 2011, 289, 489-496.

87 Blaker, J. J.; Lee, K.-Y.; Li, X., Menner, A.; Bismarck, A. Green Chem. 2009, 11, 1321-1326.

88 Binks, B. P.; Lumsdon, S. O. Langmuir, 2000, 16, 8622–863.

89 Ikem, V. O.; Menner, A.; Bismarck, A. Langmuir 2010, 26(11), 8836–8841.

90 Binks, B. P.; Curr. Opin.Colloid Interface Sci. 2002, 7, 21-41.

91 Binks, B. P.; Rodrigues, J. A. Angew. Chem. Int. Ed. 2005, 117, 445–448.

92 Zhang, S. M.; Chen, J. D. Chem. Commun. 2009, 2217-2219.

93 Agrios, G.; Pichat, P. J. Appl. Electrochem., 2005, 35, 655–663.

94 Li, Xiao-e; Green, A. N. M.; Haque, S. A.; Mills, A.; Durtant, J. R. J. Photochem. Photobiol. A, 2004, 162, 253–259.

95 Zan, L.; Tian, L. H.; Liu, Z. S.; Peng, Z. H. Appl. Catal. A, 2004,264, 237–242.

96 Webster, T. J.; Siegel, R. W.; Bizios, R. Scr. Mater., 2001, 44, 1639–1642.

97 Yonemura, K.; Fujimaru, H.; Ikushima, N.; Takahashi, K. United States Pat. 2000, 6166097.

98 Akay, G.; Downes, S.; Price, V. J. 2000, WO0034454.

99 Mork, S. W.; Rose, G. D.; Green, D. P. United States Pat. 2001, 6303834.

100 Kadonaga, K.; Mitsuhashi, A.; Fujimaru, H.; Sasabe, M.; Takahashi, K.; Izubayashi, M. PCT Int. Appl. 2001, WO 0121693.

101 Svec, F.; Tennikova, T. B.; Deyl, Z. Journal of Chromatography Library, Elsevier. Amsterdam, 2003, pp263.

102 Fujimaru, H.; Kadonaga, K.; Nagasuna, K.; Minami, K. United States Pat. 2003, 6630519.

103 Aronson, M. P.; Petko, M. F. J. Coll. Interf. Sci. 1993, 159, 134-149.

104 Kadonaga, K.; Mitsuhashi, A.; Takahashi, K. United States Pat. 2003, 6649665.

105 Carnachan, R. J.; Bokhari, M.; Przyborskibc, S. A.; Cameron, N. R. Soft Matter, 2006, 2, 608–616.

106 Mork, S. W.; Malone. B. A. United States Pat. 2001, 6299808.

107 Ruckenstein, E.; Hong, L. Polymer 1995, 36, 2857-2860.

108 Ruckenstein, E.; Sun, Y. J. Appl. Polym. Sci. 1996, 61, 1949-1956.

109 Li, N.; Benson, J. R.; Kitagawa, N. United States Pat. 2000, 6100306.

110 Zhang, H.; Cooper, A. I. Chem. Mater., 2000, 14(10), 4017–4020.

111 Butler, R.; Davies, C. M.; Cooper, A. I. Adv. Mater., 2001, 13, 1459-1463.

112 Cooper, A. I. Adv. Mater., 2003, 15. 1049-1058.

113 Butler, R.; Davies, C. M.; Hopkinson, I.; Cooper, A. I. Polymer Preprints 2002, 43(1), 744-745.

114 DeSimone, J. M. Science 2002, 297, 799-803.

115 Desimone, J. M.; Guan, Z.; Elsbernd, C. S. Science 1992, 257, 945-947.

116 Desimone, J. M.; Maury, E. E.; Menceloglu, Y. Z.; McClain, J. B.; Combes, J. R. Science 1994, 265, 356-359.

117 Deleuze, H.; Maillard, B.; Monval, O.; Bioorg, M. Med. Chem. Lett. 2002, 12, 1877-1880.

118 Krajnc, P.; Leber, N.; Stefanec, D.; Kontrec, S.; Podgornik, A. J. Chromatogr. A 2005, 1065, 69-73.

119 Parthasarathy, R. V.; Clear, S. C.; Sura, R. K.; Soo, P. P United States Pat. 2004, 6750261.

120 Hough, D. B.; Hammond, K.; Morris, C.; Hammond, R. C. United States Pat. 1991, 5071747.

121 Barby, D. European Pat., 1986, 0060138.

122 David, D.; Silverstein, M. S. J. Polym. Sci., Part A: Polym. Chem. 2009, 47, 5806-5814.

123 Palocci, C.; Barbetta, A.; Grotta, A. L.; Dentini, M. Langmuir, 2007, 23, 8243-8251.

124 Barbetta, A.; Dentini, M.; Zannoni, E.; Stefano, M. D. Langmuir, 2005, 21, 12333- 12341.

125 Collins, D. J.; Retzsch, H. L. United States Pat. 2000, 6136874.

126 Bjorksten, J.; Yager, L. L. Mod. Plast. 1952, 29, 124-188.

127 Debnath, S.; Wunder, S. L.; McCoo, J. I.; Baran, G. R. Dent. Mater. 2003, 19, 441-448.

128 Delmonte, J. Technology of Carbon and Graphite Fibre Composites; Van Nostrand Reinhold Ltd., New York, 1981, pp179.

129 Zhu, B.; Katsoulis, D. E.; Keryk, J. R.; McGarry, F. J. Polymer 2000, 41, 7559-7573.

130 Tai, H.; Sergienko, A.; Silverstein, M. S. Polymer 2001, 42, 4473-4482.

131 Lépine, O.; Birot, M.; Deleuze, H. J. Polym. Sci., Part A: Polym. Chem. 2007, 45, 4193-4203.

132 Manley, S. Advances in Experimental Methods for Characterisation of Porous Solids, Ph.D. Thesis, Imperial College, London, UK, 2009.

133 Livshin, S.; Silverstein, M. S. Macromolecules, 2007, 40, 6349-6354.

134 Lumelsky, Y.; Zoldan, J.; Levenberg, S.; Silverstein, M.S. Macromolecules, 2008, 41, 1469-147.

135 Normatov, J.; Silverstein, M. S. J. Polym. Sci., Part A: Polym. Chem. 2008, 46(7), 2357-2366.

136 Silverstein, M.S.; Tai, H.; Sergienko, A.; Lumelsky, Y.; Pavlovsky, S. 2005, Polymer, 46(17), 6682-6694.

137 Youssef, C.; Backov, R.; Treguer, M.; Birot, M.; Deleuze, H. J. Polym. Sci., Part A: Polym. Chem, 2010, 48(3), 2942-2947.

138 British Standard for Compression Test For Rigid Materials BS ISO 844:2001.

139 Rogers, C.E.; Greenhalgh E.S.; Robinson, P. Developing a mode II fracture model for composite laminates. ECCM13; 2008.

140 Greenhalgh, E, S.; Rogers, C.; Robinson, P. Composite Science and Technology 2009, 69 (14), 2345-2351.

141 Rogers, C. Investigating the Micromechanisms of Mode II Delamination in Composite Laminates, Ph.D. Thesis, Imperial College, London, UK, 2009.

142 Standard Test Method for Shear Properties of Sandwich Core Materials. Annual Book of ASTM Standards, Vol 15.03. Report No.: C273-94: 1994.

143 Jurf, R. A.; Pipes, R. B. J. Composite Materials, 1982, 16, 386-394.

144 Hong, C. S; Yoon, S. H. Proc. VI Int. Cong. On Exp. Mech., Oregon, 1988.

145 Banks-Sills, L.; Arcan, M. Int. Jour. of Fracture, 1983, 22, 9-13.

146 Hong, C. S; Yoon, S. H. Experimental Mechanics, 1990, 30, 234-239.

147 Arcan, M.; Hashin, Z.; Voloshin, A. Experimental Mechanics, 18, 1978, 141-146.

148 http://www.mae.ufl.edu/~uhk/STRENGTH.html.

149 Arcan, L.; Arcan, M.; Daniel, I. M. Fractography of Modern Engineering Materials: Composites and Metals, Masters; Au (eds.). American Society for Testing and Materials. ASTM STP 948: 1987: 41-67.

150 Gojny, F. H.; Wichmann, M. H. G.; Köpke, U.; Fiedler, B.; Schulte, K. Composites Science and Technology, 2004, 64(15), 2365-2371.

151 Ritchie, R.; Knott, J. F. J. Mech. &. Phys. Solids, 1973, 21, 395 -410.

152 Banks-Sills, L.; Arcan, M.; Bortma,Y. Engineering Fracture Mechanics, 1984, 20,145-147.

153 Pang, H. L. J.; Seetoh, C. W. Engineering Fracture Mechanics, 1997, 57, 57-65.

154 Polymer Handbook, Edited by: Brandrup, J.; Immergut, E. H.; Grulke, E. A.; Abe, A.; Bloch, D. R.© 1999; 2005 John Wiley & Sons.

155 Carnachan, R. Emulsion-derived (PolyHIPE) Foams for Structural Materials Applications, Ph.D. Thesis, University of Durham, Durham, UK, 2004.

156 Zhao, C.; Danish, E.; Cameron, N. R.; Kataky, R. J. Mater. Chem., 2007, 17, 2446-2453.

157 Barbetta, A.; Cameron, N. R. Macromolecules, 2004, 37, 3188–3201.

158 Wang, D.; Smith, N. L.; Budd, P. M. Polym. Int. 2005, 54, 297–303.

159 Hull, D. Fractography: observing, measuring, and interpreting fracture surface topography, Cambridge University Press, 1999, 122-123.

160 Frechette, V. D. Failure Analyses of Brittle Material; Advances in Ceramics, Volume 28, The American Ceramic Society, Westerville, Ohio, 1990.

161 Singh, S.; Greenhalgh, E. S. Rubber and Composites Processing and Application, 1998, 27(5), 220-226.

162 Hibbs, M. F.; Bradley, W. L. Fractography of Modern Engineering Materials: Composites and Metals, Masters; Au (eds.). American Society for Testing and Materials. ASTM STP 948, 1987, 68-97.

163 http://www.diabgroup.com/global_data_sheets/H_DS_US.pdf.

164 Noury, P. M.; Shenoi, R. A.; Sinclair, I. International Journal of Fracture 1998, 92, 131-151.

165 Grenstedt, J. L.; Hallstrom, S.; Kuttenkeuler, J. Engineering Fracture Mechanics, 1996, 54(4), 445-456.

166 Canal, C.; Gaboriau, F.; Vilchez, A.; Erra, P.; Garcia-Celma, M.; Esquen, J. Plasma Process. Polym. 2009, 6, 686–692.

167 Hainey, P.; Huxham, I. M.; Rowatt, B.; Sherrington, D. C.; Tetley, L. Macromolecules, 1991, 117-121.

168 Molina, R.; V Íchez, A.; Canal, C.; Esquena, J. Surf. Interface Anal. 2009, 41, 371–377.